20 Questions & Answers About the Ozone Layer

2022 Update

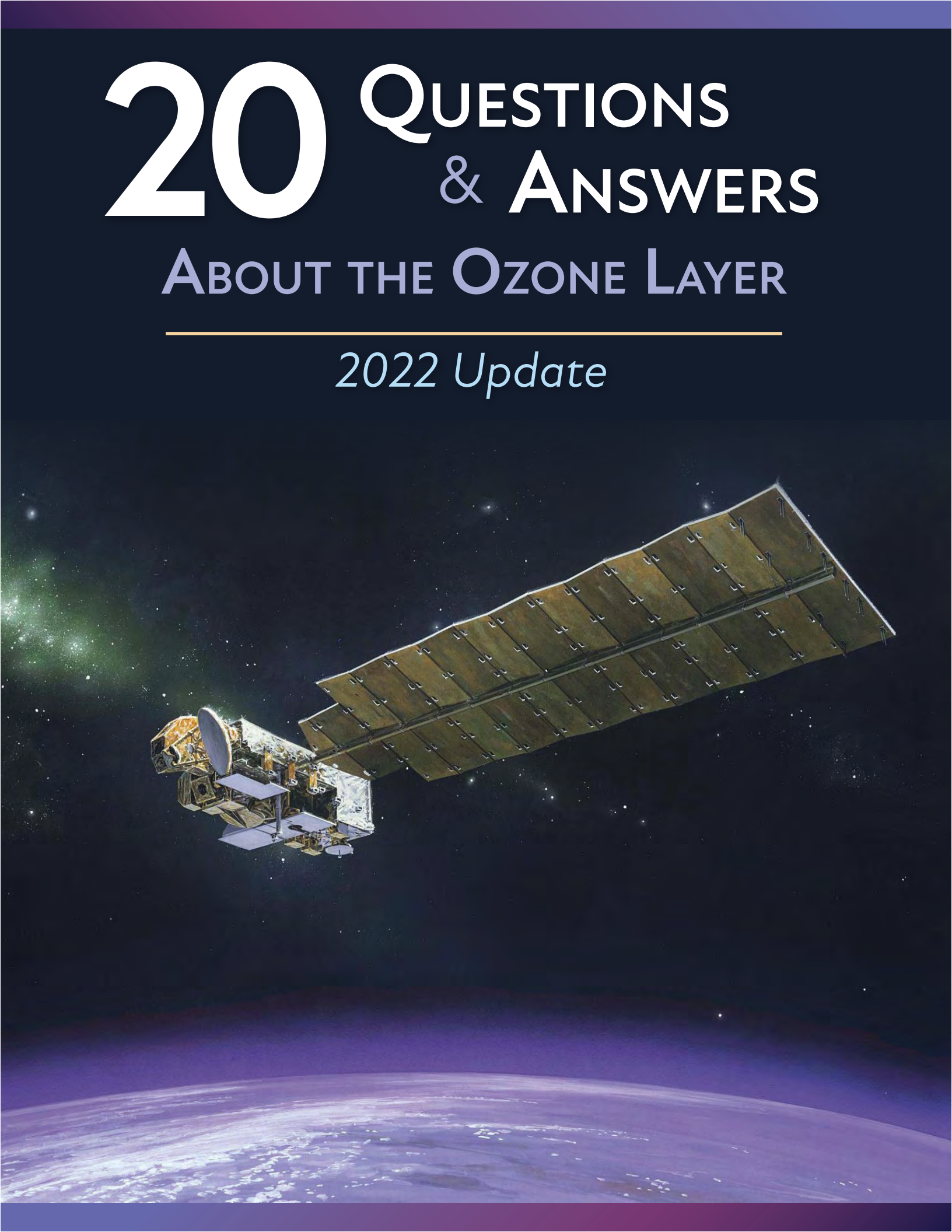

World Meteorological Organization
7bis avenue de la Paix
Case postale 2300
CH-1211 Geneva 2
Switzerland

United Nations Environment Programme
Ozone Secretariat
P.O. Box 30552
Nairobi, 00100
Kenya

US Department of Commerce
National Oceanic and Atmospheric Administration
14th Street and Constitution Avenue NW
Herbert C. Hoover Building, Room 5128
Washington, D. C. 20230

National Aeronautics and Space Administration
Earth Science Division
NASA Headquarters
300 E. Street SW
Washington, D.C. 20546-0001

European Commission
Directorate-General for Research
B-1049 Bruxelles
Belgium

Published April 2023

ISBN: 978-9914-733-98-3

Ross J. Salawitch (Lead Author), Laura A. McBride, Chelsea R. Thompson, Eric L. Fleming, Richard L. McKenzie, Karen H. Rosenlof, Sarah J. Doherty, David W. Fahey, *Twenty Questions and Answers About the Ozone Layer: 2022 Update*, *Scientific Assessment of Ozone Depletion: 2022*, 75 pp., World Meteorological Organization, Geneva, Switzerland, 2023.

This report is available on the internet at the following locations:
https://ozone.unep.org/science/assessment/sap
https://www.csl.noaa.gov/assessments/ozone/2022

Cover image: Artistic rendering of the Aura spacecraft in Earth orbit. Aura, launched in 2004 by the U.S. National Aeronautics and Space Administration (NASA), carries four instruments: the Microwave Limb Sounder (MLS), High Resolution Dynamics Limb Sounder (HIRDLS), Tropospheric Emission Spectrometer (TES) and Ozone Monitoring Instrument (OMI). The instrument suite has provided observations of stratospheric and tropospheric ozone abundances, as well as a wide range of other chemical and physical properties of the atmosphere. The observations have been used extensively to guide the scientific community's understanding of the effects of human activity on Earth's protective ozone layer. Of particular importance have been the MLS observations of the chemical conditions in the ozone layer over Antarctica, including halogen species (ClO and HCl) and nitric acid (HNO_3) (see Fig. Q7-3). Image credit: NASA.
Cover design by Chelsea R. Thompson

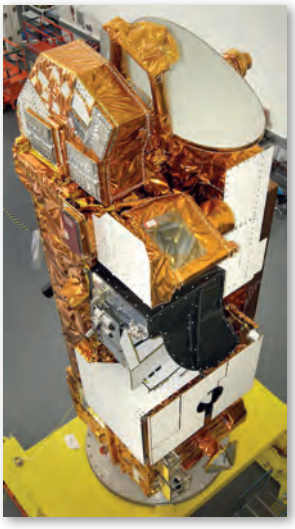

The Aura spacecraft in a clean-room, prior to launch. Photo credit: NASA

TWENTY QUESTIONS & ANSWERS ABOUT THE OZONE LAYER

2022 Update

Lead Author
Ross J. Salawitch

Coauthors
Laura A. McBride
Chelsea R. Thompson
Eric L. Fleming
Richard L. McKenzie
Karen H. Rosenlof
Sarah J. Doherty
David W. Fahey

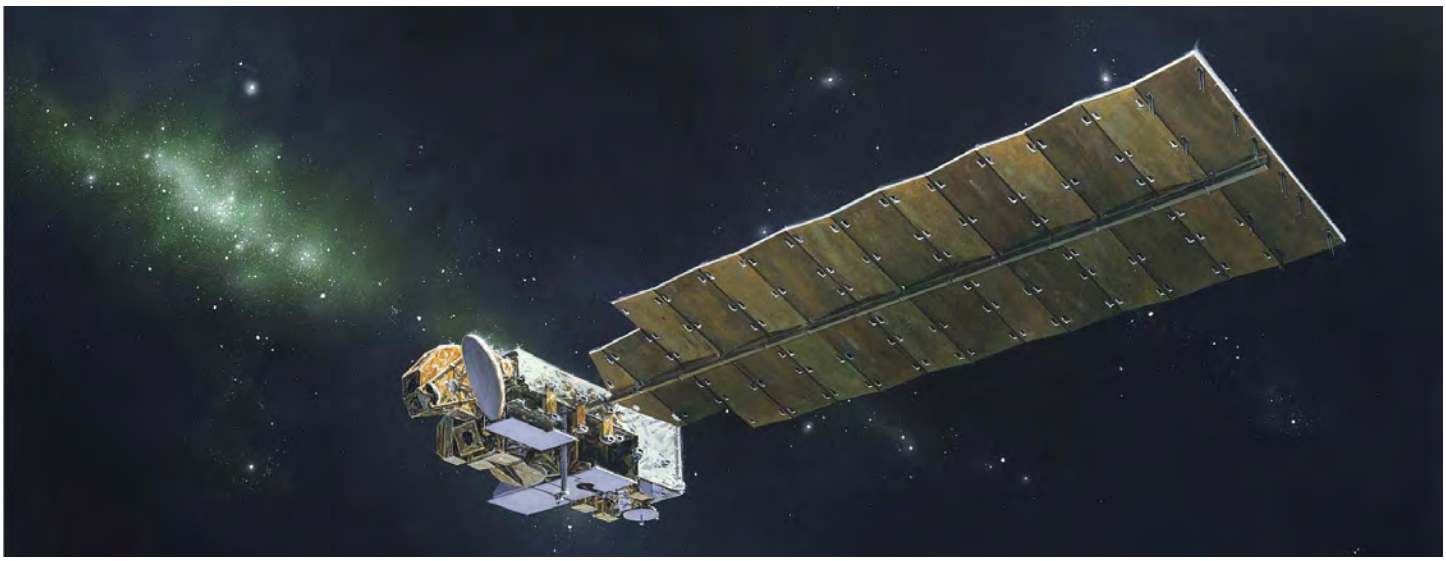

World Meteorological Organization
United Nations Environment Programme
National Oceanic and Atmospheric Administration
National Aeronautics and Space Administration
European Commission

PREFACE

This document, *Twenty Questions and Answers About the Ozone Layer: 2022 Update*, is a component of the *Scientific Assessment of Ozone Depletion: 2022* report. The report is prepared quadrennially by the Scientific Assessment Panel (SAP) of the Montreal Protocol on Substances that Deplete the Ozone Layer*. The 2022 edition of the Twenty Questions document is the fifth update of the original edition that appeared in the 2002 Assessment Report. The motivation behind this scientific publication is to tell the story of ozone depletion, ozone-depleting substances and the success of the Montreal Protocol. The questions and answers format divides the narrative into topics that can be read and studied individually by the intended audience of specialists and non-specialists. The topics range from the most basic (e.g., What is ozone?) to more recent developments (e.g., the Kigali Amendment to the Montreal Protocol). Each question begins with a short answer followed by a longer, more comprehensive answer. Figures enhance the narrative by illustrating key concepts and results. This document is principally based on scientific results presented in the 2022 and earlier Assessment Reports and has been extensively reviewed by scientists and non-specialists to ensure quality and readability.

We hope that you find this Twenty Questions and Answers edition of value in communicating the scientific basis of ozone depletion and the success of the Montreal Protocol in protecting the ozone layer and climate.

David W. Fahey, Paul A. Newman, John A. Pyle, and Bonfils Safari

Co-Chairs of the Scientific Assessment Panel

* https://ozone.unep.org/science/assessment/sap

CONTENTS

INTRODUCTION

Ozone is present only in small amounts in the atmosphere. Nevertheless, ozone is vital to human well-being as well as agricultural and ecosystem sustainability. Most of Earth's ozone resides in the stratosphere, the layer of the atmosphere that is more than 10 kilometers (6 miles) above the surface. About 90% of atmospheric ozone is contained in the stratospheric "ozone layer", which shields Earth's surface from harmful ultraviolet radiation emitted by the Sun.

In the mid-1970s scientists discovered that some human-produced chemicals could lead to depletion of the stratospheric ozone layer. The resulting increase in ultraviolet radiation at Earth's surface would increase incidents of skin cancer and eye cataracts, suppress the immune systems of humans, and also adversely affect agriculture as well as terrestrial and oceanic ecosystems.

Following the discovery of this environmental issue, researchers sought a better understanding of this threat to the ozone layer. Monitoring stations showed that the abundances of gases that are ozone-depleting substances (ODSs)[1], such as chlorofluorocarbons (CFCs), were steadily increasing in the atmosphere. These trends were linked to growing production and use of CFCs and other ODSs for spray can propellants, refrigeration and air conditioning, foam blowing, industrial cleaning, and other applications. Measurements in the laboratory and in the atmosphere characterized the chemical reactions that were involved in ozone destruction. Computer models of the atmosphere employing this information were used to simulate how much ozone depletion was already occurring and to predict how much more might occur in the future.

By the mid-1980s observations of the ozone layer showed that depletion was indeed occurring. The most severe ozone loss, unexpected at the time of discovery, was found to be recurring each springtime over Antarctica. The loss in this region is commonly called the "ozone hole" because the ozone depletion is so large and localized. A thinning of the ozone layer also has been observed over other regions of the globe, such as the Arctic and northern and southern midlatitudes.

The work of many scientists throughout the world has built a broad and solid scientific understanding of the ozone-depletion process. With this foundation, we know that ozone depletion has been occurring and we understand why. Most importantly, we know that if the most potent ODSs were to continue to be emitted and increase in the atmosphere, the result would be ever greater depletion of the ozone layer.

In 1985, the world's governments adopted the Vienna Convention for the Protection of the Ozone Layer in response to the prospect of increasing ozone depletion. The Vienna Convention provided a framework through which nations agreed to take appropriate measures to protect human health and the environment from activities that harm the ozone layer, including cooperation on systematic observations, research and exchange of information. In 1987, this framework led to the Montreal Protocol on Substances that Deplete the Ozone Layer (the Montreal Protocol), an international treaty designed to control the production and consumption of CFCs and other ODSs. As a result of the broad compliance with the Montreal Protocol and subsequent amendments and adjustments as well as industry's development and deployment of "ozone-friendly" substitutes to replace CFCs, the total global accumulation of ODSs in the atmosphere has begun to decrease.

The replacement of CFCs has occurred in two phases: first via the use of hydrochlorofluorocarbons (HCFCs) that cause considerably less damage to the ozone layer compared to CFCs, and second by the introduction of hydrofluorocarbons (HFCs) that do not deplete ozone. In response, global ozone depletion has stabilized, and initial signs of recovery of the ozone layer are being observed. With continued compliance, substantial recovery of the ozone layer is expected by the middle of the 21st century. The day the Montreal Protocol was agreed upon, 16 September, is now celebrated as the International Day for the Preservation of the Ozone Layer. The Montreal Protocol has also decreased the human drivers of global warming, because many CFCs and HFCs are potent greenhouse gases (GHGs).

The amendment and adjustment process is a vitally important aspect of the Montreal Protocol, allowing the protocol to evolve and address emerging issues as our scientific understanding matures. The Protocol was amended or adjusted between 1990 and 2007 at meetings held in London, Copenhagen, Vienna, Beijing, and Montreal (see Q14). The most recent amendment was formulated at the Meeting of the Parties of the Montreal Protocol held in Kigali, Rwanda during October 2016. The Kigali Amendment phases down future global production and consumption of some HFCs to protect future climate, an important new milestone for the Montreal Protocol (see Q19). The Kigali Amendment was motivated by projections of substantial increases in the global use of HFCs in the coming decades. The control of HFCs under this amendment marks the first time the Montreal Protocol has adopted controls solely for the protection of climate.

[1] Here and throughout, the term ozone-depleting substances (ODSs) refers to gases containing either chlorine or bromine that are released to the atmosphere as a result of human activity and are controlled under Annexes A, B, C, or E of the Montreal Protocol.

The protection of the ozone layer and climate under the Montreal Protocol is a story of notable achievements: discovery, understanding, decisions, actions, and verification. It is a success story written by many: scientists, technologists, economists, legal experts, and policymakers, in which continuous dialogue has been a key ingredient. A timeline of milestones related to the science of stratospheric ozone depletion, international scientific assessments, and the Montreal Protocol is illustrated in **Figure Q0-1**.

To help communicate the broad understanding of the Montreal Protocol, ODSs, and ozone depletion, as well as the relationship of these topics to GHGs and global warming, this component of the *Scientific Assessment of Ozone Depletion: 2022* report describes the state of this science with 20 illustrated questions and answers. The questions and answers address the nature of atmospheric ozone, the chemicals that cause ozone depletion, how global and polar ozone depletion occur, the extent of ozone depletion, the success of the Montreal Protocol, the possible future of the ozone layer, and the protection against climate change now provided by the Kigali Amendment. Computer model projections show that GHGs such as carbon dioxide (CO_2), methane (CH_4), and nitrous oxide (N_2O) will have a growing influence on global ozone in the coming decades, and in some cases may exceed the influence of ODSs on ozone by the middle of this century, given the expected future decline in the atmospheric abundance of ODSs.

For each question, a brief answer is first given in highlighted text; an expanded answer then follows. The answers are based on the information presented in the 2022 and earlier Assessment reports as well as other international scientific assessments. These reports and the answers provided here were prepared and reviewed by a large number of international scientists who are experts in different research fields related to the science of stratospheric ozone and climate[2].

[2] See Authors and Contributors at the end of this book.

Figure Q0-1. Stratospheric ozone depletion and policy milestones. This timeline highlights milestones related to the history of ozone depletion. Events represent the occurrence of important scientific findings, the completion of international scientific assessments, and milestones of the Montreal Protocol.

Scientific Milestones. A worldwide network of ground-based ozone measurement stations was initiated in 1957, as part of the International Geophysical Year. The number of atmospheric observations of ozone, CFCs, and other ODSs have increased substantially since the early 1970s. The discovery of the Antarctic ozone hole in 1985 led to a major community effort that established, within a few years, that this phenomenon was caused by the human release of various chlorine and bromine compounds. The total global emission of these compounds peaked in 1987, the year the Montreal Protocol was signed. The Nobel Prize in Chemistry in 1995 was awarded for research that identified, in 1974, the threat posed by CFCs to the global ozone layer. The graph at the bottom shows the history and near future of annual total emissions of ozone-depleting substances (ODSs) combined with natural emissions of halogen source gases. The emissions, when weighted by their potential to destroy ozone, peaked in the late 1980s after several decades of steady increases. Between the late 1980s and the present, emissions have decreased substantially as a result of the Montreal Protocol and its subsequent amendments and adjustments coming into force (see Q14). The total stratospheric halogen content peaked in the late 1990s, followed by a slow, steady decline (see Q15). In the mid-2010s scientists documented clear evidence that the rise in the abundance of upper stratospheric ozone, which had begun in the late 1990s, was caused by the decline in the stratospheric chlorine loading driven by the Montreal Protocol. At the end of 2022, the stratospheric halogen content was 18% less than the peak value (see Q15).

International Scientific Assessments. The provisions of the Montreal Protocol and its amendments and adjustments have depended on information embodied in international scientific assessments of ozone depletion that have been produced periodically since 1989 under the auspices of UNEP and WMO. These assessments incorporate new knowledge from ongoing observations, modeling studies, and analyses into a report designed to reflect the latest scientific understanding of how human activity affects the ozone layer.

International Policy Milestones. The Montreal Protocol, which is built on the framework established by the Vienna Convention, was signed on 16 September 1987. Under the Protocol, January 2010 marked the end of allowable production of CFCs and halons, with a few very small exemptions. In January 2013, a production and consumption freeze on HCFCs went into effect for all nations. In October 2016 the Kigali Amendment brought the future production of HFCs under the auspices of the Montreal Protocol (see Q19).

(A megatonne = 1 million (10^6) metric tons = 1 billion (10^9) kilograms.)

(Formally the term halogen refers to the elements fluorine, chlorine, bromine, iodine, and astatine that are in group 7A of the periodic table. Here and throughout, unless otherwise specified, halogen refers to chlorine and bromine, since source gases containing either of these two halogens constitute the ODSs controlled by the Montreal Protocol.)

EESC: Equivalent effective stratospheric chlorine | IPCC: Intergovernmental Panel on Climate Change | ODS: Ozone-depleting substance | TEAP: Technology and Economic Assessment Panel of the Montreal Protocol | UNEP: United Nations Environment Programme | WMO: World Meteorological Organization

Stratospheric Ozone Depletion Science and Policy Milestones

Scientific Milestones

- WMO World Ozone Data Centre – 1960
- Global Ozone Observing System – 1957
- Backscatter Ultraviolet satellite instrument launched – 1970
- First surface observations of CFCs – 1973
- CFC ozone-depletion hypothesis – 1974
- Start of continuous global ozone satellite record – 1978
- Ozone hole reported over Antarctica – 1985
- Peak global emissions of ODSs – 1987
- Laboratory, field, and modeling studies show chlorine and bromine deplete polar stratospheric ozone – 1985–1989
- Peak stratospheric abundance of chlorine and bromine (EESC) in midlatitudes – 1998
- Nobel Prize in Chemistry to Cruzten, Molina, and Rowland – 1995
- 2014 *Assessment* reports clear evidence that upper stratospheric ozone increased as a result of the ODS phaseout
- Stratospheric abundance of EESC in midlatitudes down 18% from peak level – 2022

International Scientific Assessments

- WMO Atmospheric Ozone – 1985
- WMO The Stratosphere 1981: Theory and Measurements
- WMO Report of the International Ozone Trends Panel – 1988
- *UNEP/WMO Scientific Assessments of Ozone Depletion :* 1989 1991 1994 1998 2002 2006 2010 2014 2018 2022
- IPCC/TEAP Special Report on Safeguarding the Ozone Layer and the Global Climate System – 2005

International Policy Milestones

- UNEP World Plan of Action on the Ozone Layer – 1977
- Vienna Convention for the Protection of the Ozone Layer – 1985
- **Montreal Protocol on Substances that Deplete the Ozone Layer – 1987**
- *Montreal Protocol Amendments :*
  - London – 1990
  - Copenhagen – 1992
  - Vienna – 1995
  - Montreal – 1997
  - Beijing – 1999
- Global production of CFCs and halons ends – 2010
- HCFC accelerated phaseout (Montreal-2007 Adjustment)
- Global consumption of ODSs reduced by 98% – 1986 to 2008
- Montreal Protocol universal ratification – 2009
- Developed countries eliminated 90% of their HCFC production and consumption; developing countries freeze their HCFC production and consumption – 2013
- Kigali Amendment enters into force – 2019
- Kigali Amendment on the control of production and consumption of some HFCs adopted – 2016

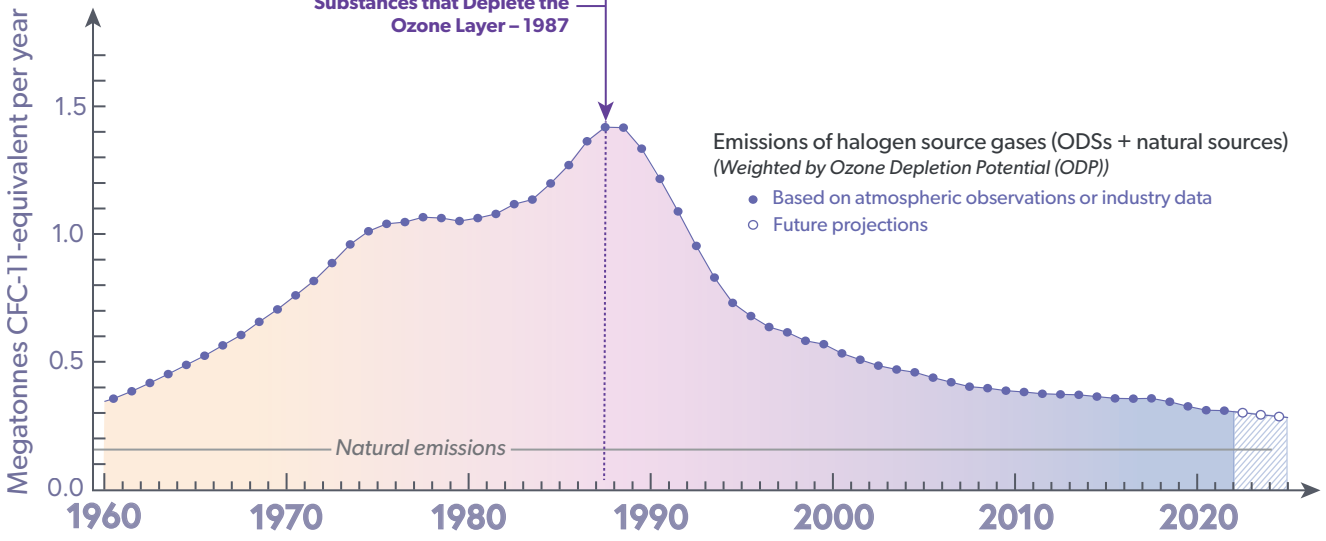

Q1 What is ozone, how is it formed, and where is it in our atmosphere?

Ozone is a gas that is naturally present in our atmosphere. Each ozone molecule contains three atoms of oxygen and is denoted chemically as O_3. Ozone is found primarily in two regions of the atmosphere. About 10% of Earth's ozone is in the troposphere, which extends from the surface to about 10–15 kilometers (6–9 miles) altitude. About 90% of Earth's ozone resides in the stratosphere, the region of the atmosphere between the top of the troposphere and about 50 kilometers (31 miles) altitude. The part of the stratosphere with the highest amount of ozone is commonly referred to as the "ozone layer". Throughout the atmosphere, ozone is formed in multistep chemical processes that are initiated by sunlight. In the stratosphere, the process begins with an oxygen molecule (O_2) being broken apart by ultraviolet radiation from the Sun. In the troposphere, ozone is formed by a different set of chemical reactions that involve naturally occurring gases as well as those from sources of air pollution.

Ozone is a gas that is naturally present in our atmosphere. Ozone has the chemical formula O_3 because an ozone molecule contains three oxygen atoms (see **Figure Q1-1**). Ozone was discovered in laboratory experiments in the mid-1800s. Ozone's presence in the atmosphere was later discovered using chemical and optical measurement methods. The word ozone is derived from the Greek word όζειν (*ozein*), meaning "to smell." Ozone has a pungent odor that allows it to be detected even at very low amounts. Ozone reacts rapidly with many chemical compounds and is explosive in concentrated amounts. Electrical discharges are generally used to produce ozone for industrial processes such as air and water purification and bleaching of textiles and food products.

Ozone location. Most ozone (about 90%) is found in the stratosphere, which begins about 10–15 kilometers (km) above Earth's surface and extends up to about 50 km altitude. The stratospheric region with the highest concentration of ozone, between about 15 and 35 km altitude, is commonly known as the "ozone layer" (see **Figure Q1-2**). The stratospheric ozone layer extends over the entire globe, with some variation in its altitude and thickness. Most of the remaining ozone (about 10%) is found in the troposphere, which is the lowest region of the atmosphere, between Earth's surface and the stratosphere. Tropospheric air is the "air we breathe" and, as such, excess ozone in the troposphere has harmful consequences (see Q2).

Ozone abundance. Ozone molecules constitute a small fraction of the gas molecules in the atmosphere. Most air molecules are either oxygen (O_2) or nitrogen (N_2). In the stratosphere, near the peak concentration of the ozone layer, there are typically a few thousand ozone molecules for every ***billion*** air molecules (1 billion = 1,000 million). In the troposphere near Earth's surface, ozone is even less abundant, with a typical range of 20 to 100 ozone molecules for each billion air molecules. The highest ozone values near the surface occur in air that is polluted by human activities. Throughout this document the word "abundance" refers to the concentration or amount of an atmospheric gas or some other physical quantity.

As an illustration of the low relative abundance of ozone in our atmosphere, one can imagine bringing all the ozone molecules in the troposphere and stratosphere down to Earth's surface and forming a layer of pure ozone that extends over the entire globe. The resulting layer would have an average thickness of about three millimeters (0.12 inches), which scientists would report as 300 Dobson Units (see Q3). Nonetheless, this extremely small fraction of the atmosphere plays a vital role in protecting life on Earth (see Q2).

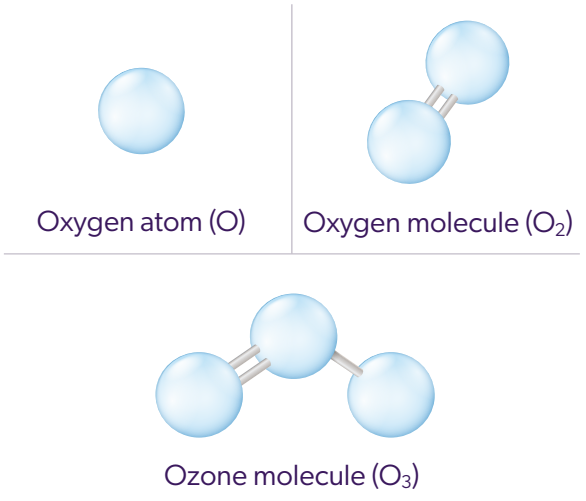

Figure Q1-1. Ozone and oxygen. A molecule of ozone (O_3) contains three oxygen atoms (O) bound together. Oxygen molecules (O_2), which constitute about 21% of the gases in Earth's atmosphere, contain two oxygen atoms bound together.

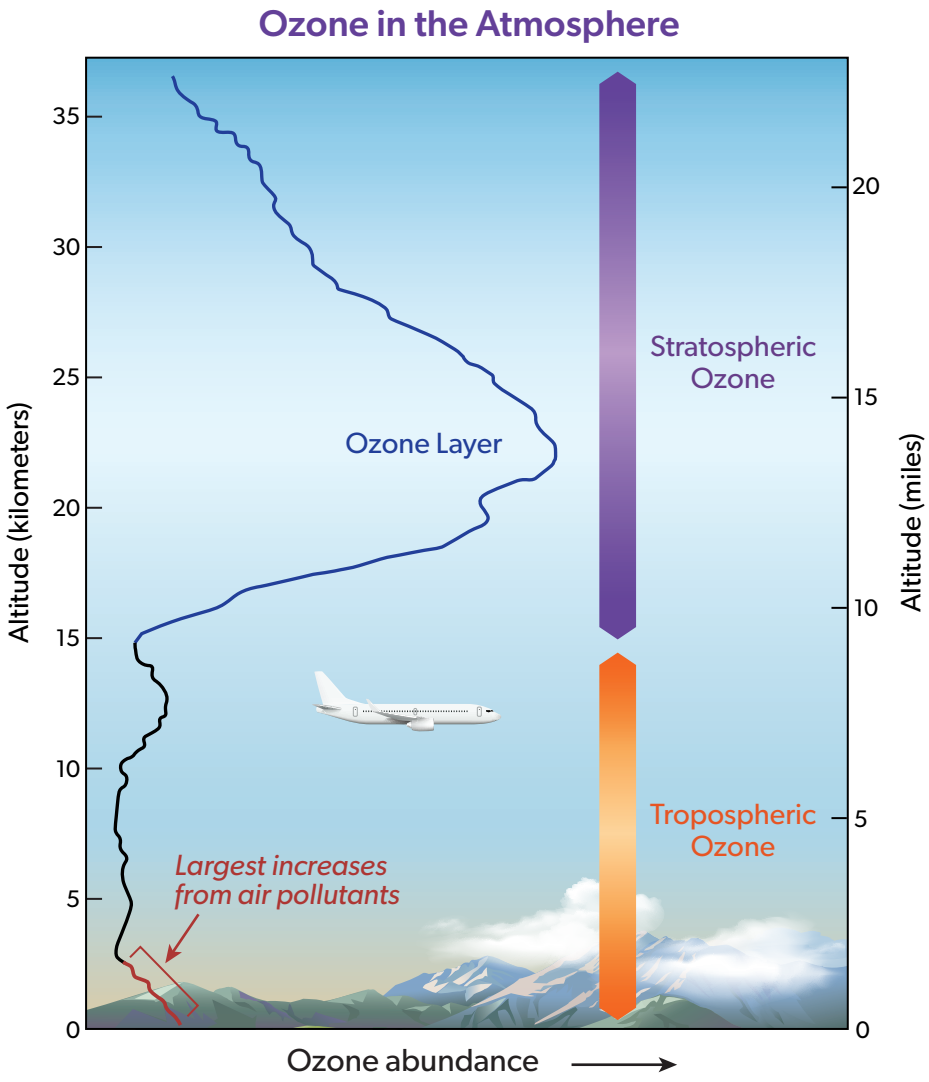

Figure Q1-2. Ozone in the atmosphere. Ozone is present throughout the troposphere and stratosphere. This profile shows schematically how ozone changes with altitude in the tropics. Most ozone resides in the stratospheric "ozone layer." The vertical extent or thickness of this layer varies from region to region and with season over the globe (see Q3). Increases in ozone near the surface are a result of air pollutants released by human activities. The direct exposure to ozone is harmful to humans and other forms of life.

Stratospheric ozone. Stratospheric ozone is formed naturally by chemical reactions involving solar ultraviolet radiation (sunlight) and oxygen molecules, which make up about 21% of the atmosphere. In the first step, solar ultraviolet radiation breaks apart one oxygen molecule (O_2) to produce two oxygen atoms (2 O) (see **Figure Q1-3**). In the second step, each of these highly reactive oxygen atoms combines with an oxygen molecule to produce an ozone molecule (O_3). These reactions occur continually whenever solar ultraviolet radiation is present in the stratosphere. As a result, the largest ozone production occurs in the tropical stratosphere.

The production of stratospheric ozone is balanced by its destruction in chemical reactions. Ozone reacts continually with sunlight and a wide variety of natural and human-produced chemicals in the stratosphere. In each reaction, an ozone molecule is lost and other chemical compounds are produced. Important reactive gases that destroy ozone are hydrogen and nitrogen oxides and those containing chlorine and bromine (see Q7). Some stratospheric ozone is regularly transported down into the troposphere and can occasionally influence ozone amounts at Earth's surface.

Tropospheric ozone. Near Earth's surface, ozone is produced by chemical reactions involving gases emitted into the atmosphere from both natural sources and human activities. Ozone production in the troposphere primarily occurs by reactions of hydrocarbon and nitrogen oxide gases, and all require sunlight for completion. Fossil fuel combustion and deforestation are the primary sources of pollutant gases that lead to production of tropospheric ozone. As in the stratosphere, ozone in the troposphere is destroyed by naturally occurring chemical reactions and by reactions involving human-produced chemicals. Tropospheric ozone can also be destroyed when ozone reacts with a variety of surfaces, such as those of soils and plants.

Balance of chemical processes. Ozone abundances in the stratosphere and troposphere are determined by the balance between chemical processes that produce and destroy ozone. The balance is determined by the amounts of reactive gases and how the rate or effectiveness of the various reactions varies with sunlight intensity, location in the atmosphere, temperature, and other factors. As atmospheric conditions change to favor ozone-producing

reactions in a certain location, ozone abundances increase. Similarly, if conditions change to favor other reactions that destroy ozone, abundances decrease. The balance of production and loss reactions, combined with atmospheric air motions that transport and mix air with different ozone abundances, determines the global distribution of ozone on timescales of days to many months (see also Q3). Global stratospheric ozone decreased from the 1970s to the late 1990s (see Q12 and Q13) because the amounts of reactive gases containing chlorine and bromine in the stratosphere increased due to human activities (see Q6 and Q15).

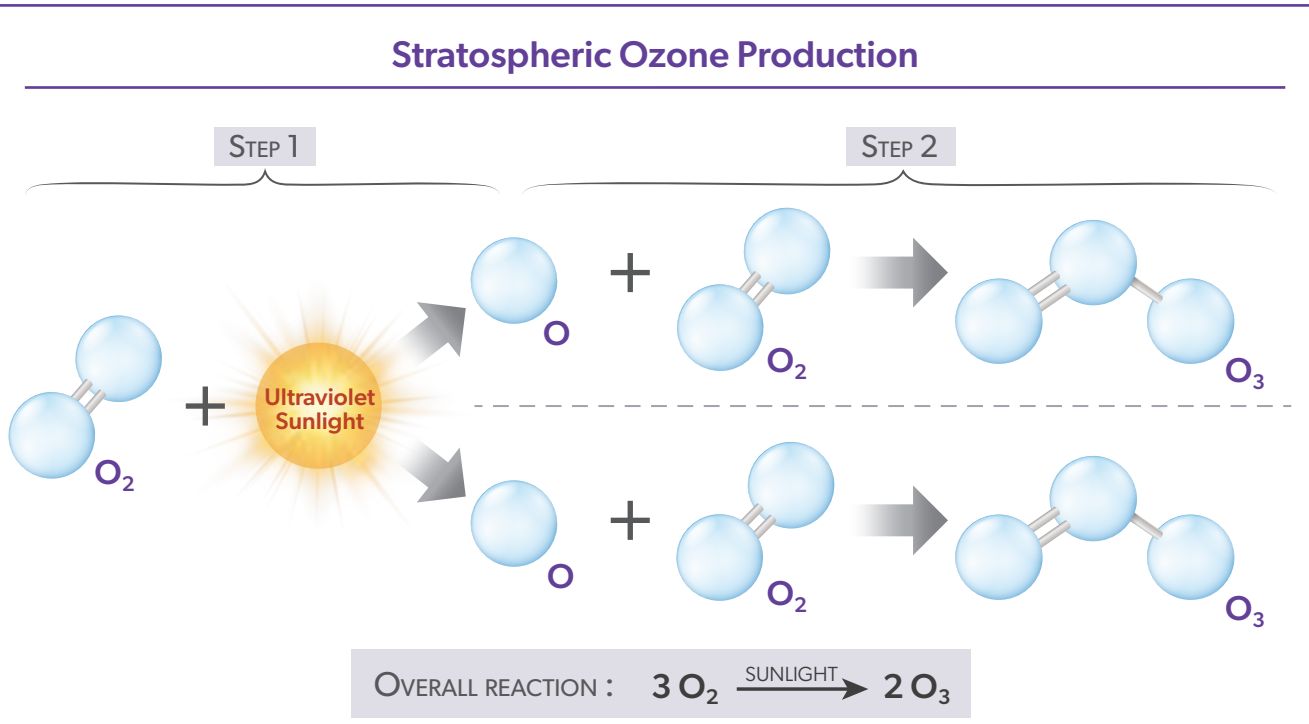

Figure Q1-3. Stratospheric ozone production. Ozone is produced naturally in the stratosphere by a two-step reaction process. In the first step, solar ultraviolet radiation (sunlight) breaks apart an oxygen molecule to form two separate oxygen atoms. In the second step, each oxygen atom collides with another oxygen molecule and forms an ozone molecule in a binding reaction. In the overall process, three oxygen molecules plus sunlight react to form two ozone molecules.

Q2 Why do we care about atmospheric ozone?

Ozone in the stratosphere absorbs a large part of the Sun's biologically harmful ultraviolet radiation. Stratospheric ozone is considered "good" ozone because of this beneficial role. In contrast, ozone formed at Earth's surface in excess of natural amounts is considered "bad" ozone because this gas is harmful to humans, plants, and animals.

Ozone in the stratosphere *(Good ozone)*. Stratospheric ozone is considered good for humans and other life forms because ozone absorbs ultraviolet (UV) radiation from the Sun (see **Figure Q2-1**). The Sun emits UV radiation that scientists categorize into three wavelength ranges: UV-C (100 to 280 nanometer (nm) wavelengths); UV-B (280 to 315 nm), and UV-A (315 to 400 nm). The energy of solar UV radiation, which cannot be seen by the human eye, is higher at shorter wavelengths. Exposure to high energy UV-C radiation is particularly dangerous to all life forms. Fortunately, UV-C radiation is entirely absorbed within the ozone layer. Most UV-B radiation emitted by the Sun is absorbed by the ozone layer; the rest reaches Earth's surface. In humans, increased exposure to UV-B radiation raises the risks of skin cancer and cataracts, and suppresses the immune system. Exposure to UV-B radiation before adulthood and cumulative exposure are both important health risk factors. Excessive UV-B exposure also can damage terrestrial plant life, including agricultural crops, single-celled organisms, and aquatic ecosystems. Low energy UV radiation, UV-A, which is not absorbed significantly by the ozone layer, causes premature aging of the skin.

Protecting stratospheric ozone. In the mid-1970s, it was discovered that gases containing chlorine and bromine atoms released by human activities could cause stratospheric ozone depletion (see Q5 and Q6). These gases, referred to as halogen source gases, and also as ozone-depleting substances (ODSs), chemically release their chlorine and bromine atoms after they reach the stratosphere.

UV Protection by the Stratospheric Ozone Layer

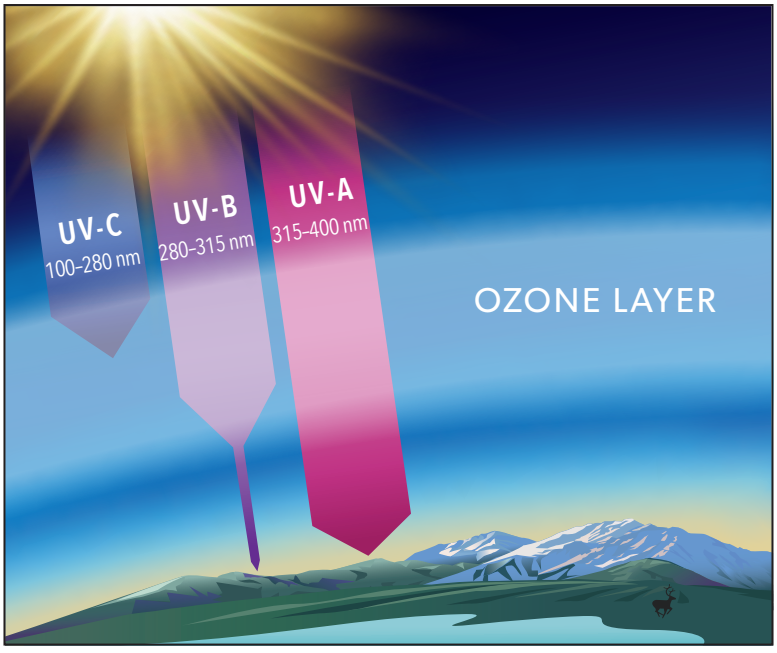

Figure Q2-1. UV protection by the ozone layer. The ozone layer is located in the stratosphere and surrounds the entire Earth. The Sun emits ultraviolet (UV) radiation that reaches the top of the ozone layer, which scientists classify according to wavelength. Solar UV-C radiation (wavelength range 100 to 280 nanometer (nm)) is extremely damaging to humans and other life forms; UV-C radiation is entirely absorbed within the ozone layer. Solar UV-B radiation (280 to 315 nm) is only partially absorbed and, as a result, humans and other life forms are exposed to some UV-B radiation. Excessive exposure to UV-B radiation increases the risks of skin cancer, cataracts, and a suppressed immune system for humans and also damages terrestrial plant life, single-cell organisms, as well as aquatic ecosystems. UV-A (315 to 400 nm), visible light, and other wavelengths of solar radiation are only weakly absorbed by the ozone layer. Exposure to UV-A is associated with premature aging of the skin and some skin cancers. Depletion of the ozone layer primarily increases the amount of UV-B radiation that reaches the surface (Q16). Avoiding ozone depletion that would increase human exposure to UV-B radiation is a principal objective of the Montreal Protocol.

(The unit "nanometer" (nm) is a common measure of the wavelength of light; 1 nm equals one billionth of a meter ($=10^{-9}$ m).)

Ozone depletion increases surface UV-B radiation above naturally occurring amounts. International efforts have been successful in protecting the ozone layer through controls on the production and consumption of ODSs (see Q14 and Q15).

Ozone in the troposphere *(Bad ozone)*. Ozone near Earth's surface in excess of natural amounts is considered bad ozone (see Figure Q1-2). Surface ozone in excess of natural levels is formed by reactions involving air pollutants emitted from human activities, such as nitrogen oxides (NO_x), carbon monoxide (CO), and various hydrocarbons (gases containing hydrogen, carbon, and often oxygen). Exposure to ozone at concentrations above natural levels is harmful to humans, plants, and other living systems because ozone reacts strongly to destroy or alter molecules that constitute biological tissue. Enhanced surface ozone caused by air pollution reduces crop yields and forest growth. In humans, exposure to high levels of ozone can reduce lung capacity; cause chest pains, throat irritation, and coughing; and worsen pre-existing health conditions related to the heart and lungs. In addition, increases in tropospheric ozone lead to a warming of Earth's surface because ozone is a greenhouse gas (GHG) (see Q17). The negative effects of excess tropospheric ozone contrast sharply with the protection from harmful UV radiation afforded by preserving the natural abundance of stratospheric ozone.

Reducing tropospheric ozone. Limiting the emission of certain common pollutants reduces the production of excess ozone near Earth's surface, where ozone can affect humans, plants, and animals. Major sources of pollutants include large cities, where fossil fuel consumption for transportation, heating, and industrial activities is concentrated, power plants that rely on coal, oil, or natural gas, as well as deforestation, wildfires, and the burning of savannah for agriculture. Many programs around the globe have been successful in reducing or limiting the emission of pollutants that cause production of excess ozone near Earth's surface.

Natural ozone. In the absence of human activities, ozone would still be present near Earth's surface and throughout the troposphere and stratosphere because ozone is a natural component of the clean atmosphere. Natural emissions from the biosphere, mainly from trees, participate in chemical reactions that produce ozone. Atmospheric ozone plays important ecological roles beyond absorbing UV radiation. For example, ozone initiates the chemical removal of many pollutants as well as some GHGs, such as methane (CH_4). In addition, the absorption by ozone of solar UV radiation as well as visible and infrared radiation is a natural source of heat in the stratosphere, causing temperatures to increase with altitude. Stratospheric temperatures affect the balance of ozone production and destruction processes (see Q1) and air motions that redistribute ozone throughout the stratosphere (see Q3).

Q3 How is total ozone distributed over the globe?

The distribution of total ozone over Earth varies with geographic location and on daily and seasonal timescales. These variations are caused by large-scale movements of stratospheric and tropospheric air and the chemical production and destruction of ozone. Total ozone is generally lowest at the equator and highest in midlatitude and polar regions.

Total ozone. The total column of ozone at any location on the globe is defined as the sum of all the ozone in the atmosphere directly above that location. Most ozone resides in the stratospheric ozone layer and a small percentage (about 5 to 10%) is distributed throughout the troposphere (see Q1). Total column ozone values are usually reported in *Dobson units* denoted as "DU." Typical values vary between 200 and 500 DU over the globe, with a global average abundance of about 300 DU (see **Figure Q3-1**). The ozone molecules required for total ozone to be 300 DU would form a layer of pure ozone gas at Earth's surface having a thickness of only 3 millimeters (0.12 inches) (see Q1), which is about the height of a stack of 2 common coins, if these molecules could be isolated and compressed. It is remarkable that a layer of pure ozone only 3 millimeters thick protects life on Earth's surface from most of the harmful UV radiation emitted by the Sun (see Q2).

Global distribution. Total ozone varies strongly with latitude over the globe, with the largest values occurring at middle and high latitudes during most of the year (see Figure Q3-1). This distribution is the result of the large-scale circulation of air in the stratosphere that slowly transports ozone-rich air from high altitudes in the tropics, where ozone production from solar ultraviolet radiation is largest, toward the poles. Ozone accumulates at middle and high latitudes, increasing the vertical extent of the ozone layer and, at the same time, total ozone. The total column of ozone is generally smallest in the tropics for all seasons. An exception since the mid-1980s is the region of low values of ozone over Antarctica during spring in the Southern Hemisphere, a phenomenon known as the Antarctic ozone hole (dark blue, Figure Q3-1; also see Q10 and Q11).

Seasonal distribution. Total ozone also varies with season, as shown in Figure Q3-1 using two-week averages of ozone taken from satellite observations acquired in 2021. March and September plots represent the early spring and autumn seasons in the Northern and Southern Hemispheres, respectively. June and December plots similarly represent the early summer and winter seasons. During spring, total ozone exhibits maximums at latitudes poleward of about 45° N in the Northern Hemisphere and between 45° and 60° S in the Southern Hemisphere. These spring maximums are a result of increased transport of ozone from its source region in the tropics toward high latitudes during late autumn and winter. This poleward ozone transport is much weaker during the summer and early autumn periods and is weaker overall in the Southern Hemisphere.

This natural seasonal cycle can be observed clearly in the Northern Hemisphere as shown in Figure Q3-1, with increasing values in Arctic total ozone during winter, a clear maximum in spring, and decreasing values from summer to autumn. In the Antarctic, however, a pronounced minimum in total ozone is observed during spring. The minimum is known as the "ozone hole", which is caused by the widespread chemical depletion of ozone in spring by pollutants known as ozone-depleting substances (see Q5 and Q10). In the late 1970s, before the ozone hole appeared each year, much higher ozone values than those currently observed were found in the Antarctic spring (see Q10). Currently, the lowest values of total ozone across the globe and all seasons are found during early spring in the Antarctic, as shown in Figure Q3-1 for 2021. After spring, these low values disappear from total ozone maps as polar air mixes with lower-latitude air containing much higher amounts of ozone.

In the tropics, the change in total ozone through the progression of the seasons is much smaller than at higher latitudes. This feature is present because seasonal changes in both sunlight and ozone transport are much smaller in the tropics compared to higher latitudes.

The abundance of ozone is larger at midlatitudes in the Northern Hemisphere (NH) than the Southern Hemisphere (SH), for all four seasons in the respective hemispheres. The thinner ozone layer at SH midlatitudes compared to NH midlatitudes is due to several factors: differences in the large-scale circulation of the two hemispheres that preceded the development of the ozone hole as well as larger abundances of tropospheric ozone in the NH compared to the SH that is caused by more pollution in the more heavily populated NH. Dilution of ozone-depleted air from the Antarctic ozone hole region starting in the 1980s further increases the hemispheric difference in total ozone. This hemispheric total ozone difference results in higher levels of UV light reaching the surface in the SH compared to the NH (see Q16).

Natural variations. Total ozone varies strongly with latitude and longitude, as seen within the seasonal plots in Figure Q3-1. These patterns come about for two reasons. First, atmospheric winds transport air between regions of the stratosphere that have high ozone values and those that have low ozone values. Tropospheric weather systems can temporarily alter the vertical extent of the ozone layer in a region, and thereby change total ozone. The regular nature of these air motions, in some cases associated with geographical features (oceans and mountains), in turn causes recurring patterns in the distribution of total ozone. Second, ozone

variations occur as a result of changes in the balance of chemical production and loss processes. This balance is very sensitive to the amount of solar UV radiation (see Q2) reaching the various parts of the atmosphere.

There is a good understanding of how chemistry and air motions work together to cause the observed large-scale features in total ozone, such as those seen in Figure Q3-1. Ozone changes are routinely monitored by a large group of scientists using satellite, airborne, and ground-based instruments. The continued analyses of these observations provide an important long-term basis to quantify the contribution of human activities to ozone depletion.

Global Satellite Maps of Total Ozone in 2021

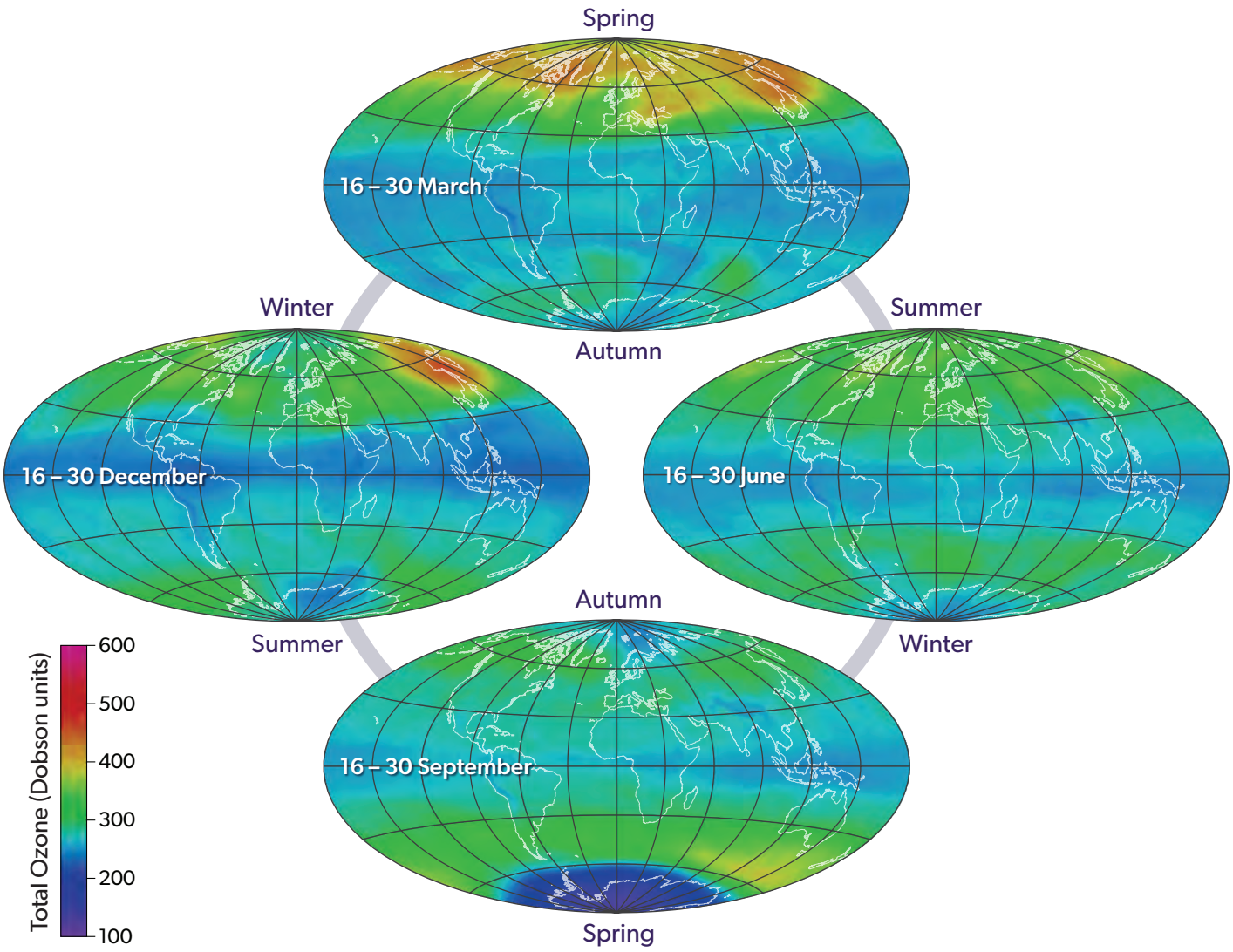

Figure Q3-1. Total ozone. Total column ozone at any location on the globe is defined as the sum of all the ozone molecules in the atmosphere directly above that location. Total ozone varies with latitude, longitude, and season, with the largest values at high latitudes and the lowest values usually found in tropical regions. The variations are demonstrated here with two-week averages of total ozone in 2021 as measured with a satellite instrument. Total ozone shows little variation in the tropics (20°N–20°S latitudes) over all seasons. Total ozone outside of the tropics varies more strongly with time on a daily to seasonal basis as ozone-rich air is moved from the tropics and accumulates at higher latitudes, with more ozone being transported in winter. The low total ozone values over Antarctica shown here in September constitute the "ozone hole" in 2021. Since the mid-1980s, the ozone hole in late winter/early spring represents the lowest values of total ozone that occur over all seasons and latitudes (see Q10).

Q4 How is ozone measured in the atmosphere?

The amount of ozone in the atmosphere is measured by instruments on the ground and carried aloft on balloons, aircraft, and satellites. Some instruments measure ozone remotely over long distances by using ozone's unique optical absorption or emission properties. Other instruments measure ozone locally by continuously drawing air samples into a small detection chamber.

The abundance of ozone in the atmosphere is measured by a variety of techniques (see **Figure Q4-1**). The techniques make use of ozone's unique optical and chemical properties. There are two principal categories of measurement techniques: local and remote. Ozone measurements by these techniques have been essential in monitoring changes in the ozone layer and in developing our understanding of the processes that control ozone abundances.

Local measurements. Local measurements of the atmospheric abundance of ozone are those that require air to be drawn directly into an instrument. Once inside an instrument's detection chamber, the amount of ozone is determined by measuring the absorption of ultraviolet (UV) radiation or by the electrical current or light produced in a chemical reaction involving ozone. The latter approach is used in "ozonesondes", which are lightweight, ozone-measuring modules suitable for launching on small balloons. The balloons ascend up to altitudes of about 32 to 35 kilometers (km), high enough to measure ozone in the stratospheric ozone layer. Ozonesondes are launched regularly at many locations around the world. Local ozone-measuring instruments using optical or chemical detection schemes are also used on research aircraft to measure the distribution of ozone in the troposphere and lower stratosphere (up to altitudes of about 20 km). High-altitude research aircraft can reach the ozone layer at most locations over the globe and can reach furthest into the layer at high latitudes. Ozone measurements are also being made routinely on some commercial aircraft flights. Local measurements of the abundance of ozone at the surface are obtained at many thousands of sites over the globe, which provide hourly data critical for assessing and improving air quality throughout the world.

Remote measurements. Remote measurements of total ozone amounts and the altitude distributions of ozone are obtained by detecting ozone at large distances from the instrument. Most remote measurements of ozone rely on its unique absorption of UV radiation. Sources of UV radiation that can be used are sunlight (and reflected sunlight from the moon), lasers, and starlight. For example, satellite instruments use the absorption of solar UV radiation by the atmosphere or the absorption of sunlight scattered from the surface of Earth to measure ozone over nearly the entire globe on a daily basis. Lidar instruments, which measure backscattered laser light, are routinely deployed at ground sites and on research aircraft to detect ozone over a distance of many kilometers along the laser light path. A network of ground-based

Measuring Ozone in the Atmosphere

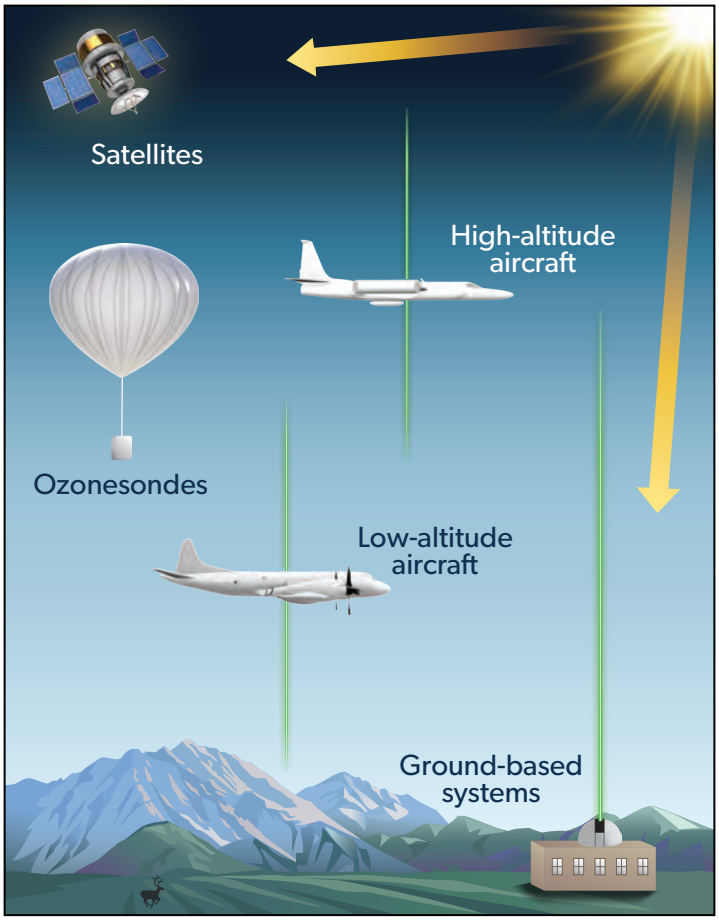

Figure Q4-1. Ozone measurements. Ozone is measured throughout the atmosphere with instruments on the ground, aircraft, high-altitude balloons, and satellites. Some instruments measure ozone locally in sampled air and others measure ozone remotely a considerable distance away from the instrument. Instruments use optical techniques with either the Sun (direct, reflected, or scattered radiation) or lasers (green lines) as light sources; detect the thermal emissions from ozone and other atmospheric molecules (not shown); or use chemical reactions that are unique to ozone (ozonesonde). At many locations over the globe, regular measurements are made to monitor ozone amounts and their variations over time.

instruments measures ozone by detecting small changes in the amount of the Sun's UV radiation that reaches Earth's surface. Other instruments measure ozone using either its absorption of infrared, visible, or ultraviolet radiation or its emission of microwave or infrared radiation at different altitudes in the atmosphere, thereby obtaining information on the vertical distribution of ozone. Emission measurements have the advantage of providing remote ozone measurements at night, which is particularly valuable for sampling polar regions during winter, when there is continuous darkness.

Global Ozone Network

The first instrument for routinely monitoring total ozone was developed by Gordon M.B. Dobson in the United Kingdom in the 1920s. The instrument, called a Féry spectrometer, made its measurements by examining the wavelength spectrum of solar ultraviolet (UV) radiation (sunlight) using a photographic plate. A small network of instruments distributed around Europe allowed Dobson to make important discoveries about how total ozone varies with location and time. In the 1930s a new instrument was developed by Dobson, now called a Dobson spectrophotometer, which precisely measures the intensity of sunlight at two UV wavelengths: one that is strongly absorbed by ozone and one that is weakly absorbed. The difference in light intensity at the two wavelengths provides a measure of the total amount of ozone above the instrument location.

A global network of total ozone observing stations was established in 1957 as part of the International Geophysical Year. Today there are hundreds of sites located around the world ranging from South Pole, Antarctica (90°S) to Ellesmere Island, Canada (83°N) that routinely measure total ozone. The Brewer spectrophotometer was introduced into the global network starting in 1982. Whereas the original Dobson instrument measures atmospheric ozone based on observations of UV light at only two wavelengths, modern Dobson instruments as well as Brewer instruments use observations from multiple pairs of wavelengths. The accuracy of these observations is maintained by regular instrument calibrations and intercomparisons. At many of the stations, observations of total ozone are augmented by measurements of the vertical distribution of ozone obtained either from twilight measurements with Dobson or Brewer instruments, by routine launches of ozonesondes, or with the use of lidar instruments. Numerous stations also quantify the atmospheric abundances of a wide variety of related compounds, taking advantage of the unique optical properties of atmospheric gases.

Data from the network have been essential for understanding the effects of chlorofluorocarbons and other ozone-depleting substances on the global ozone layer, starting before the launch of space-based ozone-measuring instruments and continuing to the present day. Ground-based instruments with excellent long-term stability and accuracy are now routinely used to help calibrate space-based observations of total ozone as well as numerous other gases and physical quantities involved in ozone chemistry.

Keeping with the tradition of naming units after pioneering scientists, the unit of measure for total ozone is called the "Dobson unit" (see Q3).

Q5 How do emissions of halogen source gases lead to stratospheric ozone depletion?

The initial step in the depletion of stratospheric ozone by human activities is the emission, at Earth's surface, of gases that contain chlorine and bromine and have long atmospheric lifetimes. Most of these gases accumulate in the lower atmosphere because they are relatively unreactive and do not dissolve readily in rain or snow. Natural air motions eventually transport these accumulated gases to the stratosphere, where they are converted to more reactive gases. Some of these gases then participate in reactions that destroy ozone. Finally, when stratospheric large-scale circulation patterns return this air to the lower atmosphere, these reactive chlorine and bromine gases are removed from Earth's atmosphere by rain and snow.

The principal steps in stratospheric ozone depletion caused by human activities are shown in **Figure Q5-1**.

Emission, accumulation, and transport. The process begins with the ***emission***, at Earth's surface, of long-lived source gases containing the halogens chlorine and bromine (see Q6). The halogen source gases, often referred to as ozone-depleting substances (ODSs), include manufactured chemicals released to the atmosphere when used in a variety of applications, such as refrigeration, air conditioning, and foam blowing. Chlorofluorocarbons (CFCs) are an important example of chlorine-containing source gases. Emitted source gases ***accumulate*** in the lower atmosphere (troposphere) and are slowly ***transported*** to the stratosphere by natural air motions. The accumulation occurs because most source gases are highly unreactive in the lower atmosphere. Furthermore, only a small amount of halogen source gases dissolve in ocean waters. The low reactivity of these manufactured halogenated gases within the lower atmosphere is one property that made them well suited for specialized applications such as refrigeration.

Some halogen gases are emitted in substantial quantities from natural sources (see Q6). These emissions also accumulate in the troposphere, are transported to the stratosphere, and participate in ozone destruction reactions. These naturally emitted gases are part of the natural balance of ozone production and destruction that predates the large release of manufactured halogenated gases and the associated observed ozone depletion.

Conversion, reaction, and removal. Halogen source gases do not react directly with ozone. Once in the stratosphere, halogen source gases are chemically ***converted*** to reactive and reservoir halogen gases by the absorption of ultraviolet radiation from the Sun (see Q7). The rate of conversion is related to the atmospheric lifetime of a gas (see Q6). Gases with longer lifetimes have slower conversion rates and survive longer in the atmosphere after emission. Lifetimes of the principal ODSs vary from about 1 to 100 years (see Table Q6-1). Emitted gas molecules with atmospheric lifetimes greater than a few decades circulate between the troposphere and stratosphere multiple times, on average, before conversion occurs.

The reactive gases formed from halogen source gases react chemically to destroy ozone in the stratosphere (see Q8). The average depletion of total ozone attributed to reactive gases is smallest in the tropics and largest at high latitudes (see Q12). In polar regions, reactions that occur on the surface of polar stratospheric clouds, which exist only at low temperatures, greatly increase the abundance of the most important reactive chlorine gas, chlorine monoxide (ClO) (see Q9). This process results in substantial ozone destruction in polar regions in late winter/early spring (see Q10 and Q11).

Air in the stratosphere is generally isolated from the troposphere. A small portion of stratospheric air returns to the troposphere every day, bringing along reactive and reservoir halogen gases. On average, it takes several years for air throughout the global stratosphere to return to the troposphere. Reactive halogen gases that are transported back to the troposphere are ***removed*** from the atmosphere by rain and other precipitation or deposited by wind onto Earth's land or ocean surfaces. These removal processes bring to an end the destruction of ozone by chlorine and bromine atoms that were first released to the atmosphere as components of halogen source gas molecules.

Tropospheric conversion. Halogen source gases with short lifetimes (less than 1 year) undergo significant chemical conversion in the troposphere, producing reactive and reservoir halogen gases. Source gas molecules that are not converted are transported to the stratosphere. Only small portions of reactive and reservoir halogen gases produced in the troposphere are transported to the stratosphere, because most are removed by precipitation. Important examples of halogen gases that undergo some tropospheric removal, prior to transport to the stratosphere, are the hydrochlorofluorocarbons (HCFCs), methyl bromide (CH_3Br), methyl chloride (CH_3Cl), and gases containing iodine (see Q6).

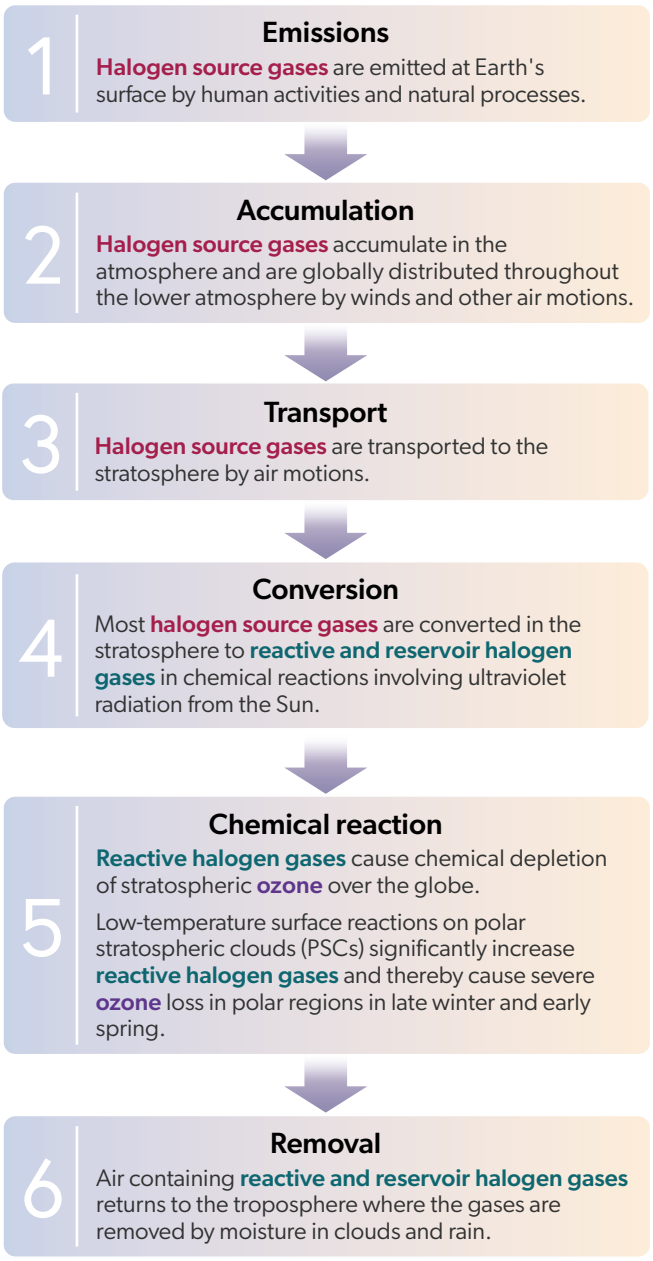

Figure Q5-1. Principal steps in stratospheric ozone depletion. The stratospheric ozone depletion process begins with the emission of halogen source gases by human activities and natural processes. These compounds have at least one carbon and one halogen atom, causing them to be chemically stable and leading to common use of the term halocarbon, an abbreviation for halogen and carbon. Many halocarbon gases emitted by human activities are also ozone-depleting substances (ODSs); all ODSs contain at least one chlorine or bromine atom (see Q7). Most of these compounds undergo little or no chemical loss within the troposphere, the lowest region of the atmosphere, and accumulate until transported to the stratosphere. Subsequent steps are the conversion of ODSs to reactive and reservoir halogen gases and chemical reactions that remove ozone (see Q8). Ozone depletion by halogen gases occurs throughout the globe (see Q12), with the largest losses occurring in the polar regions during late winter and early spring (see Q9 to Q11). Ozone depletion ends when reactive and reservoir halogen gases are removed by rain and snow in the troposphere and deposited on Earth's surface.

Understanding Stratospheric Ozone Depletion

Our understanding of stratospheric ozone depletion has been obtained through a combination of laboratory studies, computer models, and atmospheric observations. The wide variety of chemical reactions that occur in the stratosphere have been discovered and investigated in ***laboratory studies***. Chemical reactions between two gases follow well-defined physical rules. Some of these reactions occur on the surfaces of polar stratospheric clouds formed in the winter stratosphere. Reactions have been studied that involve many different molecules containing chlorine, bromine, fluorine, and iodine and other atmospheric constituents such as carbon, oxygen, nitrogen, and hydrogen. These studies have shown that several reactions involving chlorine and bromine directly or indirectly destroy ozone in the stratosphere.

Computer models have been used to examine the combined effect of the large group of known reactions that occur in the stratosphere. These models simulate the stratosphere by including representation of chemical abundances, winds, air temperatures, and the daily and seasonal changes in sunlight. These analyses show that under certain conditions chlorine and bromine react in catalytic cycles in which one chlorine or bromine atom destroys many thousands of ozone molecules. Models are also used to simulate ozone amounts observed in previous years as a strong test of our understanding of atmospheric processes and to evaluate the importance of new reactions found in laboratory studies. The response of ozone to possible future changes in the abundances of trace gases, temperatures, and other atmospheric parameters has been extensively explored with specialized computer models (see Q20).

Atmospheric observations have shown what gases are present in different regions of the stratosphere and how their abundances vary with respect to time and location. Gas and particle abundances have been monitored over time periods spanning a daily cycle to decades. Observations show that reactive halogen gases are present in the stratosphere at the amounts required to cause observed ozone depletion (see Q7). Ozone and chlorine monoxide (ClO), for example, have been observed extensively with a variety of instruments. ClO is a highly reactive gas that is involved in catalytic ozone destruction cycles throughout the stratosphere (see Q8). Instruments on the ground and on satellites, balloons, and aircraft now routinely measure the abundance of ozone and ClO remotely using optical and microwave signals. High-altitude aircraft and balloon instruments are also used to measure both gases locally in the stratosphere (see Q4). Observations of ozone and reactive gases made in past decades are used extensively in comparisons with computer models to increase confidence in our understanding of stratospheric ozone depletion.

Q6 What emissions from human activities lead to stratospheric ozone depletion?

Certain industrial processes and consumer products result in the emission of ozone-depleting substances (ODSs) to the atmosphere. Principal ODSs are manufactured halogen source gases that are now controlled worldwide by the Montreal Protocol. These gases bring chlorine and bromine atoms to the stratosphere, where they destroy ozone in chemical reactions. Important examples are the chlorofluorocarbons (CFCs), once used in almost all refrigeration and air conditioning systems, and the halons, which were used as fire extinguishing agents. Current ODS abundances in the atmosphere are known directly from air sample measurements.

Halogen source gases versus ozone-depleting substances (ODSs). Halogen source gases that are emitted by human activities and controlled by the Montreal Protocol are generally referred to as ODSs. The Montreal Protocol controls the global production and consumption of ODSs (see Q14). Halogen source gases such as methyl chloride (CH_3Cl) that have predominantly natural sources are not classified as ODSs. The contributions of various ODSs and natural halogen source gases to the total amount of chlorine and bromine entering the stratosphere are shown in **Figure Q6-1**. Total chlorine and total bromine entering the stratosphere peaked in 1993 and 1999, respectively. The difference in the timing of these peaks is a result of various phaseout schedules specified by the Montreal Protocol and its amendments and adjustments, different atmospheric lifetimes of halogen source gases, and the time delays between production and emission of the numerous source gases. Also shown are the contributions to total chlorine and bromine in 2020, highlighting the reductions of 11% and 15%, respectively, achieved by the controls of the Montreal Protocol.

Ozone-depleting substances (ODSs). The principal ODSs are manufactured for specific industrial uses or consumer products, most of which result in the eventual emission of these gases to the atmosphere. Total ODS emissions increased substantially from the middle to the late 20th century, reached a peak in the late 1980s, and are now in decline (see Figure Q0-1). Because of their long atmospheric lifetimes, a large fraction of the emitted ODSs reach the stratosphere, where they are converted to reactive and reservoir gases containing chlorine and bromine that lead to ozone depletion.

ODSs containing only chlorine, fluorine, and carbon are called ***chlorofluorocarbons***, usually abbreviated as CFCs. The principal CFCs are CFC-11 (CCl_3F), CFC-12 (CCl_2F_2), and CFC-113 (CCl_2FCClF_2). CFCs, along with carbon tetrachloride (CCl_4) and methyl chloroform (CH_3CCl_3), historically have been the most important chlorine-containing halogen source gases emitted by human activities. These and other chlorine-containing ODSs have been used in many applications, including refrigeration, air conditioning, foam blowing, spray can propellants, and cleaning of metals and electronic components. As a result of the Montreal Protocol controls, the abundances of these chlorine source gases have decreased since 1993 (see Figure Q6-1). The abundances of CFC-11 and CFC-12 in 2020 were 16% and 2.8% lower than their values in 1993, respectively.

The class of compounds known as ***hydrochlorofluorocarbons*** (HCFCs) contain hydrogen, in addition to chlorine, fluorine, and carbon. HCFC-22 (CHF_2Cl), developed in the 1930s, has been used as a refrigerant, primarily in residential air conditioners, since the 1940s. As detailed below, HCFCs are less harmful to the ozone layer compared to CFCs. In the 1990s, the use of HCFC-22 expanded and other HCFCs were developed as substitutes for CFCs. Consequently, the chlorine content of HCFCs entering the stratosphere increased by 185% between 1993 and 2020 (see Figure Q6-1). With restrictions on production starting in 1996, and globally in place since 2013, the atmospheric abundances of HCFCs are expected to peak between 2023 and 2030 (see Figures Q0-1 and Q15-1). Classes of compounds known as hydrofluorocarbons (HFCs) and hydrofluoroolefins (HFOs) constitute the replacement for many applications of HCFCs.

Another category of ODSs contains bromine. The most important of these gases are the halons and methyl bromide (CH_3Br). Halons are a group of industrial compounds that contain at least one bromine and one carbon atom; halons may or may not contain a chlorine atom. Halons were originally developed to extinguish fires and were widely used to protect large computer installations, military hardware, and commercial aircraft engines. Consequently, halons are often released directly into the atmosphere upon use or testing of these fire suppression systems. The most abundant halons emitted by human activities are halon-1211 ($CBrClF_2$) and halon-1301 ($CBrF_3$). Methyl bromide is used primarily as a fumigant for pest control in agriculture and disinfection of export shipping goods, and also has significant natural sources.

As a result of the controls of the Montreal Protocol, the contribution to the atmospheric abundance of methyl bromide from human activities decreased by 71% between 1999 and 2020 (see Figure Q6-1). The concentration of halon-1211 peaked in 2005 and has been decreasing ever since, reaching an abundance in 2020 that was 22% below that measured in 1999. The abundance of halon-1301, on the other hand, increased by 19% since 1999 and is expected to slowly decline into the next decade because

Halogen Source Gases Entering the Stratosphere

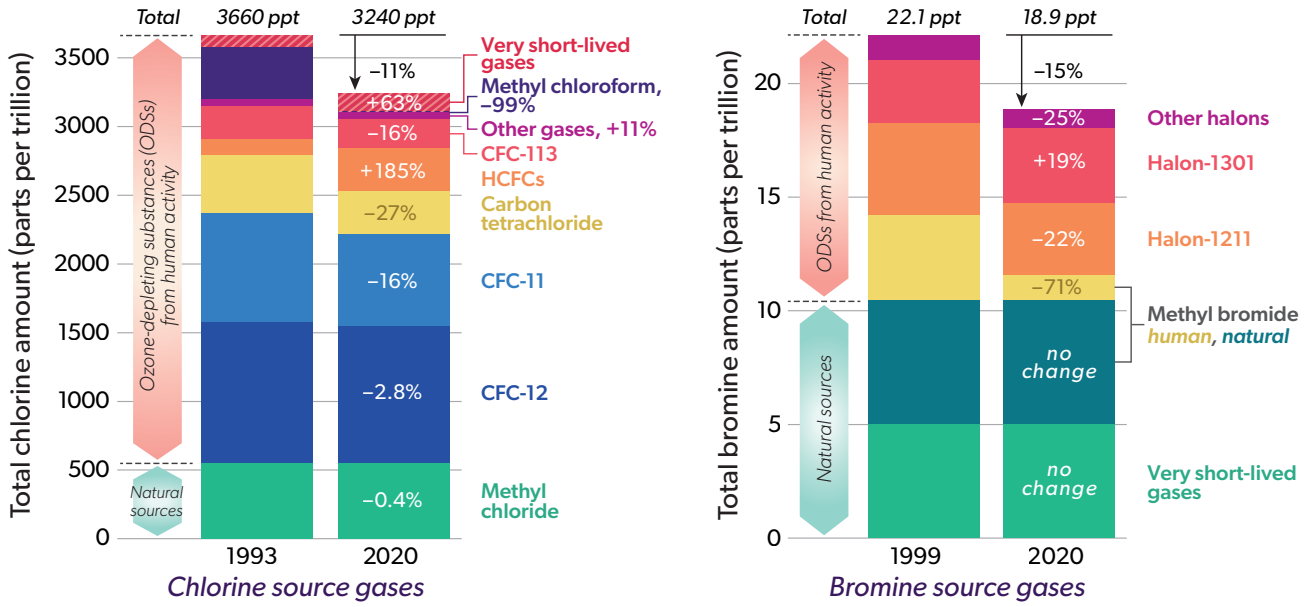

Figure Q6-1. Changes in halogen source gases entering the stratosphere. A variety of halogen source gases emitted by human activities and natural processes transport chlorine and bromine into the stratosphere. Ozone-depleting substances (ODSs) are the subset of these gases emitted by human activities that are controlled by the Montreal Protocol. These partitioned columns show the abundances of chlorine- and bromine-containing gases entering the stratosphere in 1993 and 1999, when their total amounts peaked, respectively, and in 2020. The overall reductions in the total amounts of chlorine and bromine entering the stratosphere and the changes observed for each source gas are also indicated. The amounts are derived from tropospheric observations of each gas. Note the large difference in the vertical scales: total chlorine entering the stratosphere is about 150 times greater than total bromine. Both, however, are important because bromine is about 60 times more effective on a per-atom basis than chlorine at destroying ozone. Human activities are the largest source of chlorine reaching the stratosphere and CFCs are the most abundant chlorine-containing gases. Methyl chloride is the primary natural source of chlorine. The largest decreases between 1993 and 2020 are seen in methyl chloroform, carbon tetrachloride, and CFC-11. The abundance of HCFCs, which are substitute gases for CFCs and also controlled under the Montreal Protocol, have risen substantially since 1993 and have approached expected peak atmospheric abundances (see Figure Q15-1). The abundance of chlorine-containing very short-lived gases entering the stratosphere has risen substantially since 1993; these compounds originate primarily from human activity, undergo chemical loss within the troposphere, and are not controlled by the Montreal Protocol. Halons and methyl bromide are the largest contributors to bromine entering the stratosphere. The largest decrease between 1999 and 2020 is seen in the abundance of methyl bromide attributed to human activities, because of the success of the Montreal Protocol. Halon-1301 is the only brominated ODS showing an increased abundance relative to 1999. Methyl bromide also has a natural source, which is now substantially greater than the human source due to the success of the Montreal Protocol. Natural sources, which make a much larger fractional contribution to bromine entering the stratosphere than occurs for chlorine, have remained fairly constant in the recent past.

(The unit "parts per trillion" is used here as a measure of the relative abundance of a substance in dry air: 1 part per trillion equals the presence of one molecule of a gas per trillion (=10^{12}) total air molecules.)

of continued small releases and a long atmospheric lifetime (see Figure Q15-1). In 2020, the bromine content of other halons (mainly halon-1202 and halon-2402) was 25% below the amount present in 1999.

Natural sources of chlorine and bromine. There are a few halogen source gases present in the stratosphere that have large natural sources. These include methyl chloride (CH_3Cl) and methyl bromide (CH_3Br), both of which are emitted by oceanic and terrestrial ecosystems. In addition, very short-lived source gases (defined as compounds with atmospheric lifetimes typically less than 0.5 year) containing bromine such as bromoform ($CHBr_3$) and dibromomethane (CH_2Br_2) are also released to the atmosphere, primarily from biological activity in the oceans. Only a fraction of the emissions of very short-lived source gases reaches the stratosphere because these gases are efficiently removed in the lower atmosphere. Volcanoes provide an episodic source of reactive halogen gases that sometimes reach the stratosphere in appreciable quantities.

Other natural sources of halogens include reactive chlorine and bromine produced by evaporation of ocean spray. However, these

reactive chemicals play no role in stratospheric ozone depletion because they readily dissolve in water and are removed in the troposphere.

In 2020, natural sources contributed about 17% of total stratospheric chlorine and about 56% of total stratospheric bromine (see Figure Q6-1). The amount of chlorine and bromine entering the stratosphere from natural sources is known to be fairly constant over time and, therefore, cannot be the cause of the ozone depletion observed since the 1980s.

Other human activities that are sources of chlorine and bromine gases. Other chlorine- and bromine-containing gases are released to the atmosphere from human activities. Common examples are the use of chlorine-containing solvents and industrial chemicals, and the use of chlorine gases in paper production and disinfection of potable and industrial water supplies (including swimming pools). Most of these gases are very short-lived and only a small fraction of their emissions reaches the stratosphere. The contribution of very short-lived chlorinated gases from natural sources and human activities to total stratospheric chlorine was 63% larger in 2020 than in 1993, and now contributes about 4% (130 ppt) of the total chlorine entering the stratosphere (see Figure Q6-1). The Montreal Protocol does not control the production and consumption of very short-lived chlorine source gases, although the atmospheric abundances of some (notably dichloromethane, CH_2Cl_2) have increased substantially in recent years. Solid rocket engines, such as those used to propel payloads into orbit, release reactive chlorine gases directly into the troposphere and stratosphere. The quantities of chlorine emitted globally by rockets is currently small in comparison with halogen emissions from other human activities.

Lifetimes and emissions. Estimates of global emissions in 2020 for a selected set of halogen source gases are given in **Table Q6-1**. These emissions occur from continued production of HCFCs and HFCs as well as the release of gases from banks. Emission from ***banks*** refers to the atmospheric release of halocarbons from existing equipment, chemical stockpiles, foams, and other products. In 2020 the global emission of the refrigerant HCFC-22 constituted the largest annual release, by mass, of a halocarbon from human activities. Release in 2020 of HFC-134a (CH_2FCF_3), another refrigerant, was second largest. The emission of methyl chloride (CH_3Cl) is primarily from natural sources such as the ocean biosphere, terrestrial plants, salt marshes and fungi. The human source of methyl chloride is small relative to the total natural source (see Q15).

After emission, halogen source gases are either removed from the atmosphere or undergo chemical conversion in the troposphere, stratosphere, or mesosphere. The time to remove or convert about 63% of a gas is often called its atmospheric lifetime. Lifetimes vary from less than 1 year to 100 years for the principal chlorine- and bromine-containing gases (see Table Q6-1). The long-lived gases are converted to other gases primarily in the stratosphere and essentially all of their original halogen content becomes available to participate in the destruction of stratospheric ozone. Conversely, gases with short lifetimes such as methyl bromide, methyl chloride, and some HCFCs are converted to other gases in the troposphere, which are then removed from the atmosphere by rain and snow. Therefore, only a fraction of their halogen content contributes to ozone depletion in the stratosphere. Methyl chloride, despite its large source, constituted only about 17% (540 ppt) of the halogen source gases entering the stratosphere in 2020 (see Figure Q6-1).

The amount of an emitted gas that is present in the atmosphere represents a balance between its emission and removal rates. A wide range of current emission rates and atmospheric lifetimes are derived for the various source gases (see Table Q6-1). The atmospheric abundances of most of the principal CFCs and halons have decreased since 1990 in response to smaller emission rates, while those of the important substitute gases, the HCFCs, continue to slowly increase under the provisions of the Montreal Protocol (see Q15). In the past few years, the rate of the increase of the atmospheric abundance of HCFCs has declined. In the coming decades, the emissions and atmospheric abundances of all controlled ODSs are expected to decrease under these provisions.

Ozone Depletion Potential (ODP). The effectiveness of halogen source gases at destroying stratospheric ozone is given by the ODP (see Table Q6-1 and Q17). A gas with a larger ODP destroys more stratospheric ozone than a gas with a smaller ODP. The calculation of ODP requires the use of computer models that simulate atmospheric ozone and is found relative to CFC-11, which has an ODP defined to be 1. The ODP of a gas is based upon a comparison of the amount of ozone depletion caused by the continuous emission to the atmosphere of a certain mass of that gas, relative to the amount of ozone depletion following emission of the same mass of CFC-11. Halogen source gases controlled by the Montreal Protocol have a wide range of ODPs. Halon-1211 and halon-1301 have ODPs significantly larger than that of CFC-11 and most other chlorinated gases because bromine is much more effective (about 60 times) on a per-atom basis than chlorine in chemical reactions that destroy ozone. The gases with smaller values of ODP generally have shorter atmospheric lifetimes or contain fewer chlorine and bromine atoms compared to gases with larger ODPs.

HFCs & other fluorine-containing gases. Many of the source gases in Figure Q6-1 also contain fluorine, another halogen, in addition to chlorine or bromine. After the source gases undergo conversion in the stratosphere (see Q5), the fluorine content of these gases is left in chemical forms that do not cause ozone depletion. As a consequence, halogen source gases that contain fluorine and no other halogens are not classified as ODSs. An important example of these are the HFCs, which are included in Table Q6-1 because they are common ODS substitute gases. HFCs do not contain chlorine or bromine and, consequently, all HFCs have an ODP of zero.

Many HFCs are strong greenhouse gases, as quantified by a metric termed the Global Warming Potential (GWP) (see Q17). The Kigali Amendment to the Montreal Protocol now controls the production and consumption of HFCs (see Q19), especially those HFCs with high GWPs. As a result, industry has transitioned in part to production and use of a subset of HFCs with very low GWPs known as hydrofluoroolefins (HFOs), which are also composed of hydrogen, fluorine, and carbon atoms. Here, the "O" stands for olefin, a term used by chemists to refer to the double carbon bond of these compounds that results in small tropospheric lifetimes and GWPs for HFOs. One such HFO, HFO-1234yf (CF_3CFCH_2), has a GWP of less than 1 due to its 12 day lifetime.

Iodine containing gases. Iodine is a component of several gases that are naturally emitted from the oceans and from some human activities. Research on the importance of iodine for stratospheric ozone is being conducted, in part, because trifluoroiodomethane (CF_3I) is a possible replacement for halons in fire extinguishers and also because CF_3I has been proposed as an ingredient of low-GWP refrigerant blends. Although iodine can participate in ozone destruction reactions, iodine-containing source gases all have very short lifetimes, with most of the removal occurring in the lower atmosphere within a few days. Since the last assessment, there has been an upward revision to the upper limit on the amount of iodine reaching the stratosphere, which is now estimated to be about 1 ppt. The importance for stratospheric ozone of very short-lived iodine containing source gases, including a possible enhancement of polar ozone depletion, remains an active area of investigation.

Other non-halogen gases. Other non-halogen gases that influence stratospheric ozone abundances have also increased in the stratosphere as a result of emissions from human activities (see Q20). Important examples are methane (CH_4), which reacts in the stratosphere to form water vapor and reactive hydrogen, and nitrous oxide (N_2O), which reacts in the stratosphere to form nitrogen oxides. These reactive products participate in the destruction of stratospheric ozone. Increased levels of atmospheric carbon dioxide (CO_2) alter stratospheric temperature and winds, which also affect the abundance of stratospheric ozone. Should future atmospheric abundances of CO_2, CH_4, and N_2O increase significantly relative to present-day values, these increases will affect future levels of stratospheric ozone through combined effects on temperature, winds, and chemistry (see Figure Q20-2). Efforts are underway to reduce the emissions of these gases under the Paris Agreement of the United Nations Framework Convention on Climate Change because they cause surface warming (see Q18 and Q19). Although past emissions of ODSs still dominate global ozone depletion today, future emissions of N_2O from human activities are expected to become relatively more important for ozone depletion as the atmospheric abundances of ODSs decline (see Q20).

Table Q6-1. Atmospheric lifetimes, global emissions, Ozone Deletion Potentials, and Global Warming Potentials of some halogen source gases and HFC substitute gases.

Gas	Atmospheric Lifetime (years)	Global Emissions in 2020 (kt/yr)[a]	Ozone Depletion Potential (ODP)[b]	Global Warming Potential (GWP)[b]
Halogen Source Gases				
Chlorine Gases				
CFC-11 (CCl_3F)	52	36 – 58	1	6410
Carbon tetrachloride (CCl_4)	30	27 – 60	0.87	2150
CFC-113 (CCl_2FCClF_2)	93	1 – 13	0.82	6530
CFC-12 (CCl_2F_2)	102	3 – 48	0.75	12,500
Methyl chloroform (CH_3CCl_3)	5.0	1 – 3	0.12	164
HCFC-141b (CH_3CCl_2F)	8.8	48 – 67	0.102	808
HCFC-142b (CH_3CClF_2)	17	15 – 23	0.057	2190
HCFC-22 (CHF_2Cl)	12	284 – 403	0.038	1910
Methyl chloride (CH_3Cl)	0.9	3759 – 5677	0.015	6
Bromine Gases				
Halon-1301 ($CBrF_3$)	72	1 – 2	17	7430
Halon-1211 ($CBrClF_2$)	16	1 – 5	7.1	1990
Methyl bromide (CH_3Br)	0.8	111 – 154	0.57	2
Hydrofluorocarbons (HFCs)				
HFC-23 (CHF_3)	228	16 – 18	0	14,700
HFC-143a (CH_3CF_3)	52	27 – 33	0	5900
HFC-125 (CHF_2CF_3)	31	78 – 98	0	3820
HFC-134a (CH_2FCF_3)	14	216 – 275	0	1470
HFC-32 (CH_2F_2)	5.3	56 – 77	0	749
HFC-152a (CH_3CHF_2)	1.5	41 – 63	0	153
HFO-1234yf (CF_3CFCH_2)	0.03	not available	0	less than 1

[a] Includes both human activities (production and banks) and natural sources. Emissions are in units of kilotonnes per year (1 kilotonne = 1000 metric tons = 1 gigagram = 10^9 grams). These emission estimates are based on analysis of atmospheric observations. The range of values for each emission estimate reflects the uncertainty in estimating emissions from atmospheric observations.

[b] 100-year GWP. ODPs and GWPs are discussed in Q17. Values are calculated for emissions of an equal mass of each gas. ODPs given here reflect current scientific values and in some cases differ from those used in the Montreal Protocol.

Q7 What are the reactive halogen gases that destroy stratospheric ozone?

Chlorine and bromine containing halogen source gases that enter the stratosphere arise from both human activities and natural processes (Q6). When exposed to ultraviolet radiation from the Sun, these halogen source gases are converted to other gases that also contain chlorine and bromine. Some of the gases act as chemical reservoirs, which can then be converted into ClO and BrO, the two most important reactive gases that participate in catalytic reactions that destroy ozone.

Halogen-containing gases present in the stratosphere can be divided into two groups: ***halogen source gases*** as well as ***reactive and reservoir halogen gases*** (see **Figure Q7-1**). The source gases, which include ozone-depleting substances (ODSs), are emitted at Earth's surface by natural processes and by human activities (see Q6) and are chemically inert in the lower atmosphere. Once in the stratosphere, the halogen source gases chemically convert at different rates to form the reactive and reservoir halogen gases. The conversion occurs in the stratosphere instead of the troposphere because solar ultraviolet (UV) radiation (a component of sunlight) is needed for the breakup of these compounds, and solar UV radiation is more intense in the stratosphere than the troposphere (see Q2). Reactive gases containing the halogens chlorine and bromine participate in a series of chemical reactions that remove stratospheric ozone (see Q8).

Reactive and reservoir halogen gases. The chemical conversion of halogen source gases, which involves solar ultraviolet radiation and other chemical reactions, produces a number of reactive and reservoir halogen gases. These reactive and reservoir gases contain all of the chlorine and bromine atoms originally present in the source gases. The chlorine content of all of the reactive and reservoir gases is termed ***available chlorine***, while the bromine content of similar gases is termed ***available bromine***.

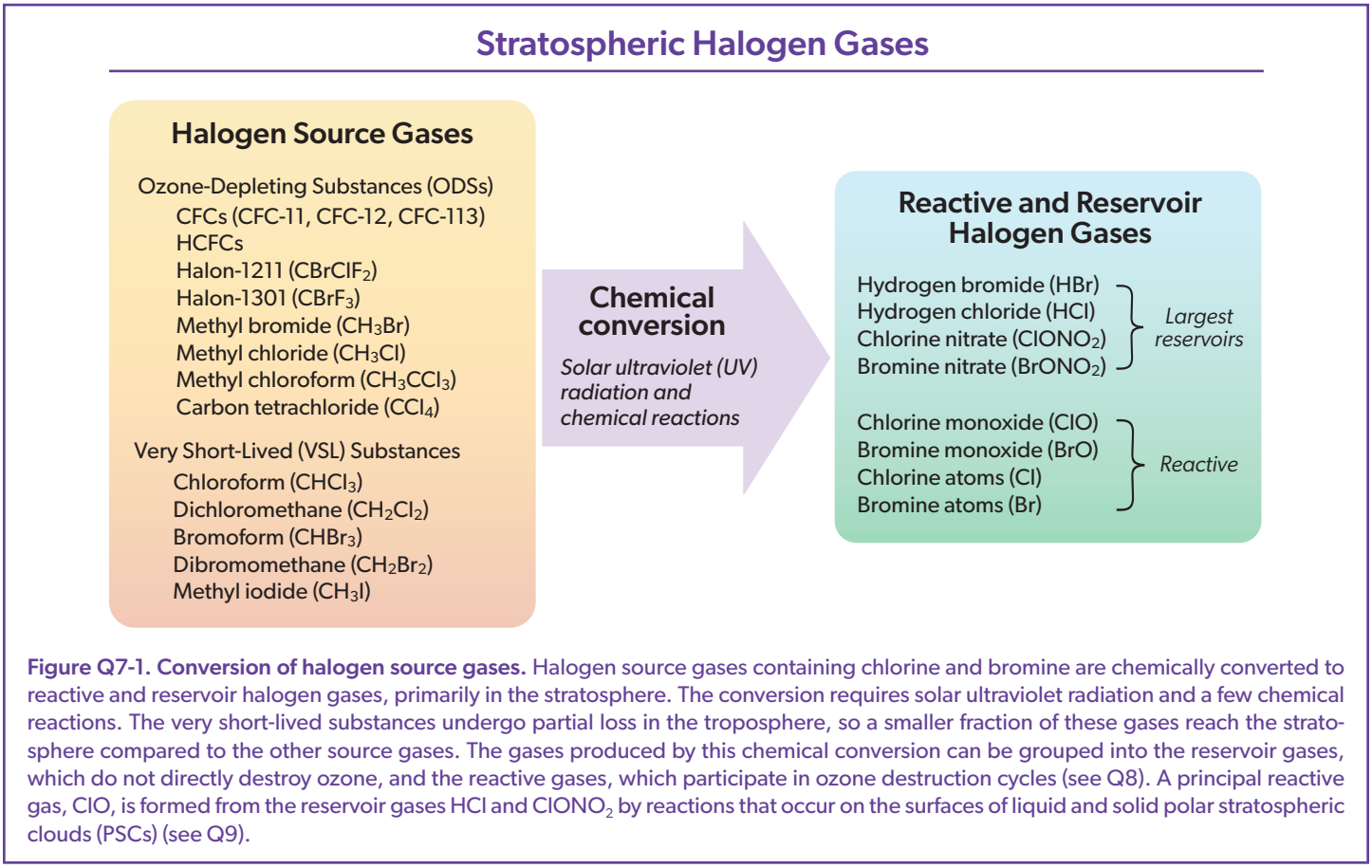

Figure Q7-1. Conversion of halogen source gases. Halogen source gases containing chlorine and bromine are chemically converted to reactive and reservoir halogen gases, primarily in the stratosphere. The conversion requires solar ultraviolet radiation and a few chemical reactions. The very short-lived substances undergo partial loss in the troposphere, so a smaller fraction of these gases reach the stratosphere compared to the other source gases. The gases produced by this chemical conversion can be grouped into the reservoir gases, which do not directly destroy ozone, and the reactive gases, which participate in ozone destruction cycles (see Q8). A principal reactive gas, ClO, is formed from the reservoir gases HCl and $ClONO_2$ by reactions that occur on the surfaces of liquid and solid polar stratospheric clouds (PSCs) (see Q9).

The most important reactive and reservoir chlorine and bromine containing gases that form in the stratosphere are shown in Figure Q7-1. Throughout the stratosphere, the most abundant are typically hydrogen chloride (HCl) and chlorine nitrate ($ClONO_2$). These two gases are considered *reservoir* gases because, while they do not react directly with ozone, they can be converted to the most reactive forms that do chemically destroy ozone. The halogens most reactive with ozone are chlorine monoxide (ClO) and bromine monoxide (BrO) molecules, as well as chlorine and bromine (Cl and Br) atoms. A large fraction of available bromine is generally in the form of BrO, whereas usually only a small fraction of available chlorine is in the form of ClO. The unusually cold conditions that occur in the polar regions during winter cause the reservoir gases HCl and $ClONO_2$ to undergo nearly complete conversion to ClO and related reactive gases. This conversion occurs through chemical reactions that take place on the surface or within polar stratospheric cloud (PSC) particles (see Q9).

Chlorine at midlatitudes. Reactive and reservoir chlorine gases have been observed extensively in the stratosphere using both local and remote measurement techniques, including observations from satellite instruments. The measurements from space displayed in **Figure Q7-2** are representative of how the amounts of chlorine-containing gases change between the surface and the upper stratosphere at middle to high latitudes. Total chlorine (see red line in Figure Q7-2) is the sum of chlorine contained in halogen source gases (e.g., CFC-11, CFC-12) and in the reservoir and reactive gases (e.g., HCl, $ClONO_2$, and ClO). Total chlorine is constant to within about 10% from the surface to above 50 km (31 miles) altitude. In the troposphere, total chlorine is contained almost entirely in the source gases described in Figure Q6-1. At higher altitudes, the source gases become a smaller fraction of total chlorine as they are converted to the reactive and reservoir chlorine gases. At the highest altitudes, total chlorine is all in the form of reactive and reservoir chlorine gases.

In the altitude range of the ozone layer at midlatitudes, as shown in Figure Q7-2, the reservoir gases HCl and $ClONO_2$ account for most of the available chlorine. The abundance of ClO, the most important reactive gas in ozone depletion, is a small fraction of total chlorine. The abundance of ClO peaks in the upper stratosphere about 40 km (24.9 miles) above the surface. In this region of the atmosphere the abundance of ozone reached a minimum in the late 1990s, at about the time the abundance of ClO in the upper stratosphere maximized. In the lower and middle stratosphere (altitudes below about 30 km, or 18.6 miles above the surface), the low abundance of ClO tends to limit the amount of ozone destruction that occurs outside of polar regions.

Chlorine in polar regions. Chlorine gases in polar regions undergo large changes between autumn and late winter. Meteorological and chemical conditions in both polar regions are now routinely observed from space in all seasons. Maps of autumn and late winter conditions at an altitude of 18 km (11.2 miles), near the center of the ozone layer (see Figure Q11-3) over the Antarctic are contrasted in **Figure Q7-3**. These observations document dramatic differences in chemistry and temperature for these two seasons.

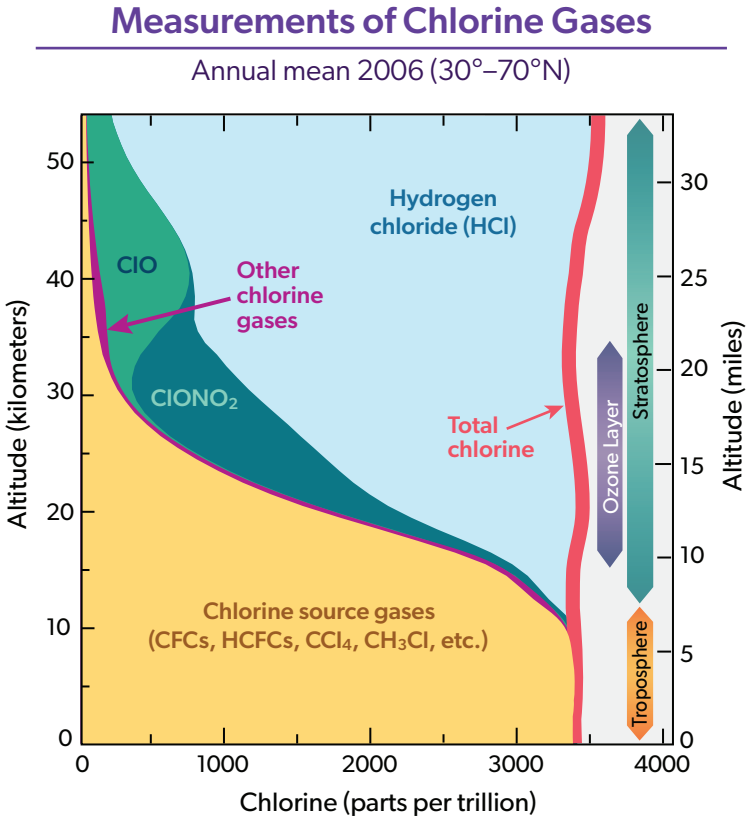

Figure Q7-2. Chlorine gas observations. The abundances of chlorine source gases as well as reactive and reservoir chlorine gases as measured in 2006, averaged over 30° to 70°N latitude, are displayed as a function of altitude. In the troposphere (below about 12 km), all of the measured chlorine is contained in the source gases. In the stratosphere, the total chlorine content of reactive and reservoir gases (termed available chlorine) increases with altitude as the amount of chlorine source gases declines. This transition is a consequence of chemical reactions initiated by solar ultraviolet radiation that convert source gases to available chlorine (see Figure Q7-1). The principal reactive and reservoir chlorine gases formed are HCl, $ClONO_2$, and ClO. Adding up the source gases with available chlorine gives "Total chlorine", which is nearly constant with altitude throughout the atmosphere. In the midlatitude ozone layer (15–35 km), chlorine source gases are still present and HCl and $ClONO_2$ constitute the most abundant forms of available chlorine.

(The unit "parts per trillion" is defined in the caption of Figure Q6-1.)

Ozone values are high over the entire Antarctic continent during autumn in the Southern Hemisphere. Temperatures are mid-range, HCl and nitric acid (HNO_3) are high, and ClO is very low. High HCl indicates that substantial conversion of halogen source gases to this reservoir gas has occurred in the stratosphere. In the 1980s and early 1990s, the abundances of the reservoir gases HCl and $ClONO_2$ increased substantially in the stratosphere following increased emissions of halogen source gases. HNO_3 is an abundant, primarily naturally-occurring stratospheric compound that plays a major role in stratospheric ozone chemistry by both moderating ozone destruction and condensing to form polar stratospheric clouds (PSCs), thereby enabling conversion of chlorine reservoirs gases to ozone-destroying forms (see Q9). The low abundance of ClO indicates that little conversion of the reservoir to reactive gases occurs in autumn, thereby limiting chemical ozone destruction.

By late winter (September), a remarkable change in the composition of the Antarctic stratosphere has taken place. Low amounts of ozone reflect substantial depletion at 18 km altitude over an area larger than the Antarctic continent. Antarctic ozone holes arise from similar chemical destruction throughout much of the altitude range of the ozone layer (see altitude profile in Figure Q11-3). The meteorological and chemical conditions in late winter, characterized by very low temperatures, very low HCl and HNO_3, and very high ClO, are distinctly different from those found in autumn. Low stratospheric temperatures occur during winter, when solar heating is reduced. Low HCl and high ClO reflect the conversion of the halogen reservoir compounds, HCl and $ClONO_2$, to the most important reactive form of chlorine, ClO. This conversion occurs selectively in winter on PSCs, which form at very low temperatures (see Q9). Low HNO_3 is indicative of its condensation to form these PSCs, some of which subsequently fall to lower altitudes through gravitational settling. High abundances of ClO generally cause ozone depletion to continue in the Antarctic region until mid-October (spring), when the lowest ozone values usually are observed (see Q10). As temperatures rise at the end of the winter, PSC formation is halted, ClO is converted back into the reservoir species HCl and $ClONO_2$ (see Q9), and ozone destruction is curtailed.

Similar changes in meteorological and chemical conditions are also observed between autumn and late winter for some years in the Arctic, leading to substantial ozone loss. In spring of 2020, Arctic ozone reached exceptionally low values. A very stable, cold, and long-lived stratospheric Arctic vortex enabled halogen-catalyzed chemical ozone loss that exceeded the previous record-breaking loss observed in spring 2011 (see Q11). Substantial chemical loss of Arctic ozone will continue to occur in cold winters/springs, as long as the concentrations of ODSs are well above natural levels.

Bromine observations. Fewer measurements are available for reactive and reservoir bromine gases in the lower stratosphere than for chlorine gases. This difference arises in part because of the lower abundance of bromine, which makes quantification of its atmospheric abundance more challenging. The most widely observed bromine gas is BrO, which can be observed from space. Estimates of the concentration of available bromine in the stratosphere are higher than expected from the decomposition of halons and methyl bromide, the most important bromine source gases that are produced by human activities. This difference was the first direct evidence that very short-lived (VSL) bromine-containing source gases reach the stratosphere. Subsequently, direct observations of VSL source gases have confirmed their importance. In 2020, slightly more than one-quarter of the total stratospheric bromine is supplied by these naturally occurring, VSL source gases (see Q6).

Figure Q7-3. Chemical conditions in the ozone layer over Antarctica. Observations of the chemical conditions in the Antarctic region highlight the changes associated with the formation of the ozone hole. Satellite instruments routinely monitor ozone, reactive and reservoir chlorine gases, and temperatures in the global stratosphere. Satellite observations are shown here for autumn (May) and late winter (September) seasons in the Antarctic region, for a narrow altitude region near 18 km (11.2 miles) within the ozone layer (see Figure Q11-3). Ozone over Antarctica has naturally high values in autumn, before the onset of ozone destruction reactions that drive widespread depletion. The high ozone is accompanied by moderate temperatures, large values of the reservoir gases HCl and HNO_3, and very low amounts of reactive ClO. When the abundance of ClO is low, significant ozone destruction from halogens does not occur. Chemical conditions are quite different in late winter when ozone undergoes severe depletion. Temperatures are much lower, HCl has been converted to ClO (the most important reactive chlorine gas), and HNO_3 has been removed by the gravitational settling of polar stratospheric cloud particles. The abundance of ClO closely surrounding the South Pole is low in September because formation of ClO requires sunlight, which is still gradually returning to the most southerly latitudes. The high values of ClO in late winter cover an extensive area that at times exceeds that of the Antarctic continent and can last for several months, leading to efficient destruction of ozone in sunlit regions in late winter/early spring. Ozone typically reaches its minimum values in early to mid-October (see Q11). Note that the first and last colors in the color bar represent values outside the indicated range of values.

(The unit "parts per billion," abbreviated "ppb," is used here as a measure of the relative abundance of a substance in dry air: 1 part per billion equals the presence of one molecule of a gas per billion ($=10^9$) total air molecules (compare to ppt in Figure Q6-1).)

Chemical Conditions Observed in the Ozone Layer Over Antarctica

Normal ozone amounts in autumn (1 May 2021) at 18 km altitude

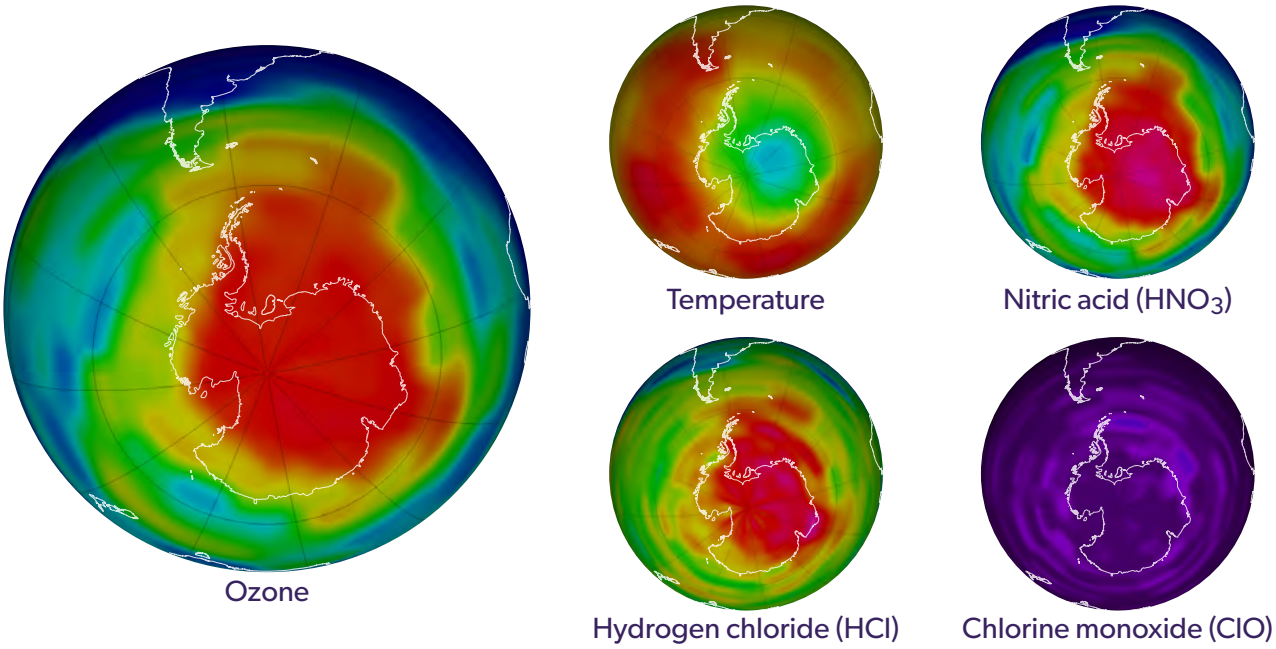

Large ozone depletion in late winter (15 September 2021) at 18 km altitude

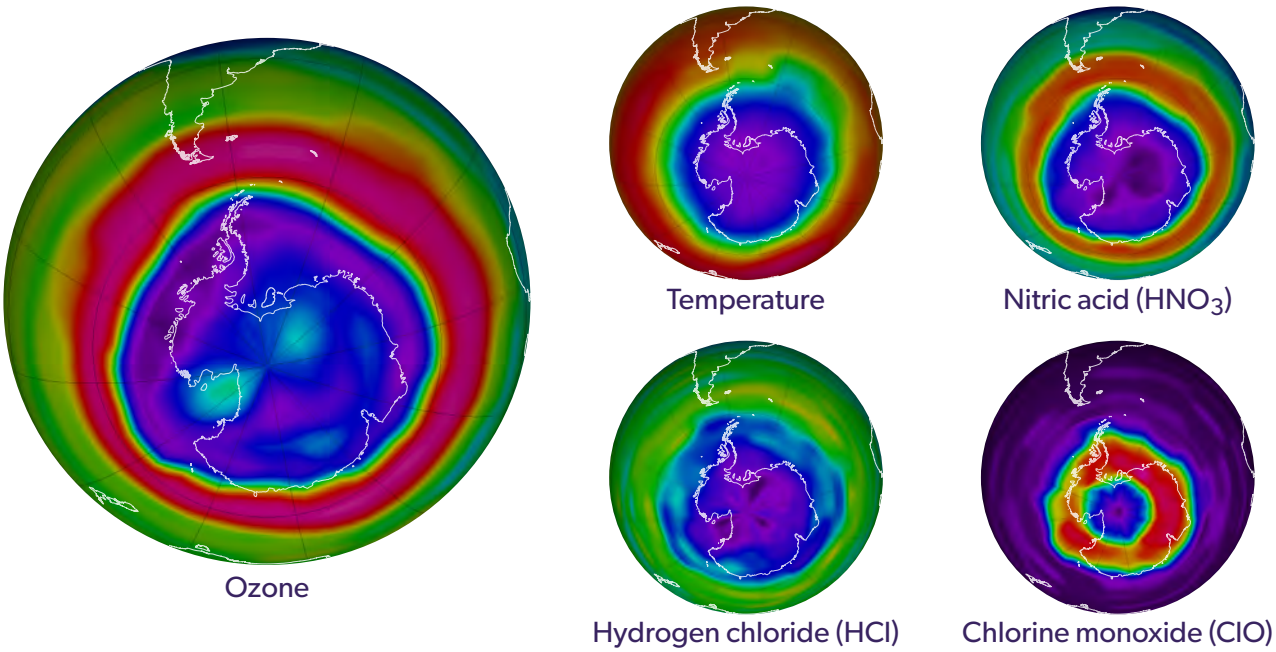

Temperatures and chemical abundances

Low		High
750	Ozone	3600 ppb
−95°	Temperature	−50° C
0.0	HNO_3	12.0 ppb
0.0	HCl	2.2 ppb
0.0	ClO	2.2 ppb

Q8 What are the chlorine and bromine reactions that destroy stratospheric ozone?

Reactive gases containing chlorine and bromine destroy stratospheric ozone in "catalytic" cycles made up of two or more separate reactions. As a result, a single chlorine or bromine atom can destroy many thousands of ozone molecules before it leaves the stratosphere. In this way, a small amount of reactive chlorine or bromine has a large impact on the ozone layer. A special situation develops in polar regions in the late winter/early spring season, where large enhancements in the abundance of the most important reactive gas, chlorine monoxide, lead to severe ozone depletion.

Stratospheric ozone is destroyed by reactions involving reactive halogen gases, which are produced in the chemical conversion of halogen source gases (see Figure Q7-1). The most reactive of these gases are chlorine monoxide (ClO), bromine monoxide (BrO), and chlorine and bromine atoms (Cl and Br). These gases participate in three principal reaction cycles that destroy ozone.

Cycle 1. Ozone destruction Cycle 1 is illustrated in **Figure Q8-1**. The cycle is made up of two basic reactions: ClO + O and Cl + O_3. The net result of Cycle 1 is to convert one ozone molecule and one oxygen atom into two oxygen molecules. In each cycle, chlorine acts as a *catalyst* because ClO and Cl react and are reformed. In this way, one Cl atom participates in many cycles, destroying many ozone molecules. For typical stratospheric conditions at middle or low latitudes, a single chlorine atom can destroy thousands of ozone molecules before it happens to react with another gas, breaking the catalytic cycle. During the total time of its stay in the stratosphere, a chlorine atom can thus destroy many thousands of ozone molecules.

Polar Cycles 2 and 3. The abundance of ClO is greatly increased in polar regions during late winter and early spring, relative to other seasons, as a result of reactions on the surfaces of polar stratospheric clouds (see Q7 and Q9). Cycles 2 and 3 (see **Figure Q8-2**)

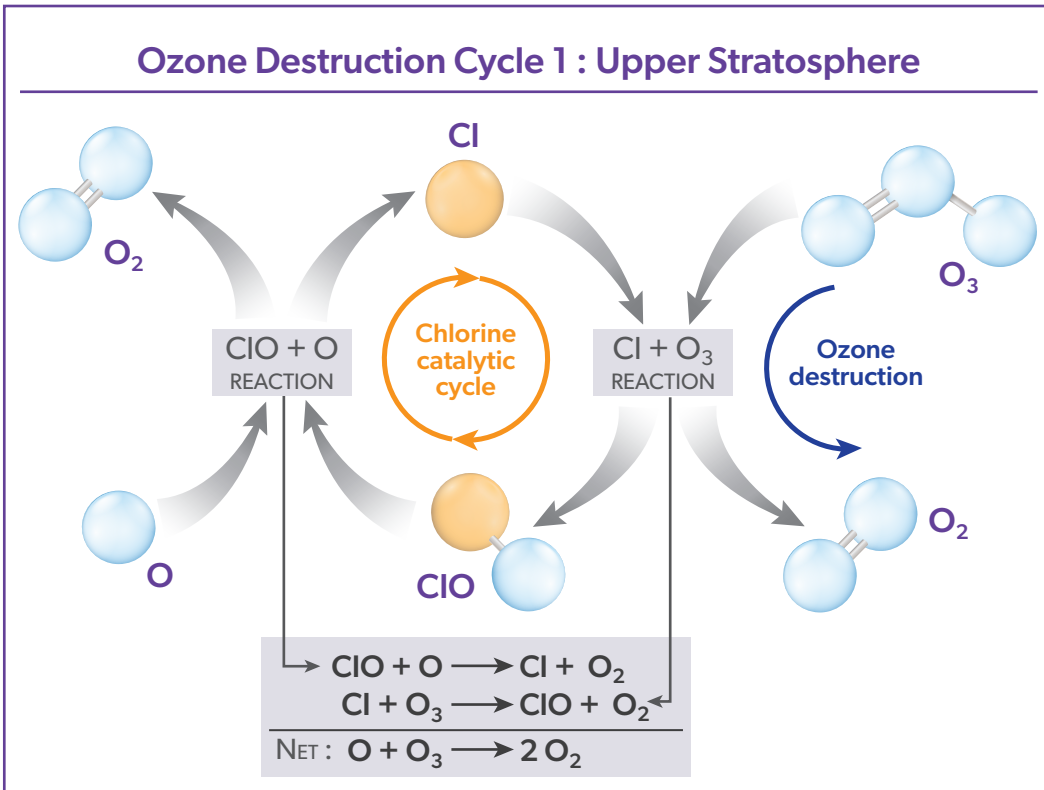

Figure Q8-1. Ozone destruction Cycle 1. The destruction of ozone in Cycle 1 involves two separate chemical reactions. The cycle can be considered to begin with either ClO or Cl. When starting with ClO, the first reaction is ClO with O to form Cl and O_2. Then, Cl reacts with O_3 and reforms ClO, consuming O_3 in the process and forming another O_2. The net or overall reaction is that of atomic oxygen (O) with ozone (O_3), forming two oxygen molecules (O_2). The cycle then begins again with another reaction of ClO with O. Chlorine is considered a catalyst for ozone destruction because Cl and ClO are reformed each time the reaction cycle is completed, and hence available for further destruction of ozone. Atomic oxygen is formed when solar ultraviolet (UV) radiation reacts with O_3 and O_2 molecules (see Figure Q1-3). Cycle 1 is most important in the stratosphere at tropical and middle latitudes, where solar UV radiation is most intense.

Ozone Destruction Cycles 2 and 3 : Polar Regions

CYCLE 2 :

$$ClO + ClO \rightarrow (ClO)_2$$
$$(ClO)_2 + sunlight \rightarrow ClOO + Cl$$
$$ClOO \rightarrow Cl + O_2$$
$$2(Cl + O_3 \rightarrow ClO + O_2)$$
$$\text{NET: } 2O_3 \rightarrow 3O_2$$

CYCLE 3 :

$$ClO + BrO \rightarrow Cl + Br + O_2$$
$$\text{or} \begin{cases} ClO + BrO \rightarrow BrCl + O_2 \\ BrCl + sunlight \rightarrow Cl + Br \end{cases}$$
$$Cl + O_3 \rightarrow ClO + O_2$$
$$Br + O_3 \rightarrow BrO + O_2$$
$$\text{NET: } 2O_3 \rightarrow 3O_2$$

Figure Q8-2. Polar ozone destruction Cycles 2 and 3. Significant destruction of ozone occurs during late winter and early spring in the polar regions when abundances of ClO reach large values. In this case, the cycles initiated by the reaction of ClO with another ClO (Cycle 2) or the reaction of ClO with BrO (Cycle 3) efficiently destroy ozone. The net reaction in both cases is two ozone (O_3) molecules forming three oxygen (O_2) molecules. The reaction of ClO with BrO has two pathways to form the Cl and Br product gases that lead to loss of ozone. The destruction of ozone by Cycles 2 and 3 is catalytic, as illustrated for Cycle 1 in Figure Q8-1, because chlorine and bromine gases react and are re-formed each time the reaction cycle is completed. Sunlight is required to complete each cycle and to help form and maintain elevated abundances of ClO. During polar night and other periods of darkness, ozone cannot be destroyed by these reactions.

become the dominant reaction mechanisms for polar ozone loss because of the high abundances of ClO and the relatively low abundance of atomic oxygen (which limits the rate of ozone loss by Cycle 1). Cycle 2 begins with the self-reaction of ClO. Cycle 3, which begins with the reaction of ClO with BrO, has two reaction pathways that produce either Cl and Br or BrCl. The net result of both cycles is to destroy two ozone molecules and create three oxygen molecules. Cycles 2 and 3 account for most of the ozone loss observed in the stratosphere over the Arctic and Antarctic regions in the late winter/early spring season (see Q10 and Q11). At high ClO abundances, the rate of polar ozone destruction can reach 2 to 3% per day.

Sunlight requirement. Sunlight is required to complete and maintain these reaction cycles. Cycle 1 requires ultraviolet (UV) radiation (a component of sunlight) that is strong enough to break apart molecular oxygen into atomic oxygen. Cycle 1 is most important in the stratosphere at altitudes above about 30 km (18.6 miles), where solar UV-C radiation (100 to 280 nanometer (nm) wavelengths) is most intense (see Figure Q2-1).

Cycles 2 and 3 also require sunlight. In the continuous darkness of winter in the polar stratosphere, reaction Cycles 2 and 3 cannot occur. Sunlight is needed to break apart $(ClO)_2$ and BrCl, resulting in abundances of ClO and BrO large enough to drive rapid loss of ozone by Cycles 2 and 3. These cycles are most active when sunlight returns to the polar regions in late winter/early spring. Therefore, the greatest destruction of ozone occurs in the partially to fully sunlit periods after midwinter in the polar stratosphere.

Sunlight in the UV-A (315 to 400 nm wavelengths) and visible (400 to 700 nm wavelengths) parts of the spectrum needed in Cycles 2 and 3 is not sufficient to form ozone because this process requires more energetic solar UV-C solar radiation (see Q1 and Q2). In the late winter/early spring, only UV-A and visible solar radiation is present in the polar stratosphere, due to low Sun angles. As a result, the rate of ozone destruction by Cycles 2 and 3 in the sunlit polar stratosphere during springtime greatly exceeds the rate of ozone production.

Other reactions. Global abundances of ozone are controlled by many other reactions (see Q1). Reactive hydrogen and reactive nitrogen gases, for example, are involved in catalytic ozone-destruction cycles, similar to those described above, that also take place in the stratosphere. Reactive hydrogen is supplied by the stratospheric decomposition of water (H_2O) and methane (CH_4). Methane emissions result from both natural sources and a wide variety of human activities. The abundance of stratospheric H_2O is controlled by the temperature of the upper tropical troposphere as well as the decomposition of stratospheric CH_4. Reactive nitrogen is supplied by the stratospheric decomposition of nitrous oxide (N_2O), also emitted by natural sources and human activities. The importance of reactive hydrogen and nitrogen gases in ozone depletion relative to reactive halogen gases is expected to increase in the future because the atmospheric abundances of the reactive halogen gases are decreasing as a result of the Montreal Protocol, while abundances of CH_4 and N_2O are projected to increase due to various human activities (see Q20).

Q9 Why has an "ozone hole" appeared over Antarctica when ozone-depleting substances are present throughout the stratosphere?

Ozone-depleting substances are present throughout the stratospheric ozone layer because they are transported great distances by atmospheric air motions. The severe depletion of the Antarctic ozone layer known as the "ozone hole" occurs because of particular meteorological and chemical conditions that exist there and nowhere else on the globe. The very low winter temperatures in the Antarctic stratosphere cause polar stratospheric clouds (PSCs) to form. Specific chemical reactions that occur on PSCs, combined with the isolation of polar stratospheric air inside the polar vortex, allow chlorine and bromine reactions to produce the ozone hole over Antarctica in springtime.

The severe depletion of stratospheric ozone in late winter and early spring in the Antarctic is known as the "ozone hole" (see Q10). The ozone hole appears over Antarctica because meteorological and chemical conditions unique to this region increase the effectiveness of ozone destruction by reactive halogen gases (see Q7 and Q8). The formation of the Antarctic ozone hole requires the combination of temperatures low enough to form polar stratospheric clouds (PSCs), isolation of polar vortex air from air in other stratospheric regions, sunlight, and sufficient amounts of available chlorine (see Q8).

Distribution of halogen gases. Halogen source gases that are emitted at Earth's surface and have lifetimes longer than about 1 year (see Table Q6-1) are present in comparable amounts through-

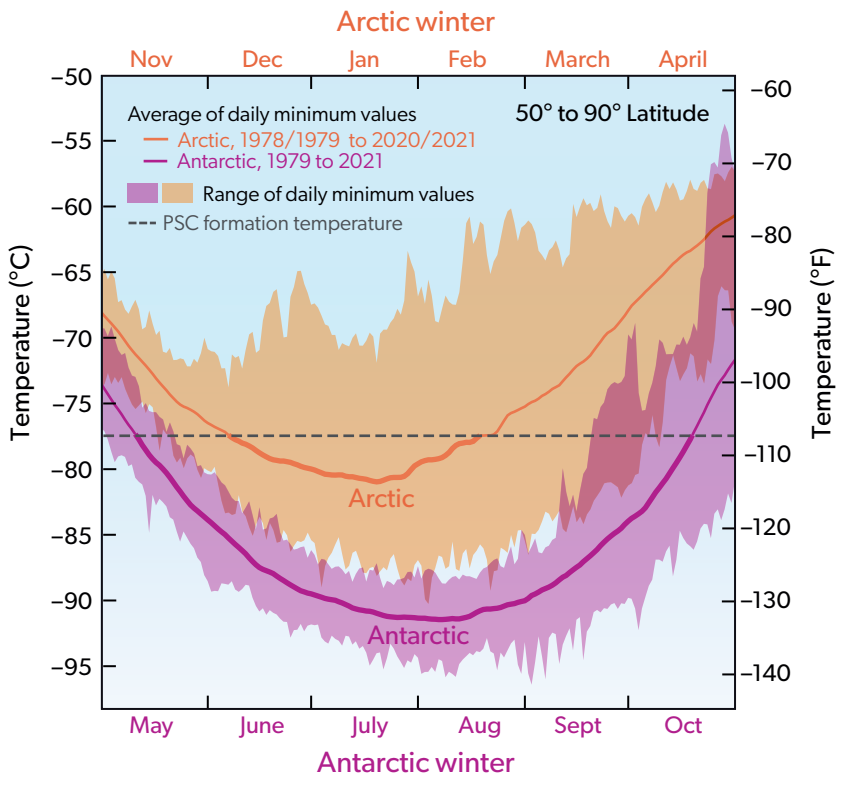

Figure Q9-1. Arctic and Antarctic temperatures. Air temperatures in the lower stratosphere of both polar regions reach minimum values in the lower stratosphere in their respective winter seasons. Average daily minimum values over Antarctica are as low as −92°C in July and August in a typical year. Over the Arctic, average minimum values are near −80°C in late December and January. Polar stratospheric clouds (PSCs) are formed in the ozone layer when winter minimum temperatures fall below their formation threshold of about −78°C. This occurs on average for 1 to 4 months over the Arctic and about 5 months over Antarctica each year (see heavy orange and magenta lines). Chemical reactions within and on the surfaces of liquid and solid PSC particles cause the highly reactive chlorine gas ClO to be formed, which catalytically destroys ozone (see Q8). The range of winter minimum temperatures found in the Arctic is much greater than that in the Antarctic. In some years, PSC formation temperatures are not reached in the Arctic, and significant ozone depletion does not occur. In contrast, PSC formation temperatures are always present for many months somewhere in the Antarctic, and severe ozone depletion occurs each winter/spring season (see Q10).

out the stratosphere in both hemispheres, even though most of the emissions occur in the Northern Hemisphere. The stratospheric abundances are comparable in both hemispheres because most long-lived source gases have no significant natural removal processes in the lower atmosphere, and because winds and convection redistribute and mix air efficiently throughout the troposphere on the timescale of weeks to months. Halogen source gases enter the stratosphere primarily from the tropical upper troposphere. Stratospheric air motions then transport these gases upward and toward the pole in both hemispheres.

Low polar temperatures. The severe ozone destruction that leads to the ozone hole requires low temperatures to be present over a range of stratospheric altitudes, over large geographical regions, and for an extended period of time. Low temperatures are important because they allow liquid and solid PSC particles to form. Chemical reactions within and on the surfaces of these PSC particles initiate a remarkable increase in the most important reactive chlorine gas, chlorine monoxide (ClO) (see below as well as Q7 and Q8). Air is usually too warm to enable the formation of clouds in the stratosphere. Only the polar regions during winter have temperatures low enough for stratospheric clouds to form, because air cools due to lack of sunlight. In the Antarctic winter, minimum daily temperatures are generally much lower and less variable than those in the Arctic winter (see **Figure Q9-1**). Antarctic temperatures also remain below PSC formation temperatures for much longer periods during winter. These and other meteorological differences occur because of variations between the hemispheres in the distributions of land, ocean, and mountains at middle and high latitudes. As a consequence, winter temperatures are low enough for PSCs to form somewhere in the Antarctic for nearly the entire winter (about 5 months), and only for limited periods (about 1 to 4 months) in the Arctic for most winters.

Isolated conditions. Stratospheric air in the polar regions is relatively isolated for long periods in the winter months. This isolation results from strong winds that encircle the poles during winter, forming a *polar vortex*, which prevents substantial transport and mixing of air into or out of the polar stratosphere. This circulation strengthens in winter as stratospheric temperatures decrease. The polar vortex circulation tends to be stronger in the Southern Hemisphere (SH) than in the Northern Hemisphere (NH), because northern latitudes have more mountainous regions and adjacent areas of ocean and land with contrasting temperatures than is present at southern latitudes. This situation leads to more meteorological disturbances in the circulation of the NH, which increase the mixing in of air from lower latitudes toward the pole, warming the Arctic stratosphere. Since winter temperatures are therefore lower in the SH than in the NH polar stratosphere, the isolation of air in the polar vortex is much more effective in the Antarctic than in the Arctic. Once temperatures drop low enough, PSCs form within the polar vortex and induce chemical changes such as an increase in the abundance of ClO (see Q8). These changes persist for many weeks to months due to the isolation of stratospheric air in the Antarctic.

Polar stratospheric clouds (PSCs). Chemical reactions within and on the surfaces of liquid and solid PSC particles can substantially increase the relative abundances of reactive chlorine gases. These reactions convert the reservoir forms of chlorine gases, hydrogen chloride (HCl) and chlorine nitrate ($ClONO_2$), to the most important reactive form, ClO (see Figure Q7-3). The abundance of ClO increases from a small fraction of available chlorine to comprise more than half of all available chlorine (see Q7). With increased ClO, the catalytic cycles involving ClO and BrO become active in the chemical destruction of ozone whenever sunlight is available (see Q8).

Different types of liquid and solid PSC particles form when stratospheric temperatures fall below about −78°C (−108°F) in polar regions (see Figure Q9-1). As a result, PSCs are often found over large areas of the winter polar regions and over extensive altitude ranges in both hemispheres, with substantially larger regions and for longer time periods in the Antarctic than in the Arctic. The most common type of PSC forms from nitric acid (HNO_3) and water

Arctic Polar Stratospheric Clouds (PSCs)

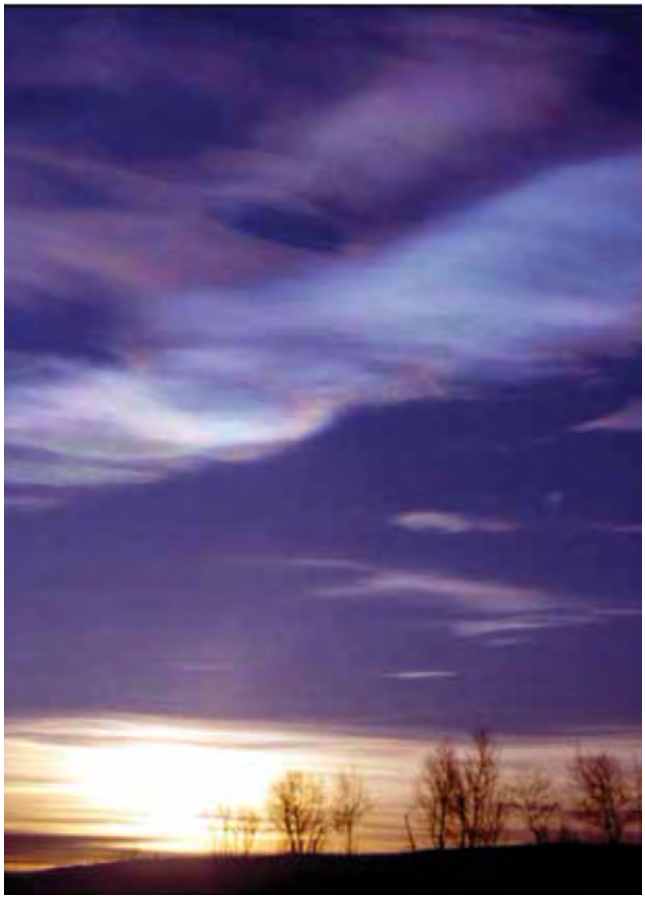

Figure Q9-2. Polar stratospheric clouds. This photograph of an Arctic polar stratospheric cloud (PSC) was taken in Kiruna, Sweden (67°N), on 27 January 2000. PSCs form in the ozone layer during winters in the Arctic and Antarctic, wherever sufficiently low temperatures occur (see Figure Q9-1). The particles grow from the condensation of water, nitric acid (HNO_3), and sulfuric acid (H_2SO_4). The clouds often can be seen with the human eye when the Sun is near the horizon. Reactions within and on PSC surfaces lead to the formation of the highly reactive gas chlorine monoxide (ClO), which is very effective in the chemical destruction of ozone (see Q7 and Q8).

condensing on pre-existing liquid sulfuric acid (H_2SO_4)-containing particles. Some of these particles freeze to form solid particles. At even lower temperatures (−85°C or −121°F), water condenses to form ice particles. PSC particles grow large enough and are numerous enough that cloud-like features can be observed from the ground under certain conditions, particularly when the Sun is near the horizon (see **Figure Q9-2**). PSCs are often found near mountain ranges in polar regions because the motion of air over the mountains can cause localized cooling in the stratosphere, which increases condensation of water and HNO_3.

When average temperatures begin increasing in late winter, PSCs form less frequently, which slows down the conversion of chlorine from reservoir to reactive forms throughout the polar region. Without continued production, the abundance of ClO decreases as other chemical reactions re-form the reservoir gases, $ClONO_2$ and HCl. When temperatures rise above PSC formation thresholds, usually sometime between late January and early March in the Arctic and by mid-October in the Antarctic (see Figure Q9-1), the most intense period of ozone depletion ends.

Nitric acid and water removal. Once formed, the largest PSC particles fall to lower altitudes because of gravity. The largest particles can descend several kilometers in the stratosphere within a few days during the low-temperature winter/spring period. Because PSCs often contain a significant fraction of available HNO_3, their descent removes HNO_3 from regions of the ozone layer. This process is called ***denitrification*** of the stratosphere. Because HNO_3 is a source for nitrogen oxides (NO_x) in the stratosphere, denitrification removes the NO_x available for converting the highly reactive chlorine gas ClO back into the reservoir gas $ClONO_2$. As a result, ClO remains chemically active for a longer period, thereby increasing chemical ozone destruction. Significant denitrification occurs each winter in the Antarctic and only for occasional winters in the Arctic, because PSC formation temperatures must be sustained over an extensive altitude region and time period to lead to denitrification (see Figure Q9-1).

Ice particles form at temperatures that are a few degrees lower than those required for PSC formation from HNO_3. If these water ice particles grow large enough, their gravitational settling can remove a significant fraction of water vapor from regions of the ozone layer over the course of a winter. This process is called ***dehydration*** of the stratosphere. Because of the very low temperatures required to form ice, dehydration is common in the Antarctic and rare in the Arctic. The removal of water vapor does not directly affect the catalytic reactions that destroy ozone. Dehydration indirectly affects ozone destruction by suppressing PSC formation later in winter, which reduces the production of ClO by reactions on PSCs.

Discovering the role of PSCs. Ground-based observations of PSCs were available many decades before the role of PSCs in polar ozone destruction was recognized. The geographical and altitudinal extent of PSCs in both polar regions was not fully known until PSCs were observed by satellite instruments starting in the late 1970s. The role of PSC particles in converting reservoir chlorine gases to ClO was not understood until after the discovery of the Antarctic ozone hole in 1985. Our understanding of the chemical role of PSC particles developed from laboratory studies of their surface reactivity, computer modeling studies of polar stratospheric chemistry, and measurements that sampled particles and reactive chlorine gases, such as ClO, in the polar stratosphere.

The Discovery of the Antarctic Ozone Hole

The first decreases in Antarctic total ozone were observed in the early 1980s over research stations located on the Antarctic continent. The measurements were made with ground-based Dobson spectrophotometers (see box in Q4) installed as part of the effort to increase observations of Earth's atmosphere during the International Geophysical Year that began in 1957 (see Figure Q0-1). The observations showed unusually low total ozone during the austral late winter/early spring months of September, October, and November. Total ozone was lower in these months in the early 1980s compared with previous observations made as early as 1957. The early published reports came from the Japan Meteorological Agency and the British Antarctic Survey. The results became widely known to the world after three scientists from the British Antarctic Survey published their observations in the prestigious scientific journal *Nature* in 1985. They suggested that rising abundances of atmospheric CFCs were the cause of the steady decline in total ozone over the Halley Bay research station (76°S) observed during successive Octobers starting in the early 1970s. Soon after, satellite measurements confirmed the spring ozone depletion and further showed that for each late winter/early spring season starting in the early 1980s, the depletion of ozone extended over a large region centered near the South Pole. The term "ozone hole" came about as a description of the very low values of total ozone, apparent in satellite images, that extend over the Antarctic continent for many weeks each October (spring in the Southern Hemisphere) (see Q10). Currently, the formation and severity of the Antarctic ozone hole are documented each year by a combination of satellite, ground-based, and balloon observations of ozone.

Very early Antarctic ozone measurements. The first total ozone measurements made in Antarctica with Dobson spectrophotometers occurred in the 1950s following extensive measurements in the Northern Hemisphere and Arctic region. Total ozone values observed in the Antarctic spring were found to be around 300 Dobson units (DU), lower than those in the Arctic spring. The Antarctic values were surprising because the assumption at the time was that the two polar regions would have similar values. We now know that these 1950s Antarctic values were not anomalous; in fact, similar values were observed near the South Pole in the early 1970s, before the ozone hole appeared (see Figure Q10-3). Antarctic total ozone values in early spring are systematically lower than those in the Arctic early spring because the Southern Hemisphere polar vortex is much stronger and colder and, therefore, much more effective in reducing the transport of ozone-rich air from midlatitudes to the pole (compare Figures Q10-3 and Q11-2).

Q10 How severe is the depletion of the Antarctic ozone layer?

Severe depletion of the Antarctic ozone layer was first reported in the mid-1980s. Antarctic ozone depletion is seasonal, occurring primarily in late winter and early spring (August–November). Peak depletion occurs in early October when ozone is often completely destroyed over a range of stratospheric altitudes, thereby reducing total ozone by as much as two-thirds at some locations. This severe depletion creates the "ozone hole" apparent in images of Antarctic total ozone acquired using satellite instruments. In most years the maximum area of the ozone hole far exceeds the size of the Antarctic continent.

The severe depletion of Antarctic ozone, known as the "ozone hole", was first reported in the mid-1980s (see box in Q9). The depletion is attributable to chemical destruction by reactive halogen gases (see Q7 and Q8), which increased everywhere in the stratosphere in the latter half of the 20th century (see Q15). Conditions in the Antarctic winter and early spring stratosphere enhance ozone depletion because of (1) the long periods of extremely low temperatures during polar night, which cause polar stratospheric clouds (PSCs) to form; (2) the large abundance of reactive halogen gases produced in reactions on PSCs; and (3) the isolation of polar stratospheric air, which allows time for chemical destruction processes to occur after the return of sunlight. The severity of Antarctic ozone depletion as well as long-term changes can be seen using satellite observations of total ozone and profiles of ozone versus altitude.

Antarctic ozone hole. The most widely used images of Antarctic ozone depletion are derived from measurements of total ozone made with satellite instruments. A map of Antarctic early spring measurements shows a large region centered near the South Pole in which total ozone is highly depleted (see **Figure Q10-1**).

Antarctic Ozone Hole

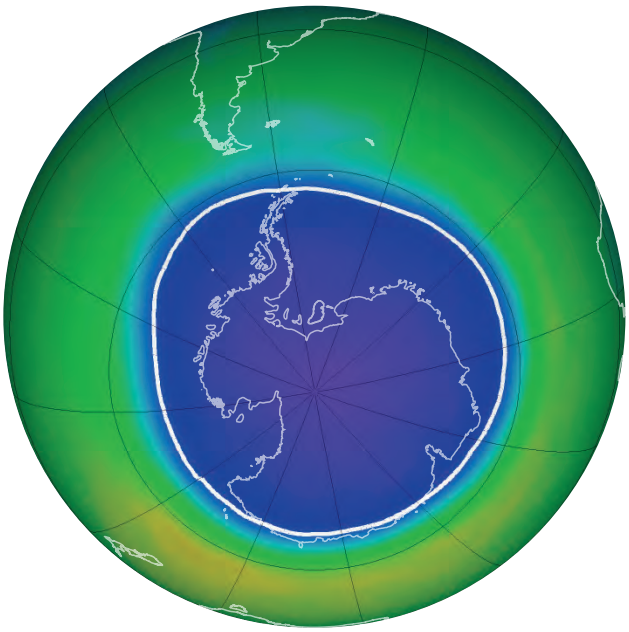

Figure Q10-1. Antarctic ozone hole. Total ozone values as measured by a satellite instrument are shown for high southern latitudes averaged over 21 to 30 September 2021. The dark blue and purple regions over the Antarctic continent show the severe ozone depletion or "ozone hole" now found every austral spring. Minimum values of total ozone inside the ozone hole are close to 150 Dobson units (DU), compared with Antarctic springtime values of about 350 DU observed in the early 1970s (see Figure Q10-3). The area of the ozone hole is usually defined as the geographical region within the 220-DU contour (thick white line) on total ozone maps. The maximum values of total ozone in the Southern Hemisphere in late winter/early spring are generally located in a crescent-shaped region (better seen in Figure Q10-3) that surrounds and is isolated from the ozone hole, due to stratospheric winds at the boundary of the polar vortex. In late spring or early summer (November–December), these atmospheric winds weaken and the ozone hole disappears due to the cessation of the ozone-depleting chemical reactions and the transport of ozone-enriched air masses towards the pole.

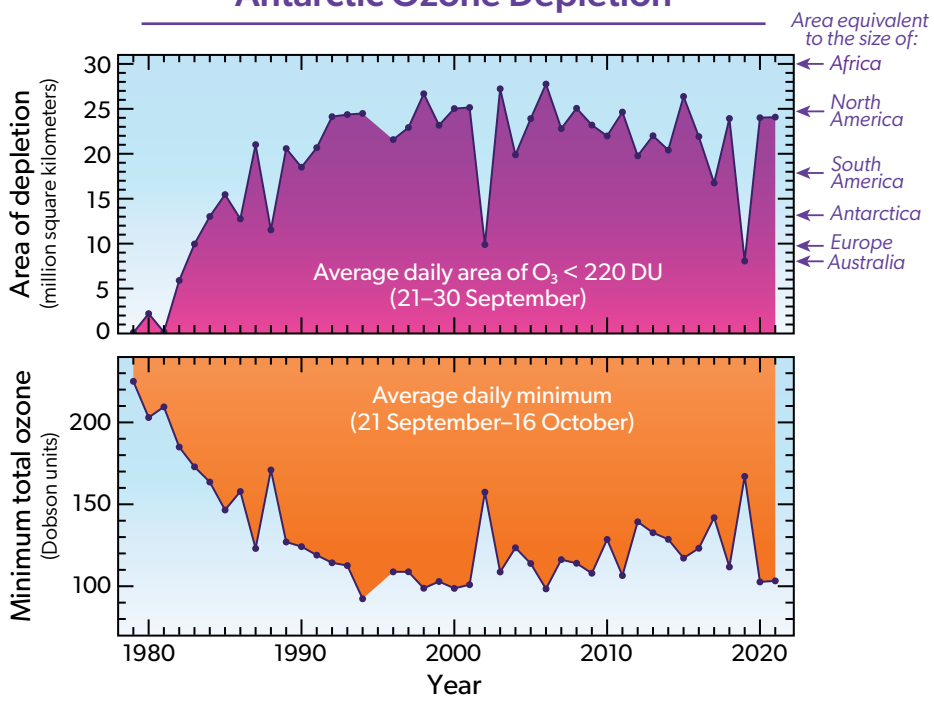

Figure Q10-2. Antarctic ozone hole features. Long-term changes are shown for key aspects of the Antarctic ozone hole: the area enclosed by the 220-DU contour on maps of total ozone (upper panel) and the minimum total ozone amount measured over Antarctica (lower panel). The values are from satellite observations and averaged for each year at a time near the peak of ozone depletion, as defined by the dates shown in each panel. The areas of continents are included for reference in the upper panel. The magnitude of Antarctic ozone depletion gradually increased beginning in 1980. In the past two and a half decades the depletion reached steady year-to-year values, except for the unusually small amount of depletion in 2002 and 2019 (see Figure Q10-4 and following box). The magnitude of Antarctic ozone depletion will steadily decline as ODSs are removed from the atmosphere (see Figure Q15-1). The return of Antarctic total ozone to 1980 values is expected to occur around the mid-2060s (see Q20).

This region has come to be called the "ozone hole" because of the near-circular contours of low ozone values in the maps. The reported area of the ozone hole for a given year is defined here as the geographical region within the 220-Dobson unit (DU) contour in total ozone maps (see white line in Figure Q10-1) averaged between 21–30 September. The area reached a maximum of 28 million square km (about 11 million square miles) in 2006, which is more than twice the area of the Antarctic continent (see **Figure Q10-2**). Minimum values of total ozone inside the ozone hole averaged in late September to mid-October are near 120 DU, which is only one-third of the springtime values of about 350 DU observed in the early 1970s (see **Figures Q10-3** and Q11-1). Low total ozone inside the ozone hole contrasts strongly with the distribution of much larger values outside the ozone hole. This common feature can be seen in Figure Q10-1, where a broad geographic region with values of total ozone around 350 DU surrounds the ozone hole in September 2021, revealing the edge of the polar vortex that acts as a barrier to the transport of ozone-rich midlatitude air into the polar region (see Q9).

Altitude profiles of Antarctic ozone. The low total ozone values within the ozone hole are caused by nearly complete removal of ozone in the lower stratosphere. Balloon-borne ozone instruments (see Q4) demonstrate that this depletion occurs within the ozone layer, the altitude region that normally contains the highest abundances of ozone. At geographic locations with the lowest total ozone values, ozonesonde measurements show that the chemical destruction of ozone has often been complete over an altitude region of up to several kilometers. For example, in the ozone profile over South Pole, Antarctica on 10 October 2020 (see red line in left panel of Figure Q11-3), ozone abundances are essentially zero over the altitude region from 14 to 20 km. The lowest winter temperatures and highest abundances of reactive chlorine (ClO) occur in this altitude region (see Figure Q7-3). The differences in the South Pole ozone profiles averaged over 1967–1971 and over 1990–2021 in Figure Q11-3 show how reactive halogen gases have dramatically altered the ozone layer. For the 1967–1971 time period, a normal ozone layer is clearly evident in the October average profile, with a peak near 16 km altitude. In the 1990–2021 average profile, a broad minimum centered near 16 km is observed, with ozone values reduced at some altitudes by up to 90% relative to normal values.

Long-term total ozone changes. Prior to 1960, the amount of reactive halogen gases in the stratosphere was insufficient to cause significant chemical loss of Antarctic ozone. Ground-based observations show that the steady decline in total ozone over the Halley Bay research station (76°S) (see box in Q9) during each October first became apparent in the early 1970s.

Satellite observations reveal that in 1979, total ozone during October near the South Pole was slightly lower than found at other high southerly latitudes (see Figure Q10-3). Computer model simulations indicate that Antarctic ozone depletion actually began in the early 1960s. Until the early 1980s, depletion of total ozone was not large enough to result in minimum values falling below the 220-DU threshold that is now commonly used to denote the boundary of the ozone hole (see Figure Q10-1). Starting in the mid-1980s, a region of total ozone well below 220 DU centered over the South Pole became apparent in satellite maps of October total ozone (see Figure Q10-3). Observations of total ozone from satellite

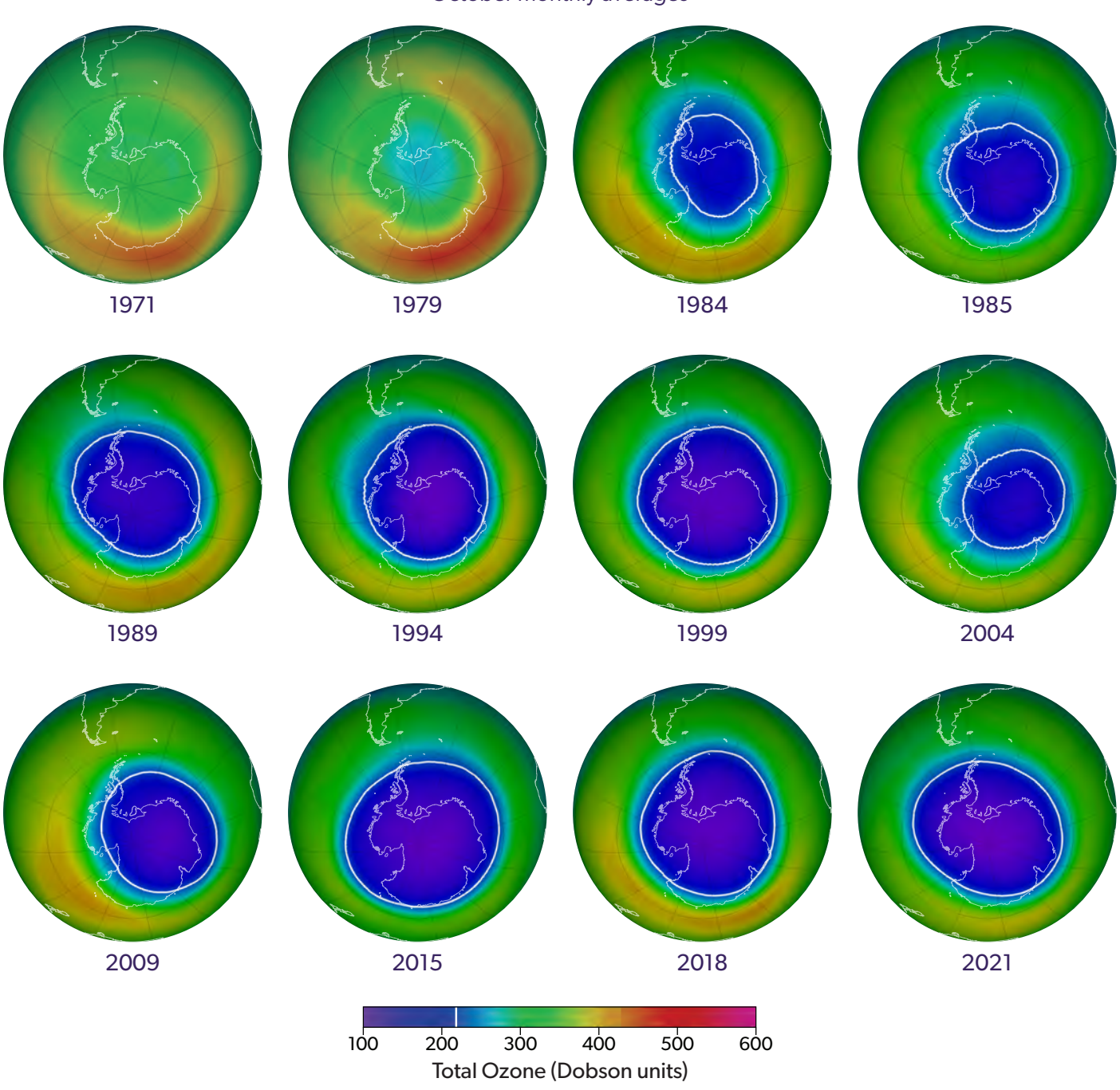

Figure Q10-3. Antarctic total ozone. Long-term changes in Antarctic total ozone are demonstrated with this series of total ozone maps derived from satellite observations. Each map is an average during October, the month of maximum ozone depletion over Antarctica. In the 1970s an ozone hole, as defined by a significant region with total ozone values less than 220 DU (thick white line), was not observed. The ozone hole initially appeared in the early 1980s and increased in size until the early 1990s. A large ozone hole has occurred each year since the mid-1980s as shown in Figure Q10-2. Maps from the mid-2010s show the large extent (about 25 million square km) of recent ozone holes. The largest values of total ozone in the Southern Hemisphere during October are found in a crescent-shaped region outside of the ozone hole. The satellite data show that these maximum values and their geographic extent have significantly diminished since the 1970s.

instruments can be used in multiple ways to examine how ozone depletion has changed in the Antarctic region over the past 50 years, including:

- First, ***ozone hole areas*** displayed in Figure Q10-2 show that the area of depletion increased after 1980, then became fairly stable in the 1990s, 2000s, and into the mid-2010s, often reaching an area of 25 million square km (about the size of North America). Exceptions are the unexpectedly low areas of depletion observed in 2002 and 2019, which are explained in the box at the end of this Question.
- Second, ***minimum Antarctic ozone*** amounts displayed in Figure Q10-2 show that the severity of the depletion increased beginning around 1980 along with the rise in the ozone hole area. Fairly constant minimum values of total ozone, near 110 DU, were observed in the 1990s and 2000s, with the exceptions of 2002 and 2019. There is some indication of an increase in the minimum value of total ozone since the early 2010s. However, in 2020 and 2021 unusually cold conditions produced large and long-lasting ozone holes, whereas in 2019 a weather disturbance resulted in a small, shallow ozone hole (see box). The ozone holes of 2019, 2020, and 2021 demonstrate the importance of year-to-year variability in ozone hole conditions, which challenges the identification of recovery due to declining levels of ODSs.
- Third, ***total ozone maps*** over the Antarctic and surrounding regions (Figure Q10-3) show how the ozone hole has developed over time. October averages show the absence of an ozone hole in the 1970s, the extent of the ozone hole around the time of its discovery in 1985 (see box in Q9), followed by the progression throughout the 1990s, the 2010s, and into the early 2020s.
- Fourth, ***values of total ozone averaged poleward of 63°S*** for each October (Figure Q11-1) show how total ozone has changed in the Antarctic region. After decreasing steeply in the early years of the ozone hole, polar-cap averages of total ozone are now approximately 30% smaller than those in pre-ozone hole years (1970–1982). Increased year-to-year variability in Antarctic-region ozone is evident since 2000.

Disappearance of the Antarctic ozone hole. Severe depletion of Antarctic ozone occurs each spring. In mid-October, temperatures in the polar lower stratosphere begin to increase (see Figure Q9-1), eventually rising to a level that prevents the formation of PSCs and production of ClO. Consequently, the most effective chemical cycles that destroy ozone are curtailed (see Q8). Typically, the polar vortex breaks down during late November or early December, ending the isolation of high-latitude air and increasing the exchange of air between the Antarctic stratosphere and lower latitudes. This exchange allows substantial amounts of ozone-rich air to be transported poleward, where it displaces or mixes with air depleted in ozone. As a result of these large-scale transport and mixing processes, the ozone hole typically disappears by mid-December.

Long-term recovery of the Antarctic ozone hole. There are emerging indications that the size and maximum ozone depletion (severity) of the Antarctic ozone hole has diminished since 2000. The signature of recovery is clearest during September, which is early spring in the Southern Hemisphere. Although accounting for the effect of natural variability on the size and depth of the ozone hole is challenging, the weight of evidence suggests that the decline in the amount of reactive halogen gases in the stratosphere since 2000 has made a substantial contribution to the observed reductions in the size and depth of the ozone hole during September. The reduction of Antarctic ozone depletion leading to full recovery of total ozone back to the value observed in the early 1980s requires continued, sustained reductions of ozone-depleting substances in the stratosphere. Even with the halogen source gas reductions already underway (see Q15), the return of Antarctic total ozone to 1980 values is not expected to occur until the mid-2060s (see Q20).

Unusual 2019 Antarctic Ozone Hole

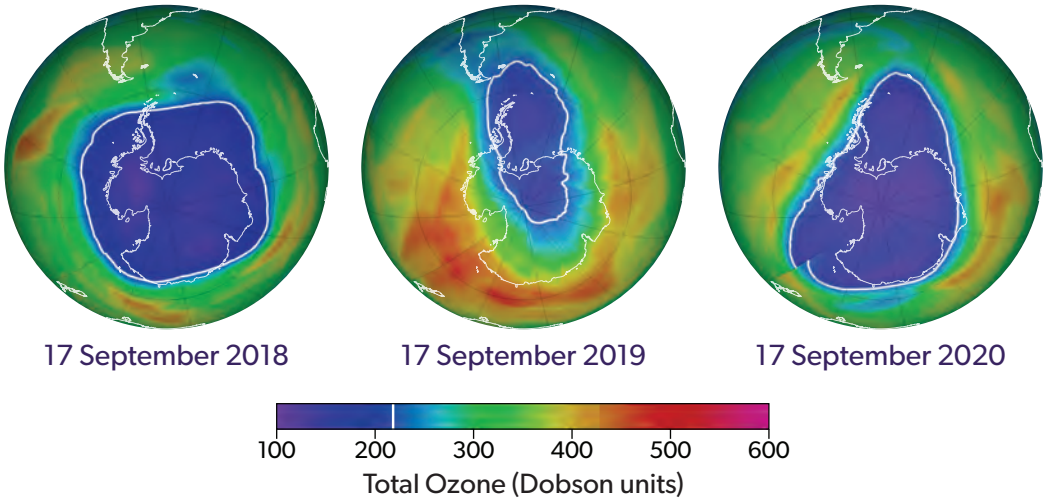

Figure Q10-4. Unusual 2019 ozone hole. Views from space of the Antarctic ozone hole are shown for 17 September for three consecutive years: 2018, 2019, and 2020. The ozone holes in 2018 and 2020 are considered typical of those observed since the late 1990s. An initially circular hole in 2019 was transformed by the significant transport of air from midlatitudes into the region of the ozone hole starting in late August. This unusual event, initiated by meteorological disturbances in the midlatitude troposphere, transported high amounts of ozone from midlatitudes into the region of the ozone hole and led to higher temperatures that reduced the rate of ozone depletion in 2019 compared to most other years. Consequently, the region of low total ozone in 2019 was displaced from the normal circumpolar position, and the amount of ozone depletion in 2019 as measured by the area of the ozone hole or minimum total ozone amounts was much less than in either 2018 or 2020 (see Figure Q10-2).

The 2019 Antarctic Ozone Hole

The 2019 Antarctic ozone hole exhibited much less ozone depletion as measured by the area of the ozone hole or minimum total ozone amounts in comparison with ozone holes in 2018 and 2020. The 2019 values, along with those observed in 2002, stand out clearly in the year-to-year changes in these quantities displayed in Figure Q10-2. Both of these anomalies are due to unusually warm meteorological conditions.

The ozone hole initially formed as expected in August 2019. At the end of August, an unusual weather pattern occurred that resulted in the transport of air from midlatitudes into the region of the ozone hole. As a result of this meteorological disturbance, the region of low total ozone was displaced from the normal circular position centered over the South Pole during September 2019 (see **Figure Q10-4**). Air with anomalously large amounts of ozone was transported from midlatitudes into the Antarctic stratosphere during the first two weeks of September 2019, resulting in the smallest ozone hole in the 21st century and one of the smallest ever observed in September since 1984, when the ozone hole was discovered (see Figure Q10-2).

The unexpected meteorological influence in 2019 resulted from specific atmospheric air motions that sometimes occur in polar regions. Meteorological analyses show that the 2019 disturbance was initiated by strong, large-scale weather systems that originated in the lower atmosphere (troposphere) at midlatitudes earlier in the year. This tropospheric weather system extended poleward and upward into the stratosphere, disturbing the normal circumpolar wind (polar vortex), transporting air with high levels of ozone into the vortex, and warming the lower stratosphere where ozone depletion was ongoing. The impact of this weather disturbance during late winter/early spring, when ozone loss processes are normally most effective, resulted in less Antarctic ozone depletion in 2019.

A similar stratospheric warming event occurred in 2002, resulting in ozone hole area and minimum total ozone amount values that are comparable to those observed in 2019 (see Figure Q10-2). Another warming event in 1988 caused somewhat smaller changes in the ozone hole features than those observed in 2002 and 2019. Large warming events are difficult to predict because of the complex conditions leading to their formation. The size and maximum ozone depletion (depth) of the ozone hole in 2020 and 2021 returned to values similar to those observed since the late 1990s (see Figures Q10-2 and Q10-3).

Q11 Is there depletion of the Arctic ozone layer?

Yes, significant depletion of the Arctic ozone layer now occurs in most years in the late winter and early spring period (January–March). However, Arctic ozone depletion is less severe than that observed in the Antarctic and exhibits larger year-to-year differences as a consequence of the more variable meteorological conditions found in the Arctic polar stratosphere. Even the most severe Arctic ozone depletion does not lead to total ozone amounts as low as those seen in the Antarctic, because Arctic ozone abundances during early winter before the onset of ozone depletion are much larger than those in the Antarctic. Consequently, an extensive and recurrent "ozone hole", as found in the Antarctic stratosphere, does not occur in the Arctic.

Significant depletion of ozone has been observed in the Arctic stratosphere in recent decades. The depletion is attributable to chemical destruction by reactive halogen gases (see Q8), which increased in the stratosphere in the latter half of the 20th century (see Q15). Arctic depletion also occurs in the late winter/early spring period (January–March), however over a somewhat shorter period than in the Antarctic (July–October). Similar to the Antarctic (see Q10), Arctic ozone depletion occurs because of (1) periods of very low temperatures, which lead to the formation of polar stratospheric clouds (PSCs); (2) the large abundance of reactive halogen gases produced in reactions on PSCs; and (3) the isolation of polar stratospheric air, which allows time for chemical destruction processes to occur after the return of sunlight. However, these conditions occur less often in the Arctic than in the Antarctic.

Total ozone observed in the Arctic during spring (see **Figure Q11-1**), even for years with significant ozone depletion, is higher than is commonly observed in the Antarctic during spring. Extensive and recurrent ozone holes as found in the Antarctic stratosphere do not occur in the Arctic. Stratospheric ozone abundances during early winter, before the onset of ozone depletion, are naturally higher in the Arctic than in the Antarctic because transport of ozone from its source region in the tropics to higher latitudes is more vigorous in the Northern Hemisphere. Furthermore, ozone depletion is limited because, in comparison to Antarctic conditions, average temperatures in the Arctic stratosphere are always significantly higher (see Figure Q9-1) and the isolation of polar stratospheric air is less effective (see Q9). These differences occur because northern latitudes have a greater prevalence of mountainous regions and contrasting areas of ocean and land than southern latitudes (compare Figures Q10-3 and Q11-2), which creates more meteorological disturbances that warm the Arctic stratosphere (see box in Q10). Consequently, the extent and timing of Arctic ozone depletion varies considerably from year to year.

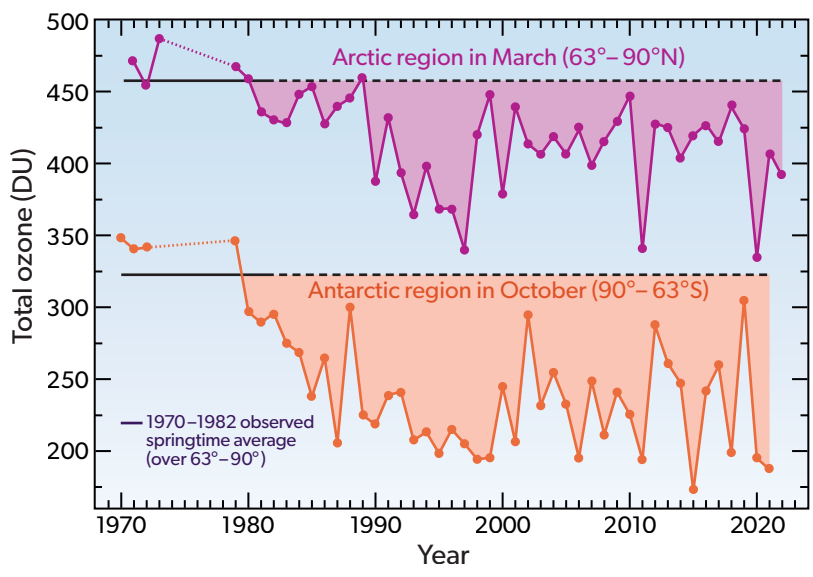

Figure Q11-1. Average total ozone in polar regions. Long-term changes in total ozone measured with satellite instruments are shown for the Antarctic and Arctic. The measurements are averaged over latitudes poleward of 63° for March (in the Arctic) and for October (in the Antarctic) and displayed as Dobson units (DU) (see box in Q4). The reference values (black lines) are averages of springtime total ozone from observations acquired between 1970 and 1982. After 1982, significant ozone depletion is found in most years in the Arctic and all years in the Antarctic. The largest average depletions have occurred in the Antarctic since 1990. The ozone changes arise from a combination of chemical destruction and natural variations in meteorological conditions that influence the year-to-year values of ozone, particularly in the Arctic. The year-to-year variation in Antarctic total ozone has increased since 2000.

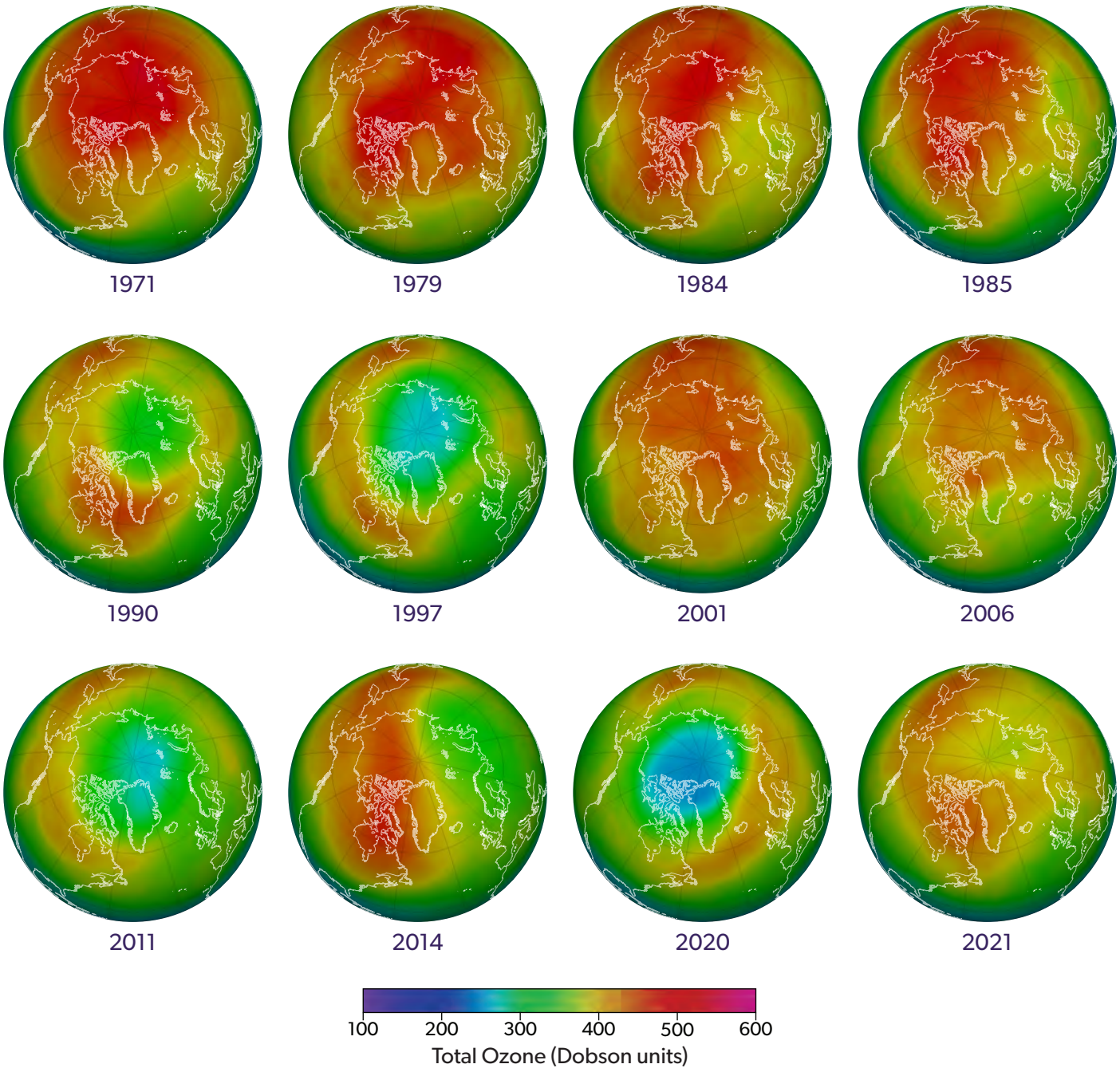

Figure Q11-2. Arctic total ozone. Long-term changes in Arctic total ozone are evident in this series of total ozone maps derived from satellite observations. Each map is an average during March, the month when some ozone depletion is usually observed in the Arctic. The years chosen are shown to highlight the strong year-to-year variability of Arctic ozone as well as the tendency towards lower values over time, during the half-century long record of satellite data. In the 1970s and 1980s, the Arctic region had normal ozone values in March, with values of 450 DU and above (red colors). Low values of total ozone on the scale of the Antarctic ozone hole do not occur in the Arctic. Instead, in late winter and early spring ozone depletion has eroded the normal high values of total ozone. For most years starting in the 1990s, the geographic extent of ozone values of 450 DU and above is reduced in comparison with the 1970s. The large regions of low total ozone in March of 1997, 2011, and 2020 (blue colors) are unusual in the Arctic record (see Figure Q11-1). Meteorological conditions during these three winters led to below-average stratospheric temperatures and strong polar vortices, conditions favorable to strong ozone depletion by reactive halogen gases.

Arctic ozone depletion in some winter/spring seasons occurs over many weeks, in others only for brief periods. These differences are controlled by the stability of and temperature within the Arctic vortex circulation system. Meteorological conditions affect the strength of the circulation of air in the Arctic stratosphere and the amount of ozone transported to the polar region. When the Arctic vortex is weak and disrupted, the polar region has larger amounts of ozone since temperatures are higher than normal and more ozone is transported by the winds to high latitudes. In contrast, a strong and stable vortex leads to lower-than-normal amounts of total ozone in the Arctic due to both more severe chemical loss and weaker poleward transport of ozone.

Long-term total ozone changes. Two important ways in which satellite observations can be used are to examine the average total ozone abundances in the Arctic region for the last half century and to contrast these values with Antarctic abundances.

- First, *total ozone averaged poleward of 63°N* for each March shows how total ozone has changed in the Arctic (see Figure Q11-1). The seasonal poleward and downward transport of ozone-rich air is naturally stronger in the Northern Hemisphere. As a result, before ozone depletion begins normal Arctic values are close to 450 DU while Antarctic values are close to 330 DU. Changes in total ozone from the 1970–1982 average value

Polar Ozone Depletion

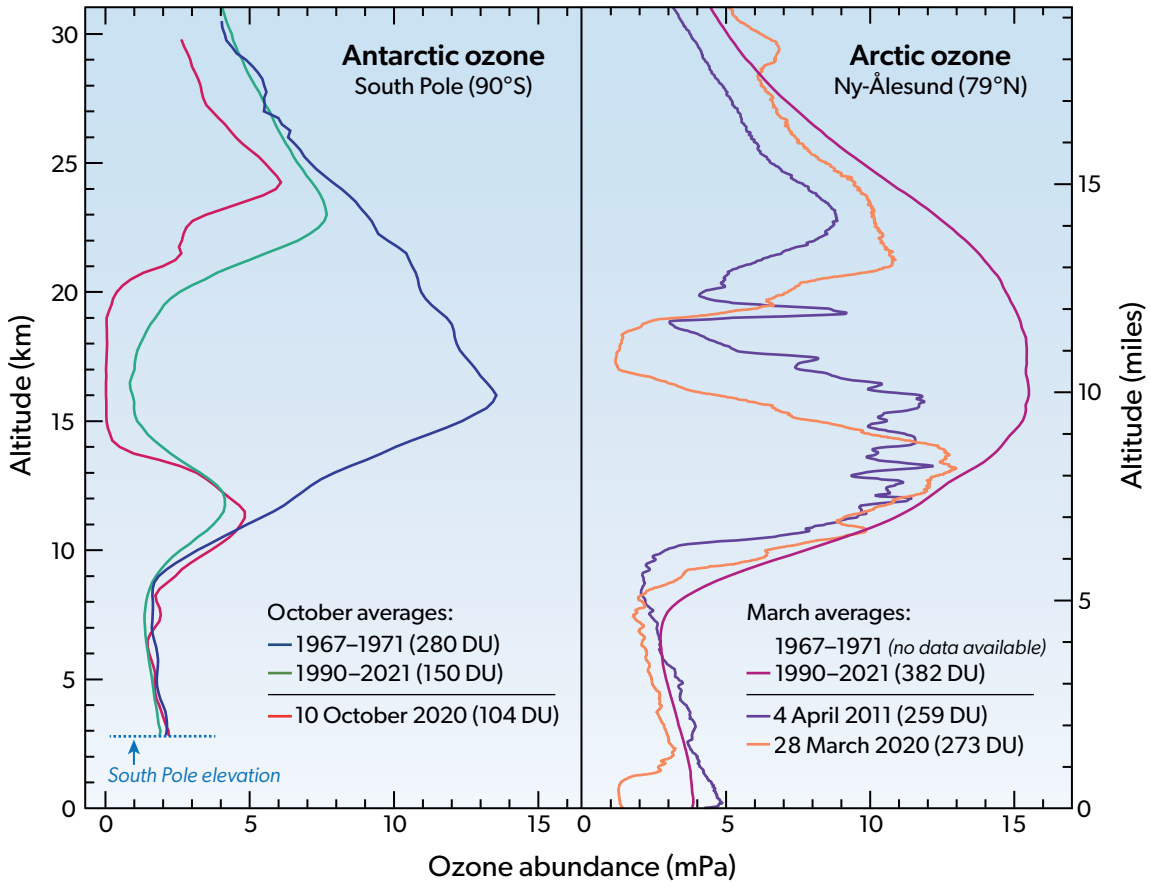

Figure Q11-3. Vertical distribution of Antarctic and Arctic ozone. At high latitudes during winter and spring, most stratospheric ozone resides between about 10 and 30 km (6 to 19 miles) above Earth's surface. Long-term observations of the ozone layer with balloon-borne ozone instruments also allow vertical profiles of ozone during winter to be compared between the Antarctic and Arctic regions. In the Antarctic at the South Pole (left panel), a normal ozone layer was observed to be present between 1967 and 1971. As shown here, ozone was almost completely destroyed between 14 and 20 km (9 to 12 miles) over the South Pole on 10 October 2020. Average October values of ozone in the last three decades (1990–2021) are 90% lower than pre-1971 values at the peak altitude of the ozone layer (16 km). For the Arctic, the average March profile for 1990–2021 as measured over the Ny-Ålesund research station is shown (right panel). No data from Ny-Ålesund are available for the 1967–1971 period. Some profiles reveal significant depletion, as shown here for 4 April 2011 and 28 March 2020. In such years, winter minimum temperatures are generally lower than normal, allowing for formation of PSCs and increases in ClO over longer periods of time. The number in parentheses for each profile is the total column ozone value in Dobson units (DU) (see box in Q4). Ozone abundances are shown here as the pressure of ozone at each altitude using the unit "milli-Pascals" (mPa) (100 million mPa = atmospheric sea-level pressure).

(horizontal line in Figure Q11-1) are due to a combination of chemical destruction by halogens and meteorological (natural) variations. In the last quarter century, these two aspects have contributed about equally to the observed year-to-year variations of ozone in the Arctic. Decreases from pre-ozone-hole average values (1970–1982) were observed in the Arctic by the mid-1980s, when larger changes were already occurring in the Antarctic. The decreases in total ozone in the Arctic are generally much smaller than those found in the Antarctic and lead to total ozone values that are typically about 10 to 20% below normal. Maximum decreases in total ozone of about 30% observed in March 1997, 2011, and 2020 for considerable regions of the Arctic (see **Figure Q11-2**) are the most comparable to Antarctic depletion. In all three Arctic winters, meteorological conditions inhibited transport of ozone-rich air to high latitudes, and in 2011 and 2020 persistently low temperatures facilitated severe chemical depletion of ozone by reactive halogens (see Q8).

- Second, ***total ozone maps*** over the Arctic and surrounding regions (see Figure Q11-2) show year-to-year changes in total ozone during March. In the 1970s, total ozone values were near 450 DU when averaged over the Arctic region in March. Beginning in the 1990s and continuing until present, values above 450 DU have been increasingly absent from the March average maps. A comparison of the maps in the 1970s and 2020, for example, shows a striking reduction of total ozone throughout the Arctic region. The large geographical extent of low total ozone in the March maps for years 1997, 2011, and 2020 represent exceptional events in the Arctic observational record of the last five decades, as noted above in the discussion of Figure Q11-1. The large-scale differences between Arctic ozone distributions observed in March 2011, 2014, 2020, and 2021 are a prime example of the influence of meteorology in driving year-to-year variations in Arctic ozone depletion. Despite the decline in the concentration of reactive gases in the polar stratosphere beginning around year 2000, there is little evidence of recovery of Arctic ozone. Detection of ozone recovery for the Arctic is made difficult by the smaller amount of depletion compared to the Antarctic, combined with larger natural variability in the year-to-year changes in the amount of Arctic ozone.

Altitude profiles of Arctic ozone. As in the Antarctic, Arctic ozone is measured using a variety of instruments (see Q4). These measurements document daily to seasonal changes within the ozone layer. Spring Arctic and Antarctic balloon-borne ozone measurements are shown in **Figure Q11-3**. Arctic profiles were obtained from the Ny-Ålesund research station at 79°N. For 1990–2021, the March average reveals the presence of a substantial ozone layer, contrasting sharply with the severely depleted Antarctic ozone layer in the October average over the same time period. This contrast further demonstrates how higher stratospheric temperatures, more variable meteorology, and larger amounts of ozone present in mid-winter have protected the Arctic ozone layer from having extended altitude regions of near-zero ozone as regularly occurs in the Antarctic, despite there being similar abundances of halogen gases (see Q7) in the two regions.

The Arctic ozone profiles shown in Figure Q11-3 for 4 April 2011 and 28 March 2020 are two of the most severely depleted in the 30-year record from Ny-Ålesund. Arctic ozone reached exceptionally low values in the spring of 2020 due to the presence of a very stable, cold, and long-lived polar vortex that led to lower-than-normal poleward transport of ozone and enabled extensive halogen-catalyzed chemical loss of ozone, which exceeded the previous record-breaking loss in spring 2011 (see Figure Q11-1). Chemical loss averaged over the Arctic vortex for March 2020 is estimated to be about 120 DU, nearly equal to the difference between the total ozone values associated with the 28 March 2020 profile and the 1991–2021 average profile shown in Figure Q11-3. Chemical loss of Arctic ozone in spring 2020 is similar in magnitude to the loss that regularly occurs over Antarctica.

Substantial chemical loss of Arctic ozone will continue to occur during cold winters and springs, as long as the concentrations of ODSs are well above natural levels. Although significant, the Arctic ozone depletion during both 2011 and 2020 resulted in amounts of ozone between 15 and 20 km altitude that are substantially larger than routinely observed in the Antarctic during October, such as in the profile from 10 October 2020 shown in Figure Q11-3. In the Antarctic stratosphere, near-complete depletion of ozone over many kilometers in altitude and over areas almost as large as North America is a common occurrence (see Figure Q10-2).

Restoring ozone in spring. As in the Antarctic, ozone depletion in the Arctic is largest in the late winter/early spring season. In spring, temperatures in the polar lower stratosphere increase (see Figure Q9-1), halting the formation of PSCs, the production of ClO, and the chemical cycles that destroy ozone. The breakdown of the polar vortex ends the isolation of air in the high-latitude region, allowing more ozone-rich air to be transported poleward, where it displaces or mixes with air in which ozone may have been depleted. As a result of these large-scale transport and mixing processes, the signature of large-scale and extensive ozone depletion at high northern latitudes typically disappears by April or earlier.

Q12 How large is the depletion of the ozone layer outside of polar regions?

The abundance of total ozone between 60°S and 60°N is now about 2–3% below the amount present during 1964–1980. The abundance of total ozone in this region declined steadily throughout the 1980s due to the increases in reactive halogen gases in the stratosphere resulting from human activities. In the early 1990s, due to additional ozone loss that followed the 1991 eruption of Mount Pinatubo, total ozone between 60°S to 60°N was depleted by 5% relative to the 1964–1980 average, the maximum depletion observed over the past six decades. In both hemispheres, total ozone depletion is small near the equator and increases toward the poles. The larger depletion at higher latitudes, particularly in the Southern Hemisphere, is driven in part by the late winter/early spring destruction of polar ozone, which influences ozone at lower latitudes following the breakdown of the polar vortex in each hemisphere.

Decreases in total ozone averaged over 60°S to 60°N, termed here *global ozone*, first became apparent in the 1980s (see **Figure Q12-1**) due to the rise in stratospheric halogens that result from human activities (see Figure Q15-1). Most of the depletion has occurred in the stratospheric ozone layer, where most ozone resides (see Figure Q1-2). Following the eruption of Mount Pinatubo in June 1991, global ozone in the early 1990s reached a minimum value that was 5% lower than the 1964–1980 average. This massive volcanic eruption dramatically increased the number of sulfuric acid-containing particles throughout the stratosphere. These particles significantly increased the effectiveness of reactive halogen gases in destroying ozone (see Q13) and, thereby, decreased global ozone by an additional 2% relative to its long-term trend for several years following the eruption. Since the mid-1990s, global ozone has gradually increased, due to the recovery of the ozone layer from this volcanically-induced perturbation as well as the slow, steady decline in stratospheric halogens driven by the Montreal Protocol (see Q14). Since 2010, global ozone has been about 2 to 3% below the 1964–1980 average.

Polar regions. Observed total ozone depletion varies significantly with latitude across the globe. The largest reductions occur at high southern latitudes as a result of the severe ozone loss over Antarctica each year during winter/spring (see Q9 and Q10). The next largest depletion is observed in the high latitudes of the Northern Hemisphere, caused in part by winter losses over the Arctic in some years (see Q11). Since ozone loss in polar regions is described extensively in the answers to other questions, the focus below is on the 60°S–60°N region, where the vast majority of the world's population resides.

Midlatitude regions. Ozone depletion is also observed at midlatitudes. Present-day (2017–2020 average) total ozone at midlatitudes of the Southern Hemisphere (SH) (35°S–60°S) is about 5% below the 1964–1980 average, whereas total ozone at midlatitudes of the Northern Hemisphere (NH) (35°N–60°N) is about 4% below the 1964–1980 average (see Figure Q12-1). Midlatitude ozone depletion has two contributing factors. First, ozone-depleted air over both polar regions is dispersed away from the poles during and after each winter/spring period, thereby reducing ozone at midlatitudes. Second, chemical destruction of ozone occurs at midlatitudes, contributing to the observed reductions in these regions. Ozone depletion at midlatitudes is much smaller than in polar regions (see Figure Q20-1) because the amount of reactive and reservoir halogen gases is lower and the dramatic seasonal increase of ClO, the most important reactive halogen gas (see Figure Q7-3), does not occur at midlatitudes. The slightly larger depletion of ozone at SH midlatitudes, compared to NH midlatitudes, is caused by the dispersion of air from the Antarctic ozone hole.

Tropical region. Total ozone in the tropics (20°S–20°N latitude) has been only weakly affected by chemical depletion. Present-day total ozone in the tropics is about 1% below the 1964–1980 average. In the tropical lower stratosphere, air is transported from the lower atmosphere (troposphere) over about an 18-month period. As a result, the fraction of ozone-depleting substances (ODSs) (halogen source gases) that is converted to reactive and reservoir halogen gases (see Figure Q7-1) is small. With little reactive and reservoir halogen gases available, total ozone depletion in this region is also small. In addition, net ozone production occurs in the tropics because of high average amounts of solar ultraviolet radiation. In contrast, stratospheric air in polar regions has been in the stratosphere for about 4 to 7 years, allowing time for significant conversion of ODSs to reactive and reservoir halogen gases (see Figure Q5-1). These systematic differences in the composition of stratospheric air are a consequence of large-scale atmospheric transport: air enters the stratosphere in the tropics, moves poleward in both hemispheres, and then descends and ultimately returns to the troposphere in the middle to high latitudes.

Ozone recovery. The Montreal Protocol, strengthened by its amendments and adjustments, has successfully controlled the production and consumption of ODSs, which act to destroy the ozone layer (see Q14). As a result, a quantity termed equivalent effective stratospheric chlorine (EESC; the total chlorine and bromine abundances in the stratosphere) peaked in the late 1990s and is now decreasing (see Q6 and Q15). An increase in upper stratospheric

Global and Regional Total Ozone Changes

Observed changes relative to the 1964–1980 average

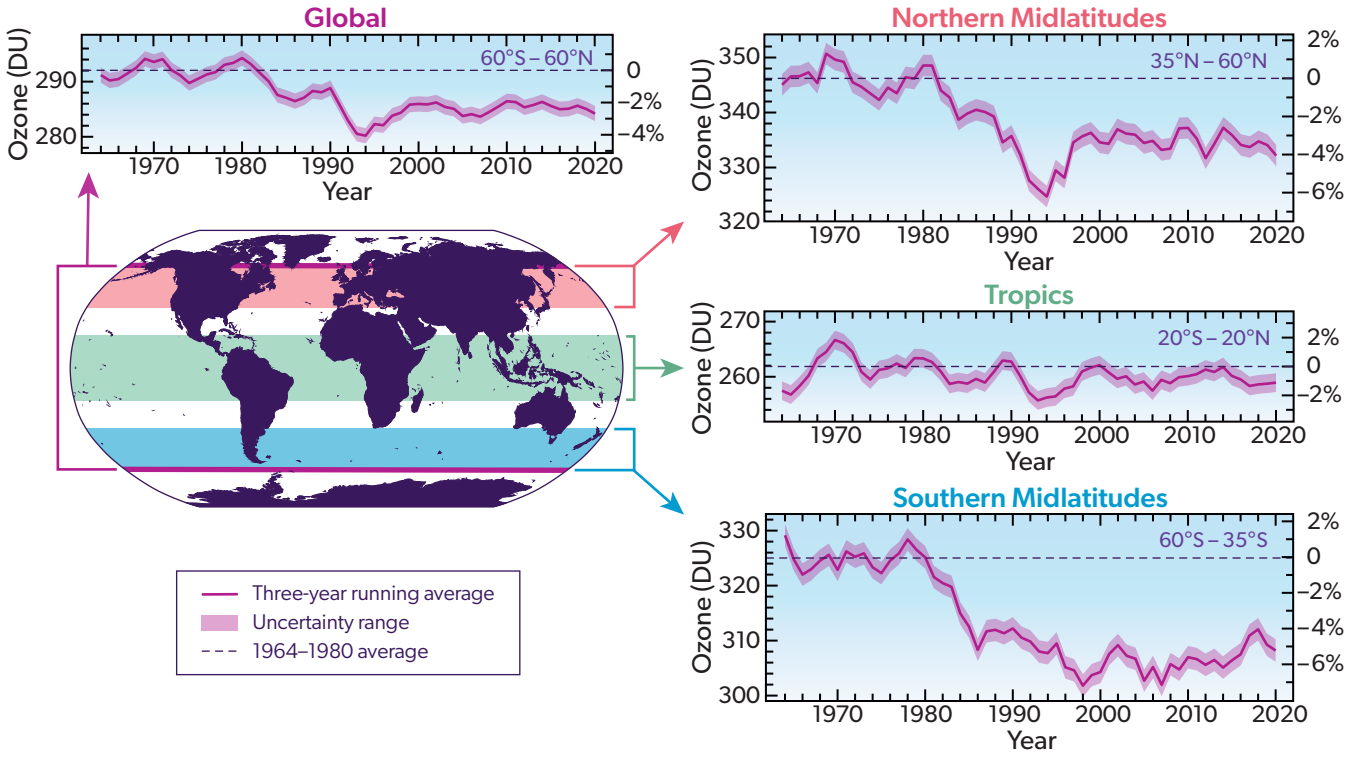

Figure Q12-1. Global total ozone changes. Ground-based and satellite observations show depletion of global total ozone beginning in the 1980s. The various panels compare the difference between annual averages of total ozone averaged over 60°S–60°N ("Global"), 35°N–60°N ("Northern Midlatitudes"), 20°S–20°N ("Tropics"), and 35°S–60°S ("Southern Midlatitudes") to the amount of ozone that was present in these regions during the period 1964–1980. Seasonal effects have been removed from the observational data set. A 1964–1980 baseline is used because large amounts of ozone depletion had not occurred during these years, as evident in the data record. Global ozone decreased between 1980 and 1990. The depletion worsened for a few years after 1991 due to the effect of volcanic aerosols from the eruption of Mount Pinatubo (see Q13). Since 2010, global ozone has been about 2 to 3% below the 1964–1980 average, ozone in the northern and southern midlatitudes has been about 2 to 5% and 4 to 7% below the 1964–1980 average, respectively, and ozone in the Tropics is about 0 to 2% below the 1964–1980 average.

ozone coincident with the decline in EESC is well documented, constituting an important initial sign of the recovery of the ozone layer. However, ozone in the upper stratosphere makes only a small contribution to total ozone.

The depletion of total ozone over 1979 to 1995 varies as a function of latitude, with the largest losses occurring at the highest latitudes in both hemispheres (see **Figure Q12-2**). Over this time period EESC nearly doubled. The pattern of ozone loss as a function of latitude is caused by two factors: 1) the tendency for larger levels of reactive and reservoir halogen gases to be present at higher latitudes due to the pattern of large-scale atmospheric transport along with the time required for significant conversion of ODSs to reactive and reservoir halogen gases as described above (see Q5 and Q7) and 2) greater influence of the dispersal of severely ozone-depleted air from the Antarctic (Q10) and Arctic (Q11) vortices at the end of their respective winters at the higher latitudes.

Over the time period 1996 to 2020, there has been a rise in total ozone of 0.4 % per decade averaged over 60°S–60°N (see Figures Q12-1 and Q12-2) that is consistent with the decline in the abundance of ODSs (see Q14 and Q15). The data indicate most of this increase in total ozone occurs between 35°–60° of the Southern Hemisphere. For the tropics (20°S–20°N), trends in total ozone over 1996 to 2020 are small and not statistically significant. The abundance of EESC at midlatitudes declined by about 15% from 1996 to 2020. The smaller decline of EESC over this 24-year time period compared to the doubling of EESC over the shorter 1979 to 1995 time period is due to the long lifetime for atmospheric removal of ODSs (see Table Q6-1), combined with the rapid growth in the emissions of ODSs in the 1970s and 1980s (see Figure Q0-1). The small increase in ozone shown in Figure Q12-2 for 1996 to 2020 is consistent with the scientific community's current understanding of the processes that control the abundance of atmospheric ozone.

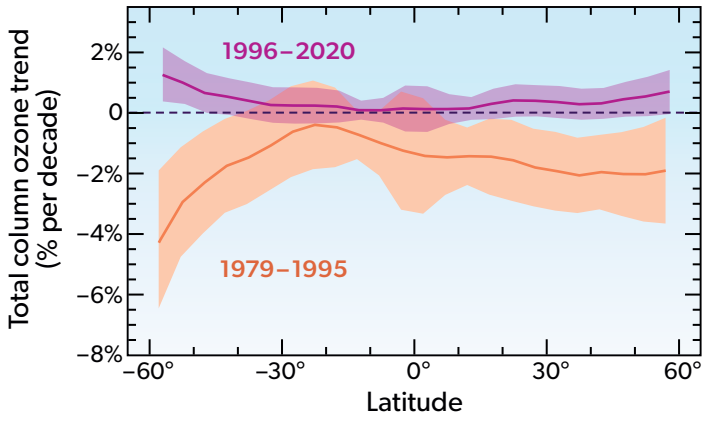

Figure Q12-2. The change in total ozone due to ODSs as a function of latitude, from 60°S to 60°N, for two time periods, 1979–1995 and 1996–2020, expressed as percent change per decade. The trends are based on a statistical model analysis of measurements of total ozone from numerous ground-based and satellite instruments. The model analysis includes the effects on total ozone from ozone-depleting substances (ODSs), stratospheric aerosols, solar ultraviolet (UV) radiation emitted by the Sun, and stratospheric air motions. The figure isolates the resulting chemically-driven change in total ozone due to trends in ODSs only for two time periods (solid lines), along with the total uncertainty (shaded regions).

Identifying an ozone increase that is attributable to the observed decrease in the amount of ODSs is challenging because halogen levels are not the only factor that determines the abundance of stratospheric ozone. Total ozone declined over most of the globe (60°S–60°N) during the 1980s and early 1990s, reaching a minimum in 1993 due to the combined effects of ODSs and the eruption of Mount Pinatubo in 1991 (see Figures Q12-1 and Q13-1). This global ozone minimum was observed half a decade before the EESC maximum was reached due to the strong global ozone response to enhanced amounts of stratospheric sulfate aerosol after the volcanic eruption of Mount Pinatubo, which led to increased ozone depletion for several years. Observed global ozone increases in the mid-1990s were caused by the steady removal of volcanic aerosol from the stratosphere by natural processes, which occurred at the time EESC was approaching its maximum (see Q13).

Another factor complicating the identification of ozone recovery in different regions of the atmosphere is the year-to-year variation of the stratospheric circulation. In most regions of the atmosphere, these variations lead to ozone variability that is currently still larger than the increases in ozone expected from the observed decrease in EESC. Finally, increases in greenhouse gases (GHGs) such as carbon dioxide (CO_2), which warm the lower atmosphere, affect ozone by decreasing stratospheric temperatures and by strengthening the stratospheric circulation. A colder stratosphere slows down the rate of ozone loss reactions (outside of polar regions), while a stronger circulation enhances the transport of ozone from the tropics to middle and high latitudes.

The impact on stratospheric ozone from accumulated emissions of most ODSs will continue for several decades because of the long atmospheric lifetime of these gases. Assuming compliance with the Montreal Protocol, EESC will continue to decline over the coming decades and will return to pre-1980 levels around 2066 (see Figure Q15-1). Increases in the abundance of most GHGs are expected to accelerate this EESC-driven return of the global ozone layer to pre-1980 levels. However, not all ozone-depleting gases are halogen compounds. Nitrous oxide (N_2O), a GHG with sources attributed to natural processes and various human activities, is projected to increase in the future, which will result in additional ozone depletion (see Q20). Finally, as long as atmospheric abundances of ODSs remain elevated, the possibility of substantial reductions in total ozone following major volcanic eruptions (see Q13) will persist.

Q13 Do changes in the Sun and volcanic eruptions affect the ozone layer?

Yes, factors such as changes in solar radiation and the formation of stratospheric aerosol particles after explosive volcanic eruptions do influence the ozone layer. Global ozone abundances vary by 1–2% between the maximum and minimum of the 11-year solar cycle. The abundance of global ozone decreased by about 2% for a few years after the June 1991 eruption of Mount Pinatubo, due to volcanic enhancement of stratospheric sulfate aerosols. However, neither factor can explain the observed decrease in global total ozone or the severe ozone depletion observed in polar regions over the past half century. The primary influence on long-term changes in total global ozone is the abundance of stratospheric halogens.

Changes in solar radiation and increases in stratospheric aerosols (small particles) from volcanic eruptions both affect the abundance of stratospheric ozone. Global total ozone in the early 1990s decreased by about 5% when compared to the 1964–1980 average, and is now about 2 to 3% below this value (see Q12). The long-term depletion of ozone is primarily attributed to increases in halogen source gases, with additional depletion in the early 1990s associated with the volcanic eruption of Mount Pinatubo. Equivalent effective stratospheric chlorine (EESC) (see definition in Q15) is often used as a measure of the potential of reactive and reservoir halogen gases to deplete ozone. Comparisons of the long-term changes in solar radiation, stratospheric volcanic aerosol, and EESC are useful in evaluating the contribution of these factors to long-term changes in total ozone.

Total ozone and solar changes. The formation of stratospheric ozone is initiated by ultraviolet (UV) radiation emitted by the Sun (see Q1). As a result, an increase in the Sun's UV radiation output increases the amount of ozone in Earth's atmosphere. Since the 1960s, ground-based and satellite instruments have recorded variations in the total energy emitted by the Sun, which is well correlated with changes in solar UV radiation. The Sun's radiation output varies over the well-documented 11-year solar cycle, as shown in **Figure Q13-1** in the quantity labeled incoming solar radiation. The long-term solar record exhibits alternating maximum and minimum values of total output, with maximum values separated by about 11 years. Global total ozone is relatively high compared to surrounding years during times of solar maxima and is relatively low during solar minima due to the sensitivity of ozone production to UV radiation, which increases during solar maxima. Analysis of measurements of ozone and incoming solar radiation shown in Figure Q13-1 shows that ozone levels vary by 1 to 2% between the maximum and minimum of a typical solar cycle. In addition to this 11-year variation, the total ozone record exhibits a long-term downward trend from the early 1980s to the early 2000s. If a decline in incoming solar radiation were the primary cause of the long-term decline in global total ozone, then the solar radiation would exhibit a similar long-term decrease. Instead, incoming solar radiation varies about a stable baseline over the modern instrument record. This comparison demonstrates that the observed long-term decline in global total ozone does not result from changes in the Sun's UV radiation output.

Total ozone and past volcanoes. Explosive volcanic eruptions inject sulfur gases directly into the stratosphere, causing new sulfate aerosol particles to be produced. These particles initially form downwind of the volcano and then disperse over large regions, as air is transported by stratospheric winds. The largest impact on global ozone usually takes place after explosive volcanic eruptions in the tropics, because the stratospheric circulation efficiently spreads tropical volcanic plumes to both hemispheres. A principal method of detecting the presence of volcanic particles in the stratosphere is to measure the transmission of solar radiation through the stratosphere to the ground, which is termed stratospheric aerosol optical depth (SAOD). When large amounts of new particles form over an extensive region of the stratosphere, SAOD increases and solar transmission is measurably reduced. Figure Q13-1 shows the long-term record of SAOD averaged over the entire stratosphere, based on measurements from ground-based and satellite instruments. Large increases in SAOD (reductions in solar transmission) are apparent after the explosive eruptions of Mount Agung (1963), Volcán de Fuego (1974), El Chichón (1982), and Mount Pinatubo (1991), all of which occurred in the tropics. Reduced transmission of solar radiation persists for a few years after each of these eruptions, until the stratospheric circulation and gravitational settling bring the volcanic sulfate aerosol particles back to the troposphere, where they are removed by precipitation.

Volcanic aerosol is primarily composed of sulfur compounds (sulfate). Chemical reactions on the surface of sulfate aerosol particles destroy stratospheric ozone by increasing the abundance of chlorine monoxide (ClO), a highly reactive chlorine gas (see Q7). The extent of ozone depletion depends on both the amount of sulfate aerosol produced following the eruption and the value of EESC (see Q15). Global ozone decreased for a few years following the eruptions of Mount Agung, Volcán de Fuego, El Chichón, and Mount Pinatubo. The ozone reduction from the eruption of Mount Pinatubo stands out in the global ozone record because it occurred at a time when EESC was near its peak and the perturbation to stratospheric sulfate aerosol was especially large (see Figures Q12-1 and Q13-1). Analysis of ozone observations shows that global total

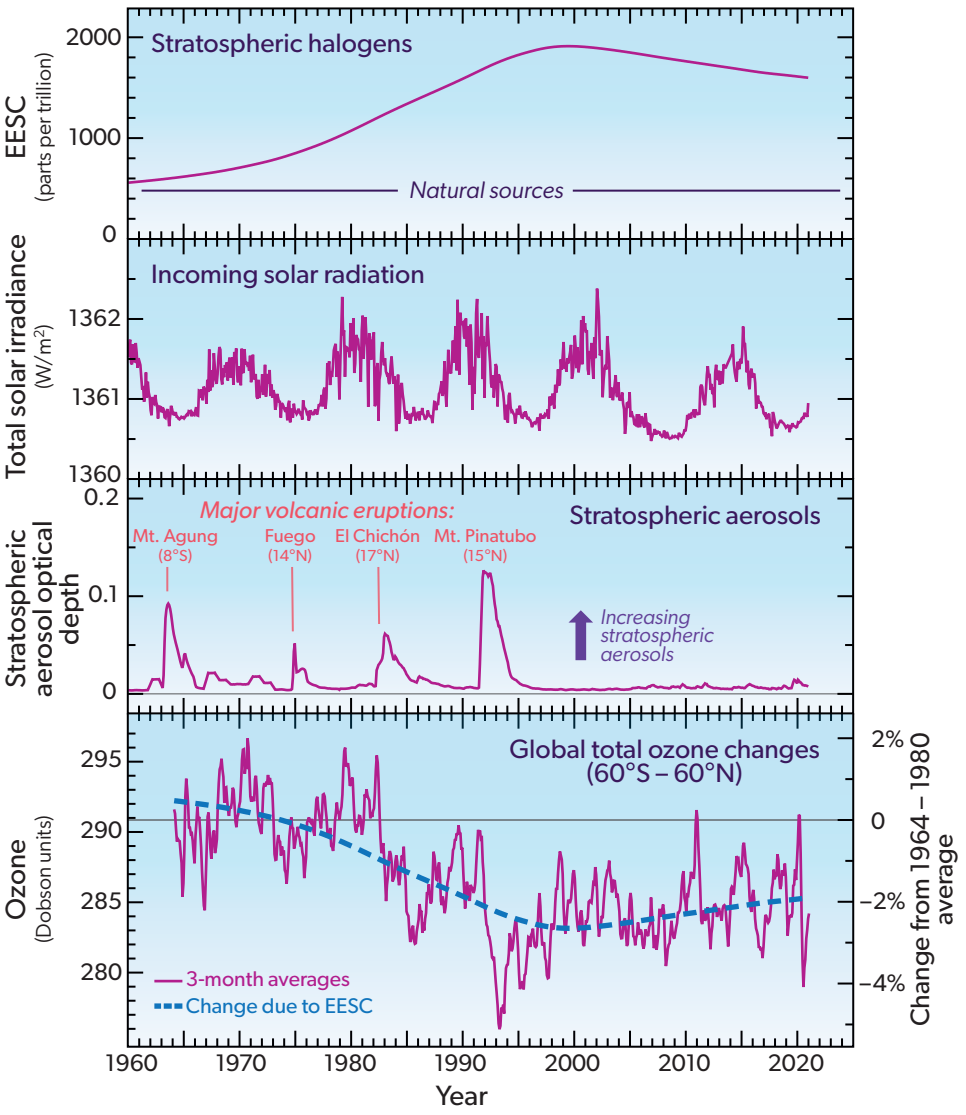

Figure Q13-1. The effects on ozone of EESC, solar changes, and volcanic eruptions. A comparison of the long-term variation in EESC, total solar radiation, and a measure of the abundance of stratospheric sulfate particles with global total ozone provides a basis to evaluate the primary influences on ozone over the past half century. The top panel shows the record of equivalent effective stratospheric chlorine (EESC) for the midlatitude, lower stratosphere (about 19 km altitude). EESC represents the potential for stratospheric ozone depletion by halogens, which result primarily from human activities (see Q15). The second panel shows the total energy of incoming solar radiation, with peaks and valleys defining the maxima and minima of the 11-year solar cycle. Following the explosive volcanic eruptions marked on the third panel, the number of sulfur-containing particles in the stratosphere exhibits a dramatic rise. These particles decrease the transmission of solar radiation through the stratosphere, which is recorded by an increase in the quantity termed stratospheric aerosol optical depth. The bottom panel shows differences in global total ozone, averaged over 60°S to 60°N latitude, from the 1964–1980 average value. Global total ozone is 1 to 2% higher at solar maxima than solar minima due to enhanced formation of ozone by solar ultraviolet radiation (see Q1). Reactions on sulfate particles enhance the abundance of highly reactive chlorine compounds, increasing the depletion of stratospheric ozone after major volcanic eruptions. The maximum depletion of ozone occurs in mid-1993, after the eruption of Mount Pinatubo. The bottom panel also shows the change in global total ozone attributed to EESC, found using an analysis that considers the effects on ozone of numerous natural and human-related factors. The long-term changes in ozone are consistent with the variation of EESC: prior to the mid-1990s EESC steadily rose while global ozone declined, and since the late 1990s EESC has declined and global ozone has risen. This figure illustrates that the primary influence on changes in global total ozone over the past half century is the abundance of stratospheric halogens.

ozone declined by about 2% following the eruption of Mount Pinatubo in June 1991, and that this effect persisted for 2 to 3 years after the eruption. At times of relatively low EESC, such as the early 1960s, total ozone is not as sensitive to a volcanically induced increase in stratospheric aerosol as during current times, when values of EESC are much higher than background levels.

If changes in the abundance of volcanic aerosol in the stratosphere were the primary cause of the long-term decline in global total ozone, then the record of stratospheric aerosol optical depth (marker of volcanic sulfate particles) would exhibit a slow, gradual rise. Instead, stratospheric volcanic aerosol has been quite low since 1995, a period of time over which global total ozone has been about 2 to 3% below the 1964–1980 value. The data record shown in Figure Q13-1 provides evidence that the long-term decrease in global total ozone relative to the 1964–1980 average does not result from changes in volcanic aerosol.

Total ozone and EESC. Values of EESC are derived from surface observations of ozone-depleting substances (ODSs) and repre-

sent the potential for ozone depletion from halogens at particular times and locations of the stratosphere (see Q15). The EESC record for the midlatitude, lower stratosphere rose well above the natural background level in the 1980s, peaked in 1998, and in 2022 was 18% below the peak value. The bottom panel of Figure Q13-1 compares the observed long-term record of global total ozone (magenta line) to the variation in ozone attributed to the changes in EESC (blue dashed line). This attribution curve is computed by a statistical model that considers the effects on ozone of EESC, stratospheric sulfur containing particles, variations in the total energy of incoming solar radiation, as well as a few factors related to changes in stratospheric circulation. The observed record of global total ozone follows the same general tendencies of the EESC attribution curve over the past half century, providing strong evidence that changes in stratospheric halogens in response to human activities are the primary factor responsible for the long-term variation of ozone depletion. Further evidence linking ODSs and long-term variations in total column ozone is provided by the climate-chemistry model simulations highlighted in Q20.

Halogen gases from volcanic eruptions. Explosive volcanic eruptions have the potential to inject halogens directly into the stratosphere, in the form of gases such as hydrogen chloride (HCl), bromine monoxide (BrO), and iodine monoxide (IO). Although HCl does not react directly with ozone, stratospheric injections of HCl and other chlorine-containing gases following explosive volcanic eruptions can lead, through chemical reactions, to elevated amounts of reactive chlorine monoxide (ClO) that destroys ozone (see Figure Q7-3). Eruption plumes also contain a considerable amount of water vapor, which forms rainwater and ice in the rising fresh plume. Rainwater and ice efficiently scavenge and remove HCl while the plume is still in the lower atmosphere (troposphere). Most of the HCl in the explosive plume of Mount Pinatubo did not enter the stratosphere because of this scavenging by precipitation. The amount of injected halogens depends on the chemical composition of the magma, conditions of the eruption such as its explosivity and the local meteorology. Recent analyses of several historic, extremely large volcanic eruptions show the potential for quite large ozone loss from the stratospheric injection of halogens. A volcanic eruption of this nature has not occurred during the time period of the modern observational record.

Antarctic volcanoes. Volcanoes on the Antarctic continent are of special interest due to their close proximity to the Antarctic ozone hole. An explosive eruption could in principle inject volcanic aerosol or halogens directly into the stratosphere over Antarctica and contribute to ozone depletion. To be a possible cause of the annually recurring ozone hole beginning in the early 1980s, explosive eruptions of Antarctic volcanoes large enough to inject material into the stratosphere would need to have occurred at least every few years. This is not the case. Mount Erebus and Deception Island are the only two currently active volcanoes in Antarctica. No explosive eruptions of these volcanoes, or any other Antarctic volcano, have occurred since 1980. Explosive volcanic eruptions in the last three decades have not caused the Antarctic ozone hole and, as noted above, have not been sufficient to cause the long-term depletion of global total ozone.

Total ozone and future volcanoes. The abundance of EESC will remain high for much of the 21st century due to the long atmospheric lifetime of ODSs (see Figure Q15-1). With its slow decline, EESC will remain above the 1960 value throughout this century. Consequently, throughout the rest of this century, increases in the abundance of stratospheric sulfate aerosol particles caused by large volcanic eruptions similar to Mount Pinatubo have the potential to reduce global total ozone values for a few years. The ozone layer will be most vulnerable to such an eruption until midcentury, since EESC is projected to return to the 1980 value around 2066. Following an explosive eruption much larger than Mount Pinatubo, or an eruption that injects halogens into the stratosphere, peak ozone losses could both be greater than previously observed and persist for longer periods of time.

Q14 Are there controls on the production of ozone-depleting substances?

Yes, the production and consumption of ozone-depleting substances (ODSs) are controlled under a 1987 international agreement known as the "Montreal Protocol on Substances that Deplete the Ozone Layer" and its subsequent amendments and adjustments. The Protocol, now ratified by 198 parties, establishes legally binding controls on the global production and consumption of ODSs. Production and consumption of controlled ODSs by developed and developing nations will be almost completely phased out by 2030.

The Vienna Convention and the Montreal Protocol. In 1985, a treaty called the Vienna Convention for the Protection of the Ozone Layer was signed by 26 nations. The signing nations agreed to take appropriate measures to protect the ozone layer from human activities. The Vienna Convention was a framework agreement that supported research, exchange of information, and future protocols. In response to growing concern, the Montreal Protocol on Substances that Deplete the Ozone Layer was signed in 1987 and, following ratification, entered into force in 1989. The Protocol has been successful in establishing and enforcing legally binding controls for developed and developing nations on the production and consumption of halogen source gases known to cause ozone depletion. Halogen source gases containing chlorine and bromine that are emitted by human activities and are controlled under the Montreal Protocol are referred to as ozone-depleting substances (ODSs). National consumption of an ODS is defined as production plus imports of the controlled substance, minus exports of the substance. Inadvertent emissions of ODSs used as feedstock (raw material used to synthesize other substances through a process of chemical transformation) are not controlled by the Montreal Protocol. Nations are, however, required to report imports, exports, and production of ODSs used as feedstocks. The Protocol provisions are structured for developed countries to act first and for developing countries to follow with financial assistance, technology transfer, and the sharing of knowledge for mitigation of emissions of ODSs as well as the destruction of ODSs within equipment or products. In 2009, the Montreal Protocol became the first multilateral environmental agreement to achieve universal ratification.

Amendments and Adjustments. As the scientific basis of ozone depletion became more certain after 1987 and substitutes and alternatives became available to replace ODSs, the Montreal Protocol was strengthened with amendments and adjustments. Each amendment is named after the city in which the Meeting of the Parties to the Montreal Protocol took place and by the year of the meeting. The timeline in Figure Q0-1 shows some of the major decisions that have been adopted. These decisions brought additional ODSs under control, accelerated the timing of existing control measures, or prescribed phaseout dates for the production and consumption of certain gases. The initial Protocol measures were a 50% reduction in chlorofluorocarbon (CFC) production and consumption by 1998 and a freeze on halon production and consumption. The 1990 London Amendment called for a phaseout of the production and consumption of the most damaging ODSs in developed nations by 2000 and in developing nations by 2010. The 1992 Copenhagen Amendment accelerated the phaseout date for CFCs, halons, carbon tetrachloride, and methyl chloroform to 1996 in developed nations and also initiated controls on future production and consumption of hydrochlorofluorocarbons (HCFCs) in developed nations. Further controls on ODSs were agreed upon in later meetings in Vienna (1995), Montreal (1997, 2007), and Beijing (1999). The latest development is the 2016 Kigali Amendment (see Q19), which expanded the Montreal Protocol to control production and consumption of hydrofluorocarbons (HFCs) with high global warming potentials (GWPs) (see Table Q6-1). As explained below, HFCs are greenhouses gases (GHGs) which warm climate in the lower atmosphere and do not cause ozone depletion.

Influence of the Montreal Protocol. Montreal Protocol phase down schedules for each group of ODSs are based on several factors including (1) the effectiveness in depleting stratospheric ozone in comparison with other substances (see Ozone Depletion Potential, ODP, in Q17), (2) the availability of suitable substitutes, and (3) the potential impact of controls on developing nations. The influence of Montreal Protocol provisions on stratospheric ODS abundances can be demonstrated with long-term changes in equivalent effective stratospheric chlorine (EESC).

Calculations of EESC combine the amounts of chlorine and bromine present in air near Earth's surface to form an estimate of the potential for ozone destruction in a particular stratospheric region on an annual basis (see definition in Q15). EESC values in the coming decades will be influenced by (1) the slow natural removal of ODSs present in the atmosphere, (2) emissions from continued production and use of ODSs, and (3) emissions from existing ODS banks. The phrase ***ODS banks*** refers to long-term containment of ODSs in various applications. Examples are CFCs in refrigeration and air-conditioning equipment as well as insulating foams, and halons in fire-extinguishing equipment. Annual emissions are projected based on release from existing banks and any new production and consumption of ODSs. The long-term changes in EESC at midlatitudes are shown in **Figure Q14-1**, based upon estimates of future emissions of ODSs that were published in year 2007 for the following cases:

- **No Protocol.** In a world-avoided scenario without the Montreal Protocol, the production, use, and emissions of CFCs and other ODSs continue to increase unabated after 1987. This No Protocol scenario is illustrated using an annual growth rate of 3% for the emissions of all ODSs. As a result, EESC increases nearly 10-fold by the mid-2050s compared with the 1980 value. Computer models of the atmosphere show that EESC under the No Protocol scenario dramatically increases global total ozone depletion between 1990 and 2020 relative to what actually occurred, and increases ozone depletion much more by midcentury. As a result, harmful UV-B radiation would have roughly doubled at Earth's surface by the middle of the 21st century, causing damage to ecosystem health, and a global rise in skin cancer and cataract cases (see Q16). Since ODSs are powerful GHGs, the climate forcing from ODSs increases substantially without the Montreal Protocol (see Q18).
- **Montreal Protocol provisions.** International compliance with only the 1987 provisions of the Montreal Protocol and the later 1990 London Amendment substantially slowed the projected growth of EESC relative to the world-avoided (No Protocol) scenario. The projections show a decrease in future EESC values for the first time with the 1992 Copenhagen Amendments and Adjustments. The provisions became more stringent with the amendments and adjustments adopted in Beijing in 1999 and Montreal in 1997 and 2007. Now, with full compliance to the Protocol, ODSs will ultimately be phased out, with some exemptions for critical uses (see Q15). Global EESC is slowly decaying from its peak value in 1998 and is expected to reach 1980 values around 2066. The success of the Montreal Protocol to date is demonstrated by the decline in ODP-weighted emissions of ODSs shown in Figure Q0-1. Total emissions peaked in 1987 at values about 10-fold higher than natural emissions

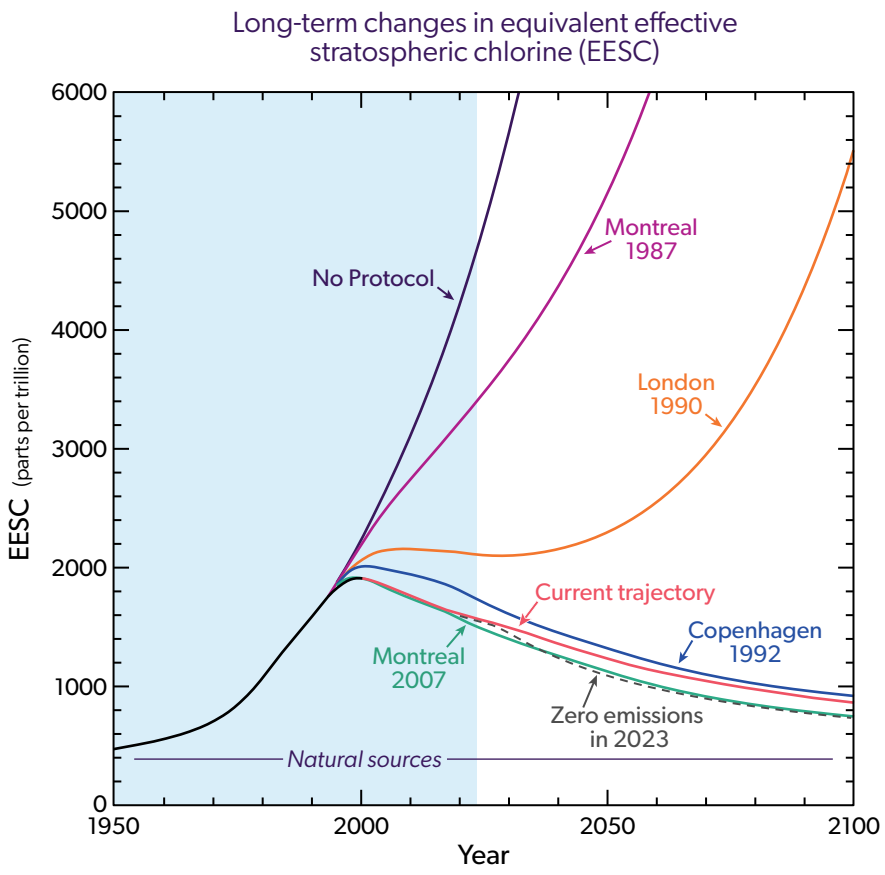

Figure Q14-1. Effect of the Montreal Protocol. The Montreal Protocol protects the ozone layer through control of the production and consumption of ozone-depleting substances (ODSs) by the world's nations. Equivalent effective stratospheric chlorine (EESC) is a quantity that represents the abundance of halogens available for ozone depletion in the stratosphere. Values of EESC are based upon either analysis of surface observations of ODSs (see Q15) or projections of future abundances of ODSs. Projections of EESC for the midlatitude lower stratosphere (about 19 km altitude) are shown separately for: no Protocol provisions; the provisions of the original 1987 Montreal Protocol and some of its subsequent amendments and adjustments as projected in in 2007; the current trajectory for EESC (red solid curve); and for future EESC assuming zero emissions of ODSs starting in 2023 (black dashed curve). The city names and years indicate where and when changes to the original 1987 Protocol provisions were agreed upon (see Figure Q0-1). Without the Protocol, EESC values would have increased significantly in the 21st century, leading to large amounts of ozone depletion throughout the world, including over highly populated regions. Only with the Copenhagen (1992) and subsequent Amendments and Adjustments do projected EESC values show a long-term decrease. The EESC values from observations shown in Figure Q15-1 lie above the Montreal 2007 projection due mainly to the use of larger emissions of ODSs from banks as well as increased emissions of ODSs from feedstocks used to manufacture various other chemicals than was considered in the original Montreal 2007 projection. Upward revision of the lifetime of CFC-11 and a few other ODSs since 2007, as well as unreported emissions of CFC-11, make small contributions to the slower decline in EESC than projected in 2007. If future emissions of ODSs from feedstocks, banks, and quarantine and pre-shipment applications of CH_3Br currently allowed under the Montreal Protocol could all be eliminated starting in 2023 (black dashed line), EESC would fall below the trajectory of full compliance following the Montreal 2007 Adjustment, as had been projected in 2007 (green line). The contributions from very short-lived gases (see Figure Q6-1), which have been minor to this point, are not included in any of these EESC time series.

(The unit "parts per trillion" is defined in the caption of Figure Q6-1.)

from methyl chloride and methyl bromide (see Q15). Between 1987 and 2022, the emissions of ODSs from human activities decreased by almost 80%.

Figure Q14-1 also shows long-term changes in EESC for two additional cases from the 2022 Scientific Assessment of Ozone Depletion report:

- **Current trajectory.** The current trajectory of EESC shown in Figure Q14-1 is based on observed abundances of ODSs from 2007 to 2021 and projected future abundances, assuming compliance with the Montreal Protocol. The current trajectory for EESC lies above the Montreal 2007 curve for two reasons: increased emissions of ODSs from banks as well as from feedstocks used for production of other chemicals, both relative to the assumptions of the original Montreal 2007 projection. The upward revision of the lifetime of CFC-11 and a few other ODSs since 2007, as well as unreported emissions of CFC-11, make small contributions to the slower decline of EESC than was projected in 2007.
- **Zero emissions.** The zero emissions scenario demonstrates the reduction in EESC that occurs if emissions of all ODSs are set to zero beginning in 2023. This assumption eliminates the emissions from new production, feedstocks, and banks. Significant differences from the current trajectory are evident in the first decades following 2023 because the phaseout of all ODS production under the Protocol will not be complete in 2023 and continued bank emissions are substantial. In the zero-emissions scenario, EESC returns to the 1980 value about a decade earlier than currently projected (solid red and dashed black lines, Figure Q14-1).

HCFC substitute gases. The Montreal Protocol provides for the use of hydrochlorofluorocarbons (HCFCs) as transitional, short-term substitute compounds for ODSs with higher ODPs, such as CFC-12. HCFCs are used for refrigeration, in making insulating foams, and as solvents, all of which were primary uses of CFCs. HCFCs are generally more reactive in the troposphere than other ODSs because they contain hydrogen (H) in addition to chlorine, fluorine, and carbon. Per amount emitted to the atmosphere, HCFCs are 88 to 98% less effective than CFC-11 in depleting stratospheric ozone because their chemical removal occurs primarily in the troposphere (see ODPs in Table Q6-1). The dominance of tropospheric removal for HCFCs prevents most of the halogen content this group of ODSs from reaching the stratosphere. In contrast, CFCs and some other ODSs release all their halogen content in the stratosphere because they are chemically inert in the troposphere (see Q5).

Under the provisions of the Montreal Protocol, developed and developing countries may continue to produce and import HCFCs over the rest of this decade before they are ultimately phased out. In the 2007 Adjustment to the Protocol, the phaseout of HCFCs was accelerated so that nearly all production ceased by 2020 for developed countries and ceases by 2030 for developing countries, about a decade earlier than in previous provisions. In making this decision, the Parties reduced the contribution of HCFC emissions to both long-term ozone depletion and future climate forcing (see Q17 and Q18).

HFC substitute gases. Hydrofluorocarbons (HFCs) are transitional substitute compounds for CFCs, HCFCs, and other ODSs. HFCs contain hydrogen, fluorine, and carbon. HFCs do not contribute to ozone depletion because they contain no chlorine or bromine. However, most HFCs and ODSs are also GHGs with long atmosphere lifetimes, so they contribute to human-induced climate change (see Q18 and Q19). Under the auspices of the United Nations Framework Convention on Climate Change (UNFCCC), HFCs are included in the basket of GHGs for which regular reporting of national annual emissions are required. The Paris Agreement of the UNFCCC is an international accord designed to reduce the emissions of GHGs in order to limit global warming to well below 2.0°C relative to the start of the Industrial Era and pursue efforts to limit global warming to 1.5°C warming. Future growth in the production and consumption of HFCs with high GWPs is now limited by the 2016 Kigali Amendment to the Montreal Protocol (see Q19).

Very short-lived (VSL) chlorine source gases. VSL halogenated source gases, defined as compounds with atmospheric lifetimes typically shorter than 0.5 years, are primarily converted to reactive halogen gases in the lower atmosphere (troposphere). Atmospheric release of most very short-lived chlorine source gases, such as dichloromethane (CH_2Cl_2, which is also known as methylene chloride) and chloroform ($CHCl_3$), results primarily from human activities. This class of compounds is not controlled by the Montreal Protocol and therefore they are not included in the estimates of EESC shown in Figure Q14-1. The atmospheric abundance of VSL chlorine source gases has increased substantially since the early 1990s and these gases presently contribute about 4% (130 ppt) to the total chlorine entering the stratosphere (see Figure Q6-1). Furthermore, the fraction of VSL gases that reach the stratosphere varies as a function of the location where the gases are emitted into the atmosphere. Should this class of compounds ever come under the control of the Montreal Protocol, future actions would be effective at lowering atmospheric abundances rather quickly, because these compounds are removed from the atmosphere within a few years.

Q15 Has the Montreal Protocol been successful in reducing ozone-depleting substances in the atmosphere?

Yes, as a result of the Montreal Protocol, the overall abundance of ozone-depleting substances (ODSs) in the atmosphere has been decreasing for the past two decades. If the nations of the world continue to comply with the provisions of the Montreal Protocol, the decrease will continue throughout the 21st century. Those gases that are still increasing in the atmosphere, HCFC-22 (CHF_2Cl) and HCFC-141b (CH_3CCl_2F), will begin to decrease this decade if compliance with the Protocol continues. However, it is only after midcentury that the abundance of ODSs is expected to fall to values that were present before the Antarctic ozone hole was first observed in the early 1980s, due to the long atmospheric lifetime of these gases.

The Montreal Protocol and its amendments and adjustments have been very successful in reducing the atmospheric abundances of ozone-depleting substances (ODSs). ODSs are halogen source gases released by human activities whose production and consumption are now controlled by the Montreal Protocol (see Q14). The success of the Montreal Protocol controls is documented by (1) observed changes and future projections of the atmospheric abundances of the principal ODSs and (2) the long-term decrease in *equivalent effective stratospheric chlorine* (EESC).

Individual ODS reductions. The reduction in the atmospheric abundance of an ODS in response to controls on production and consumption depends principally on how rapidly this ODS is used and released to the atmosphere after being produced, as well as the atmospheric lifetime of the ODS (see Table Q6-1). For example, the abundances of ODSs with short lifetimes, such as methyl chloroform, respond quickly to emission reductions. In contrast, the abundances of ODSs with long lifetimes such as CFC-11 and CFC-12 respond slowly to emission reductions. Estimates of long-term changes in the atmospheric abundances of ODSs are based upon: (1) their measured abundances in air trapped for years within accumulated snow in polar regions, (2) observed atmospheric abundances using ground-based measurements, (3) projections of future abundances based on estimated future demand and compliance with Montreal Protocol provisions for the production and consumption of ODSs, and (4) emissions from ODS banks. The term *bank* refers to the total amounts of ODSs contained in existing equipment, chemical stockpiles, foams, and other products that have not yet been released to the atmosphere. The destruction of ODSs in banks prevents the eventual release of these compounds into the atmosphere. The long-term changes of the atmospheric abundances of individual ODSs and the natural chlorine and bromine source gases, methyl chloride (CH_3Cl) and methyl bromide (CH_3Br), assuming compliance with the Montreal Protocol, are shown in **Figure Q15-1**. Key aspects of families of ODSs shown in this figure are:

- **CFCs.** Chlorofluorocarbons (CFCs) include some of the most destructive chlorine-containing ODSs. CFC-11 and CFC-12, with large Ozone Depletion Potentials (ODPs) of 1 and 0.75, are the most abundant CFCs in the atmosphere owing to large historical emissions and long atmospheric lifetimes of about 50 and 100 years, respectively (see Table Q6-1). Under the Montreal Protocol, allowed production and consumption of CFCs ended in January 1996 for developed countries and in January 2010 for developing countries. As a consequence, the atmospheric abundances of CFC-11 and CFC-113 peaked in 1994 and 1996, respectively, and have been declining for more than two decades. In contrast, the abundance of CFC-12 peaked in 2002 and has been slowly decreasing, owing to its longer lifetime (about 100 years) and continuing emissions from CFC-12 banks, namely, refrigeration and air conditioning equipment and thermal insulating foams. With no further global production of the principal CFCs, except for the use of certain CFCs (mainly CFC-113 and CFC-114) as feedstocks and some limited exempted uses, along with some continuing emissions from banks, CFC abundances are projected to decline steadily throughout this century. From 2012 to 2018, the annual decline in CFC-11 slowed measurably compared to the expected decline, due to unreported production outside the provisions of the Montreal Protocol. In 2019 and 2020, global emissions of CFC-11 declined in a manner indicative of the elimination of most of these unreported emissions.
- **Halons.** Halons are currently the most important bromine-containing ODSs. Halon-1211 and halon-1301 account for a significant fraction of bromine from all ODSs (see Figure Q6-1). Under the Montreal Protocol, production and consumption of halons for controlled uses ended in January 1994 for developed countries and in January 2010 for developing countries, with some essential use exemptions for both developed and developing countries. Atmospheric abundances of halon-1211 show significant decreases since peak concentrations were measured in the mid-2000s. Halon-2402 abundances have been decreasing slowly for the past two decades while those of halon-1301 have nearly peaked and are expected to decline in coming decades. The slow decline in the emission of halon-1301 is likely due to substantial banks in fire-extinguishing

Past and Projected Atmospheric Abundances of Halogen Source Gases

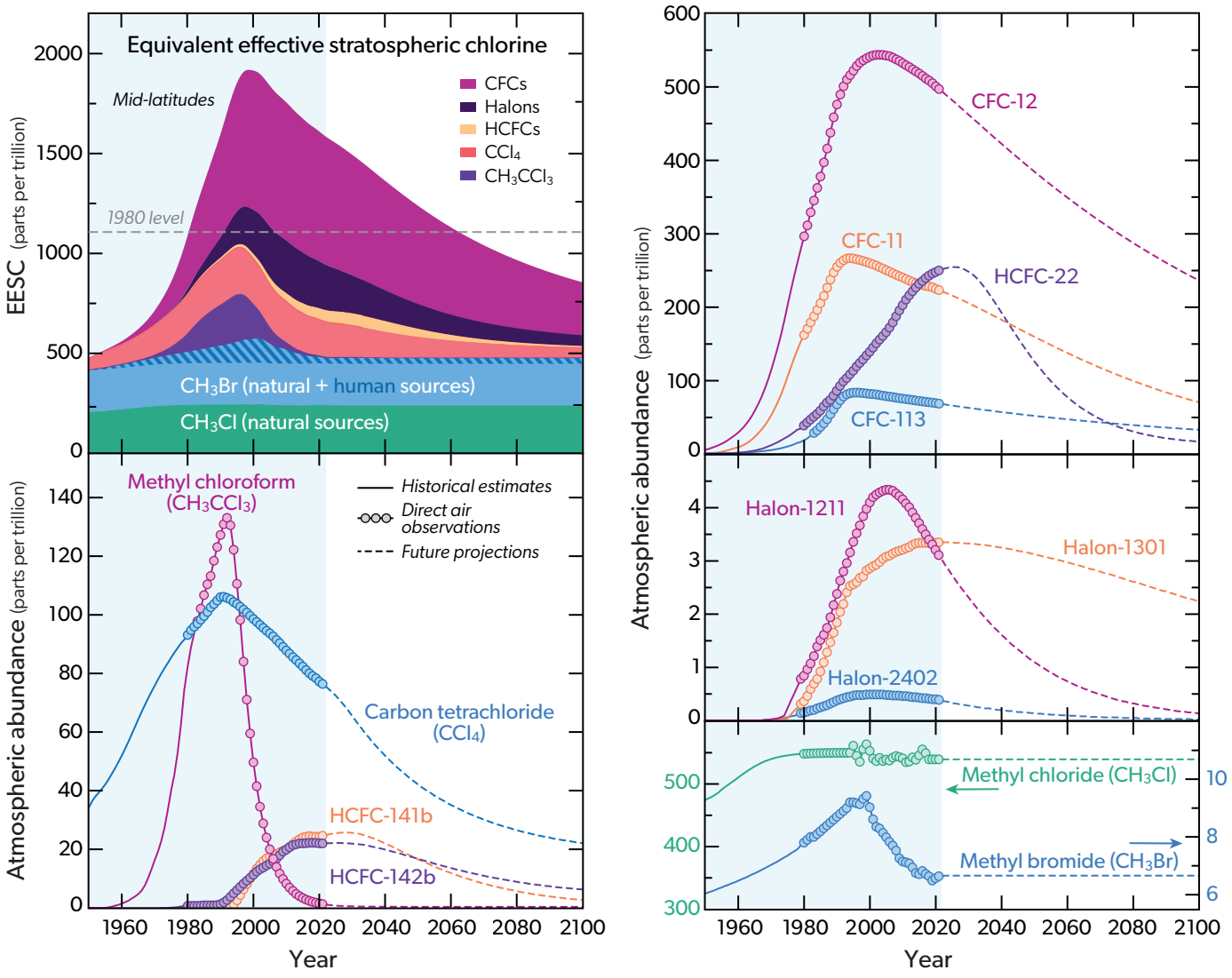

Figure Q15-1. Halogen source gas changes and contributions to EESC. The surface abundances of individual gases shown here were obtained using a combination of direct atmospheric measurements, estimates of historical abundances, and future projections of abundances assuming compliance with the Montreal Protocol. The gases are all ODSs except for methyl chloride, which is primarily emitted from natural processes. Therefore methyl chloride is not controlled by the Montreal Protocol and its abundance is projected to be constant in the future. The past increases of the principal CFCs shown in the figure, along with those of carbon tetrachloride, methyl chloroform, halon-1211, and halon-2402, have slowed and reversed in the last three decades. The abundances of most HCFCs, which are used as transitional substances to replace CFCs, will likely peak during this decade before production and consumption are completely phased out. The abundance of halon-1301 has nearly peaked and is expected to slowly decline in coming decades because of continued small releases and a long atmospheric lifetime. Future decreases in methyl bromide are expected to be modest, since most of the current source is from natural processes and the industrial production of methyl bromide is now much smaller than occurred in the 1990s. Values of EESC shown in the upper left panel are for the midlatitude lower stratosphere (about 19 km altitude), based on observations and projections (see Q14-1). The colored shaded regions depict contributions to EESC from CH_3Cl, CH_3Br, CH_3CCl_3, CCl_4, HCFCs, halons, and CFCs and the top of the magenta shaded region is the sum of all contributions, or EESC. The value of EESC rose rapidly during the latter half of the prior century, peaking in the late 1990s. Since the late 1990s, the trend in EESC has reversed due to the effectiveness of the Montreal Protocol in reducing the production and consumption of ODSs. In the midlatitude stratosphere EESC is projected to return to its 1980 value around 2066. In polar regions EESC is projected to return to 1980 values about two decades later. International compliance with the provisions of the Montreal Protocol is required to ensure that EESC will continue to decrease as projected (see Q14). Over 2012 to 2018, the decline in CFC-11 slowed measurably compared to the expected decline, due to unreported production. In 2019 and 2020, CFC-11 declined in a manner indicative of the elimination of most of this unreported production. The contributions from very short-lived gases (see Figure Q6-1) are not included in this EESC time series.

(The unit "parts per trillion" is defined in the caption of Figure Q6-1.)

and other equipment that gradually release this compound to the atmosphere years after production. The abundance of halon-1301 is expected to remain high well into the 21st century because of its long lifetime (72 years) and continued release. Atmospheric emissions of halons continue to occur due to the use of halon-containing equipment in various fire-fighting applications.

- **Carbon tetrachloride.** Production and consumption of carbon tetrachloride (CCl_4) for controlled uses in developed countries was phased out in 1996 and that in developing countries in 2010, with some essential use exemptions. As a result, atmospheric abundances of carbon tetrachloride have been decreasing for two decades. The decline is considerably less rapid than expected, suggesting that actual emissions are larger than the emissions derived from the reported consumption. Carbon tetrachloride that is used as raw material (feedstock) to make other chemicals is exempted when calculating the controlled levels of production and consumption under the Montreal Protocol, and some residual emissions do occur. Current understanding of global sources suggests emissions of carbon tetrachloride are presently dominated by inadvertent production and subsequent release during the chemical manufacturing processes of other compounds, as well as release from landfills and contaminated soils.
- **Methyl chloroform.** The largest reduction to date in the abundance of an ODS (99% from its peak value) has been observed for methyl chloroform (CH_3CCl_3). Production and consumption of methyl chloroform in developed countries ended in January 1996 and that in developing countries ended in January 2015, with limited essential use exemptions. Atmospheric abundances responded rapidly to the reduced emissions starting in the mid-1990s because methyl chloroform has a short atmospheric lifetime of about 5 years. Methyl chloroform was used mainly as a solvent and had typically been emitted soon after production. This compound is now approaching complete removal from the atmosphere due to the success of the Montreal Protocol.
- **HCFC substitute gases.** The Montreal Protocol allows for the use of hydrochlorofluorocarbons (HCFCs) as short-term, transitional substitutes for CFCs and in other specific applications. As a result, the atmospheric abundances of HCFC-22, HCFC-141b, and HCFC-142b continue to grow in response to continued production, mainly in the developing world. HCFCs pose a lesser threat to the ozone layer than CFCs, because HCFCs have lower ODP values (less than about 0.1; see Table Q6-1). The 2007 Montreal Adjustment to the Protocol accelerated the phaseout of HCFCs by a decade for both developed countries (2020) and developing countries (2030) (see Q14). Future projections indicate that the principal HCFCs will all reach peak values between 2023 and 2030, and steadily decrease thereafter. The response of atmospheric abundances to decreasing emissions (due to gradual releases from existing banks such as insulating foams) will be relatively rapid because of the short atmospheric lifetimes of HCFCs (less than 17 years).
- **Methyl chloride and methyl bromide.** Both methyl chloride (CH_3Cl) and methyl bromide (CH_3Br) are distinct among halogen source gases because substantial fractions of their emissions are associated with natural processes (see Q6). Methyl chloride is not controlled under the Montreal Protocol. The abundance of CH_3Cl in the atmosphere has remained fairly constant throughout the last 40 years (see Figure Q15-1). Current sources of methyl chloride from human activities are thought to be small relative to its natural source, and to be dominated by the combustion of coal and chemical manufacturing.

  In contrast, methyl bromide is controlled under the Montreal Protocol. Methyl bromide was primarily used as a fumigant. Nearly all developed country production and consumption of methyl bromide ended in January 2005 and that in developing countries ended in January 2015. The Protocol currently provides limited exemptions for methyl bromide production and use as a fumigant in agriculture as well as for quarantine and pre-shipment applications. Atmospheric abundances of methyl bromide declined rapidly in response to the reduced emissions starting in 1999, because its atmospheric lifetime is less than 1 year (see Figure Q15-1). Future projections show only small changes in methyl bromide abundances based on the assumptions of unchanged contributions from natural sources and small continued critical use exemptions. An important uncertainty in these projections is the future amount that will be produced and emitted under Montreal Protocol critical use, quarantine, and pre-shipment exemptions.

Equivalent effective stratospheric chlorine (EESC). Important measures of the success of the Montreal Protocol are the past and projected changes in the values of equivalent effective stratospheric chlorine, which was introduced in Figures Q13-1 and Q14-1. EESC is one measure of the potential for ozone depletion in the stratosphere that can be calculated from atmospheric surface abundances of ODSs and natural chlorine and bromine gases. The calculation considers CFCs, HCFCs, methyl chloroform, carbon tetrachloride, halons, as well as methyl chloride and methyl bromide. For both past and future EESC values, the required atmospheric abundances are derived from measurements, historical estimates, or future projections based on compliance with the provisions of the Montreal Protocol.

EESC is derived from the amount of chlorine and bromine available in the stratosphere to deplete ozone. The term equivalent indicates that bromine gases, scaled by their greater per-atom effectiveness in depleting ozone, are included in EESC. Although chlorine is much more abundant in the stratosphere than bromine (about 150-fold) (see Figure Q6-1), bromine atoms are about 60 times more efficient than chlorine atoms in chemically destroying ozone in the lower stratosphere. The term effective indicates that only the estimated fractions of ODSs that have been converted to reactive and reservoir halogen gases, for a particular region of the stratosphere at a specified time, are included in the computed value of EESC value (see Q5 and Q7). Long-term changes of EESC generally depend on the altitude and latitude region in the stratosphere under consideration. The EESC curve shown in Figure Q15-1 is for the midlatitude, lower stratosphere (about 19 km altitude).

Long-term changes in EESC. In the latter half of the 20th century up until the 1990s, EESC values steadily increased (see Figure Q15-1), causing global ozone depletion. As a result of the Montreal Protocol regulations, the long-term increase in EESC slowed,

values reached a peak in 1999, and EESC then began to decrease. By 2022, EESC at midlatitudes had declined by about 18% from the peak value. The initial decrease came primarily from the substantial, rapid reductions in the atmospheric abundance of methyl chloroform, which has a lifetime of only 5 years. The decrease is continuing with declining abundances of CFCs, carbon tetrachloride, and halon-1211. Decreases depend on natural processes that gradually decompose and remove halogen-containing gases from the global atmosphere (see Q5). Reduction of EESC to 1980 values or lower will require four more decades because the most abundant ODS gases now in the atmosphere have lifetimes ranging from 10 to 100 years (see Table Q6-1).

Q16 Does depletion of the ozone layer increase ground-level ultraviolet radiation?

Yes, ultraviolet radiation at Earth's surface increases as the amount of overhead total ozone decreases because ozone absorbs ultraviolet radiation from the Sun. Measurements by ground-based instruments and estimates made using satellite data provide evidence that surface ultraviolet radiation has increased in large geographic regions in response to ozone depletion.

Depletion of stratospheric ozone leads to an increase in solar ultraviolet radiation at Earth's surface. The increase occurs primarily in the ultraviolet-B (UV-B) component of the Sun's radiation. UV-B is defined as radiation in the wavelength range of 280 to 315 nanometers, which is invisible to the human eye. Long-term changes in UV-B radiation reaching the surface have been measured directly and can be estimated from changes in total ozone (see Q3).

Exposure to UV-B radiation can harm humans, other life forms, and materials (see Q2). Most of the effects of sunlight on the human body are caused by UV-B radiation. A principal effect is sunburn, which first appears as reddening of the skin, also called erythema. Excess exposure to UV-B radiation can lead to skin cancer. Erythemal radiation is regularly reported to the public in many countries in the form of the UV Index (UVI), which is proportional to the erythemally weighted UV radiation at Earth's surface. The UVI ranges from zero at night to more than 20 at noon for high elevations in the tropics.

Surface UV-B radiation. The amount of UV-B radiation reaching Earth's surface at a particular location depends in large part on total column ozone (see Q3) in the atmosphere at that location. Ozone molecules in the stratosphere and in the troposphere absorb UV-B radiation, thereby significantly reducing the amount that reaches Earth's surface (see Q2). If conditions occur that reduce the abundance of ozone molecules somewhere in the troposphere or stratosphere, total ozone is reduced and the amount of UV-B radiation reaching Earth's surface is increased proportionately.

Additional causes of UV changes. The actual amount of UV-B radiation reaching Earth's surface at a specific location and time depends on a number of other factors, in addition to the amount of total ozone. The primary additional factor is the elevation of the Sun in the sky, which changes at any location with daily and seasonal cycles. Other factors include the altitude of the location, local cloudiness, the amount of ice or snow cover, and the amounts of atmospheric particles (aerosols) in the atmosphere above the location. Changes in clouds and aerosols are partially related to air pollution and greenhouse gas emissions from human activities. The seasonal change in the Earth–Sun distance is also a significant factor affecting the amount of UV-B radiation reaching the surface.

Measurements indicate that both increases and decreases in UV radiation at certain locations have resulted from variations in one or more of these factors. Estimating the impact of changes in these factors is complex. For example, an increase in cloud cover usually results in a reduction of UV radiation below the clouds and at the same time could increase UV radiation at a location in the mountains above the clouds. Conversely, if clouds don't sufficiently block the direct beam from the Sun, reflections from cloud particles can result in an increase in the amount of UV-B reaching the surface.

Biologically-weighted UV and the UV Index (UVI). The effect of ozone on the amount of biologically relevant UV that arrives at the Earth's surface is governed by the wavelength dependence of the biological action involved, which typically — as in the case for skin damage — increases towards shorter (higher energy) UV-B wavelengths. Effects are commonly reported in terms of the UVI. All else being equal, the UVI rises as the abundance of total ozone declines. This inverse relationship between total ozone and the UVI measured at surface locations at stations throughout the world is shown in **Figure Q16-1**. The observations show that a 50% decline in total ozone is associated with a factor of two increase in the UVI.

The UVI is used internationally to increase public awareness about the detrimental effects of UV on human health and to guide the need for personal protective measures. Largest values of the UVI occur in the tropics, where the midday Sun has the highest elevation throughout the year and total ozone values tend to be low (see Figure Q3-1). At all latitudes, the UVI is larger in mountainous areas (due to less overhead air to scatter or absorb the radiation) and over snow- or ice-covered regions (due to increased surface reflectivity). Values of the UVI greater than 10 are considered 'extreme': under this circumstance, damage to sensitive fair skin can occur within 15 minutes of exposure.

The expected variation of the UVI with respect to total ozone is shown by the line marked "Model" in Figure Q16-1, which is in excellent agreement with the observations. The sensitivity of UV-B to ozone change is similar to that for the UVI, whereas other biological weightings exhibit different sensitivities. For example, the sensitivity for damage to DNA as a function of total ozone is about twice as large as that for the UVI and UV-B, while the sensitivity for the production of Vitamin D in the skin is intermediate between those for DNA-damage and erythema.

Long-term surface UV changes. Changes in surface UV since

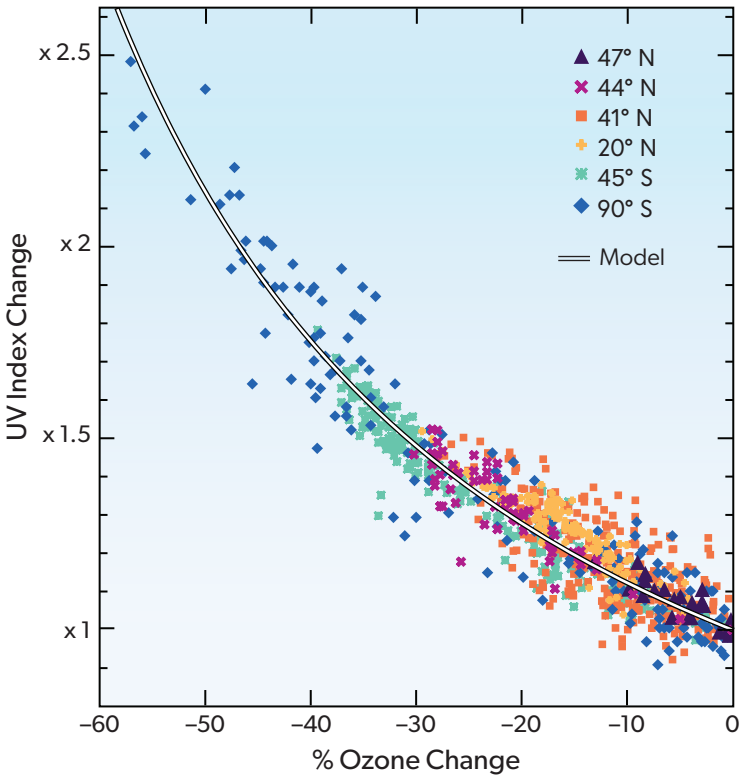

Figure Q16-1. Relationship between changes in total column ozone and the UVI measured at six sites distributed throughout the world. All data are for cloud-free conditions and are acquired at the same solar elevation for each site during the 1990s. The observed variations in ozone are large. For example, at the South Pole the ozone amount is sometimes reduced by more than 50% from its maximum. The corresponding UVI for that lowest ozone amount is a factor of 2.5 larger than for the highest ozone amount. At lower latitudes, ozone changes are smaller, but increases in the UVI can still exceed a factor of 1.5. UVI data for all sites show a similar ozone dependence, which agrees well with the dependence predicted using a model of radiative transfer through the atmosphere, as shown by the smooth curve labeled "Model".

the onset of ozone depletion are not well documented. Estimated changes derived from satellite measurements of ozone are incomplete because the backscattered radiation used by the satellites does not fully penetrate the lowermost portion of the atmosphere. Consequently, effects on UV radiation at Earth's surface due to interactions of sunlight with atmospheric aerosols and clouds must be estimated using computer models. Few ground-based measurements of UV radiation suitable for long term trend analysis were available prior to the early 1990s, during the period of most pronounced ozone depletion (see Q12). The start of the UV instrument record is further complicated by the volcanic eruption of Mount Pinatubo in 1991 (see Q13). Stratospheric aerosols from this eruption contributed to widespread ozone loss and also directly blocked solar radiation, including UV radiation, for more than a year.

The maximum daily UVI varies dramatically with location and season due largely to its strong dependence on solar elevation angle. Ground-based measurements since the early 1990s from the Palmer research station on the Antarctic Peninsula, the city of San Diego in southern California, and at Point Barrow near Utqiaġvik in northern Alaska enable a direct comparison between the UVI at polar and lower latitudes. The data show that the large geographical differences in the historical UVI have been dramatically affected by ozone depletion, especially at the Antarctic site, where the increases exceed historical geographic differences (see **Figure Q16-2**).

For San Diego and Point Barrow, the daily maximum UVI is largest during summer, when the midday Sun is closest to being overhead. For the Antarctic site, the daily maximum UVI now peaks in spring, the season of lowest total ozone due to the ozone hole (see Q10). The daily maximum UVI decreases significantly after mid-December due to the seasonal recovery of total ozone, following the break-up of the ozone hole (see Q10).

Prior to the development of the Antarctic ozone hole, the UVI was always much higher at San Diego (32°N) than at Palmer Station (64°S). Measurements at Palmer Station demonstrate the dramatic effect of Antarctic ozone depletion. There, estimates of the UVI for the years 1970 to 1976, a period before the appearance of the ozone hole, are compared with measurements for the period 1990–2020 when Antarctic ozone depletion increased the UVI throughout spring and into summer (orange shading). The development of the ozone hole led to large enhancements of the UVI that persist for many months, with the greatest increases occurring during spring.

The maximum UVI at Palmer Station is now larger by about a factor of 2.5 compared with the pre-ozone-hole period. The highest UVIs observed in spring now exceed those measured in spring and early summer in San Diego, despite San Diego's much lower latitude. The large levels of UV radiation reaching the surface due to the Antarctic ozone hole have had an adverse effect on the microscopic plants and animals at the base of the food chain in the high-latitude marine environment.

At San Diego, measurements of the UVI since 1992 and UVI values reconstructed based on pre-ozone depletion values are almost indistinguishable. This small change is consistent with the small variation in total ozone observed at subtropical latitudes (see Q12) and with the finding that the maximum daily UVI has remained essentially constant at these latitudes over about the past 20 years. At the Arctic site near Point Barrow, the UVI has increased by approximately 20% since the 1970s.

Modeling UV changes. Despite the short data record, trends in the UVI measured at unpolluted sites since the early 1990s agree well with trends calculated from changes in total ozone. These measurements show that the change in the UVI from 1996 (around the time that stratospheric chlorine peaked, see Figure Q15-1) to 2020 have been small.

Model simulations of ozone in a world without the Montreal Protocol show that large increases in the UVI due to ozone depletion occur during the period 1996 to 2020. In these simulations, at mid-southern latitudes the UVI in summer increases by

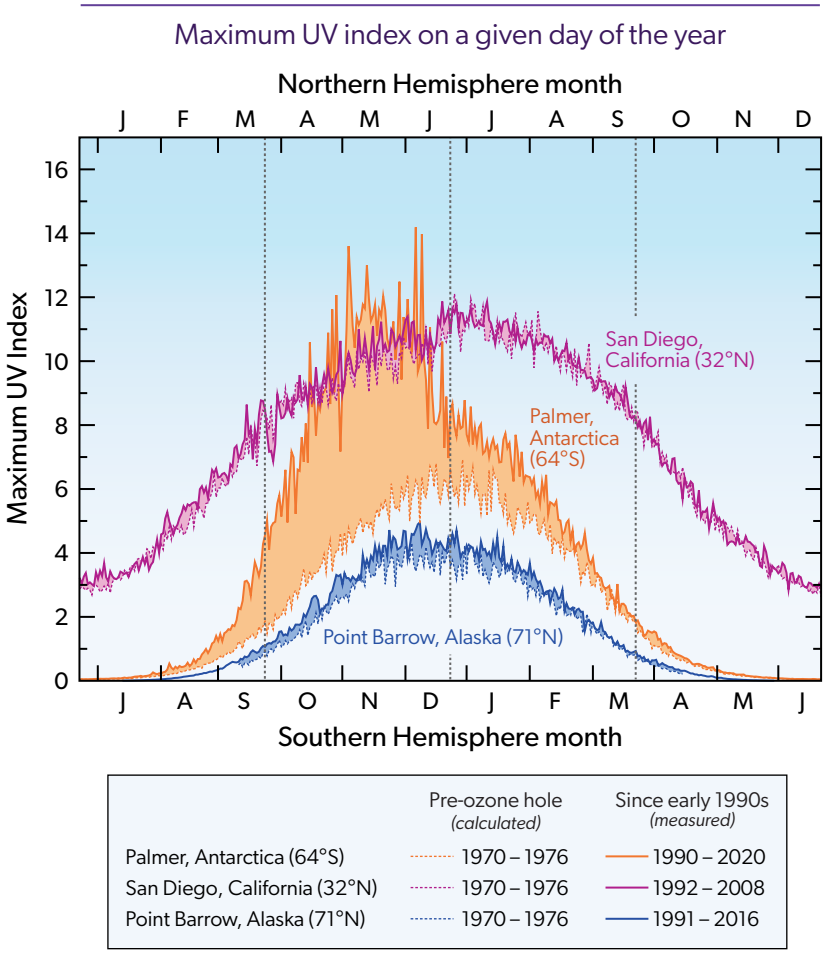

Figure Q16-2. Long-term changes in the UV Index (UVI), which is a measure of the erythemal radiation that reaches the surface. The figure shows the daily maximum UVI at three locations: San Diego, California; Point Barrow near Utqiaġvik in northern Alaska; and Palmer Station in Antarctica. The daily maximum UVI is shown for two time periods: a more recent period corresponding to the availability of measurements starting in the early 1990s (solid lines, as indicated) and a pre-ozone hole time period of 1970–1976, computed using simulated total ozone values at the three locations for this time period. The shaded region for each measurement site represents the difference between the pre-ozone hole UVI and the observed UVI, starting with early 1990s data. The UVI observations from Palmer, Antarctica demonstrate the importance of ozone depletion on the amount of erythemal radiation reaching the surface. For 1990–2020, springtime values of the daily maximum UVI at Palmer equaled or exceeded those measured in spring at San Diego, which is located at a much lower latitude and, as a consequence, experienced much larger values of the daily maximum UVI than Palmer prior to the development of the ozone hole. The three thin vertical dotted lines show the dates of the spring equinox, the summer solstice, and the autumn equinox.

about 20%, and in springtime the UVI in Antarctica doubles without the Montreal Protocol. These illustrative estimates serve as a powerful testament to the benefit of the Montreal Protocol's role in protecting human health and the environment.

UV changes and human health. Over the past several decades, depletion of the stratospheric ozone layer together with societal changes in lifestyle have increased UV radiation exposure for many people. Increased UV exposure has adverse health effects, primarily associated with eye and skin disorders. UV radiation is a recognized risk factor for eye cataracts. For the skin, the most common threat is skin cancer. Over the past decades, the incidence of several types of skin tumors has risen significantly among people of all skin types. On the other hand, an important human health benefit of UV-B radiation exposure is the production of vitamin D, which plays a significant role in bone metabolism and the immune system. Human exposure to solar UV-B radiation requires a careful balance to maintain adequate levels of vitamin D, while minimizing the risks of skin and eye disorders.

Skin cancer in humans typically occurs long after exposure to UV radiation that causes sunburn. Even under the current provisions of the Montreal Protocol and its amendments and adjustments, projections of additional skin cancer cases associated with ozone depletion are largest in the first half of the 21st century. This projection represents a significant global health issue. Since recovery to 1980 values of total ozone averaged over 60°S to 60°N is projected to occur around the middle of this century (see Figure Q20-1), ozone depletion will continue to contribute to adverse human health effects over the coming decades.

In addition to detrimental effects on human health, increases in UV radiation reaching the surface also impact air quality, aquatic and terrestrial plants and ecosystems, biogeochemical cycling, and outdoor materials. The impacts of UV radiation are discussed in greater detail in reports by the Environmental Effects Assessment Panel (EEAP) of the Montreal Protocol on Substances that Deplete the Ozone Layer[3].

[3] https://ozone.unep.org/science/assessment/eeap

Q17 Is depletion of the ozone layer the principal cause of global climate change?

No, ozone depletion is not the principal cause of global climate change. Ozone depletion and global climate change are linked because both ozone-depleting substances and their substitutes are greenhouse gases. The best estimate is that stratospheric ozone depletion has led to a small amount of surface cooling. Conversely, increases in tropospheric ozone and other greenhouse gases lead to surface warming. The effect on global climate change from stratospheric ozone depletion is small compared to the warming from the greenhouse gases responsible for observed global climate change. Since the early 1980s, the Antarctic ozone hole has contributed to changes in Southern Hemisphere surface climate through effects on the atmospheric circulation.

While stratospheric ozone depletion is not the principal cause of climate change, aspects of ozone depletion and climate change are closely linked. Both processes involve gases released to the atmosphere by human activities. The links are best understood by examining the contribution to climate change of the gases involved: ozone; ozone-depleting substances (or halogen source gases) and their substitutes; and other leading greenhouse gases.

Greenhouse gases and the radiative forcing of climate. The warming of Earth's surface and troposphere by the Sun is enhanced by the presence of greenhouse gases (GHGs). The natural abundances of GHGs in Earth's atmosphere absorb outgoing infrared radiation, trapping heat in the atmosphere and warming the surface. The most important natural GHG is water vapor. Without this natural greenhouse effect, Earth's surface would be much colder than current conditions. Human activities have led to significant increases in the atmospheric abundances of a number of long-lived and short-lived GHGs since 1750, the start of the Industrial Era, leading to warming of Earth's surface and associated climate changes. This group includes carbon dioxide (CO_2), methane (CH_4), nitrous oxide (N_2O), tropospheric ozone, and halocarbons. Ozone-depleting substances (ODSs) and their substitutes make up a large fraction of the halocarbons in today's atmosphere. Increases in the abundances of these gases from human activities cause more outgoing infrared radiation to be absorbed and reemitted back to the surface, further warming the atmosphere and surface. This change in Earth's energy balance caused by human activities is called a ***radiative forcing of climate*** or, more simply, a ***climate forcing***. The magnitude of this energy imbalance is usually evaluated at the top of the troposphere (tropopause) and is expressed using units of watts per square meter (W/m^2). The potential for climate change rises as this radiative forcing increases.

A summary of radiative forcings of climate in 2019 resulting from the increases in the principal long-lived and short-lived GHGs from human activities since 1750 is shown in **Figure Q17-1**. Positive forcings lead to warming and negative forcings lead to cooling of Earth's surface. Climate forcings also lead to other changes, for example reductions in glacier and sea-ice extent, variations in precipitation patterns, and more extreme weather events. International climate assessments conclude that much of the observed surface warming and changes in other climate parameters over the last several decades are due to increases in the atmospheric abundances of CO_2 and other GHGs, which result from a variety of human activities.

Carbon dioxide, methane, and nitrous oxide. All three of these GHGs have both human and natural sources. The accumulation of CO_2 since 1750 represents the largest climate forcing caused by human activities. Carbon dioxide concentrations continue to increase in the atmosphere primarily as the result of burning fossil fuels (coal, oil, and natural gas) for energy and transportation, as well as from cement manufacturing. The global mean atmospheric abundance of CO_2 exceeded 416 parts per million (ppm) in 2021, which is about 50% larger than the abundance of CO_2 present in 1750. Carbon dioxide is considered a long-lived gas, since a significant fraction remains in the atmosphere 100 to 1000 years after emission.

Methane is a ***short-lived*** climate gas (atmospheric lifetime of about 12 years). Sources related to human activities include livestock, fossil fuel extraction and use, rice agriculture, and landfills. Natural sources include wetlands, termites, and oceans. The global mean atmospheric abundance of CH_4 has more than doubled since 1750.

Nitrous oxide is a ***long-lived*** climate gas (atmospheric lifetime of about 109 years). The largest source related to human activities is agriculture, especially the use of fertilizer. Microbial processes in soils that are part of natural biogeochemical cycles represent the largest natural source. In the stratosphere, nitrous oxide is the principal source of reactive nitrogen species that participate in ozone destruction cycles (see Q8). The global mean atmospheric abundance of nitrous oxide has increased by about 22% since 1750.

Halocarbons. Halocarbons in the atmosphere contribute to both ozone depletion and climate change. The halocarbons considered in Figures Q17-1 and **Q17-2** are gases containing chlorine, bromine, or fluorine atoms that are either controlled under the Montreal Protocol or are GHGs that fall under the auspices of the United Nations Framework Convention on Climate Change (UNFCCC). Historically, ODSs were the only halocarbons controlled under the Montreal Protocol. In 2016, the Kigali Amend-

Greenhouse Gases and Climate Change

Climate forcing due to changes in greenhouse gases caused by human activities between 1750 and 2019

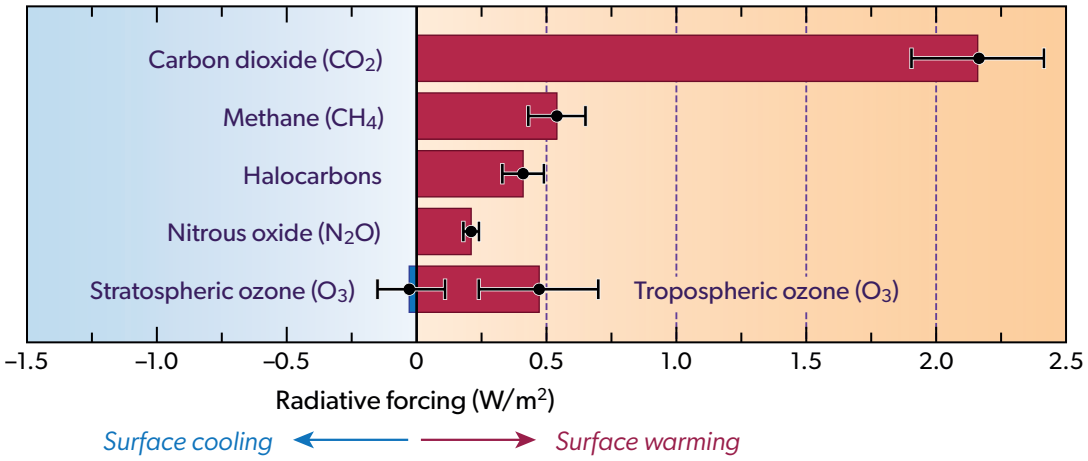

Figure Q17-1. Radiative forcing of greenhouse gases and ozone depletion. Human activities since the start of the Industrial Era (around 1750) have caused increases in the atmospheric abundance of greenhouse gases (GHGs). Rising levels of GHGs lead to an increase in the radiative forcing (RF) of climate by trapping infrared radiation released by Earth's surface. Here, values of RF are for the time period from 1750 to 2019 and are expressed in units of watts per square meter (W/m^2); black whiskers on each bar show uncertainties. Positive values of RF (shown in red) contribute to global warming and negative values (shown in blue) contribute to climate cooling. The largest positive RFs are due to carbon dioxide (CO_2), methane (CH_4), tropospheric ozone (O_3), halocarbons, and nitrous oxide (N_2O). Halocarbons include all ozone-depleting substances, hydrofluorocarbons, and a few other gases (see Figure Q17-2). The RF due to ozone is shown as the separate response to changes in ozone within two layers of the atmosphere: the troposphere and stratosphere. Tropospheric ozone increases result from the emission of air pollutants and lead to a positive RF whereas stratospheric ozone depletion leads to a small RF that could be negative or positive.

ment to the Montreal Protocol established controls on the future production and consumption of certain hydrofluorocarbon (HFC) gases. Perfluorocarbons (PFCs) and sulfur hexafluoride (SF_6) are in the UNFCCC group of GHGs that now fall under the Paris Agreement. Perfluorocarbons are compounds that contain only carbon and fluorine atoms, such as carbon tetrafluoride (CF_4) and perfluoroethane (C_2F_6). Technically, SF_6 is not a halocarbon since it lacks carbon. However, the environmental effects of SF_6 are commonly examined with those of halocarbon gases since all of these compounds contain at least one halogen atom.

In 2019, the halocarbon contribution to the radiative forcing (RF) of climate was 0.41 W/m^2, which is the fourth largest GHG forcing following carbon dioxide, methane, and tropospheric ozone (see Figure Q17-1). The contributions of individual halocarbon gases controlled by the Montreal Protocol are highlighted in Figure Q17-2. Within the halocarbons, CFC-12, CFC-11, and CFC-113 combined contribute the largest percentage (67%) to radiative forcing in 2019. The intermediate-term ODS substitutes, hydrochlorofluorocarbons (HCFCs), make the next largest contribution (15%). The long-term ODS substitutes HFCs plus PFCs and SF_6 contribute 13%. Finally, CCl_4 and CH_3CCl_3 contribute an additional 3% and the minor CFCs and halons contribute 2% to radiative forcing in 2019.

The large contribution of the CFCs to radiative forcing has been gradually decreasing following the decline in their atmospheric abundance and is expected to further decrease (see Figure Q15-1). Based on their long lifetimes, CFCs will still make a significant contribution, and most likely the largest contribution from ODSs, to the radiative forcing by halocarbons at the end of this century. Even with adherence to the provisions of the Kigali Amendment to the Montreal Protocol, the radiative forcing from HFCs is projected to increase for another two to three decades before starting to slowly decline (see Figure Q19-2).

Stratospheric and tropospheric ozone. Ozone in both the stratosphere and the troposphere absorbs infrared radiation emitted from Earth's surface, trapping heat in the atmosphere. Ozone also significantly absorbs solar ultraviolet (UV) radiation. As a result, increases or decreases in stratospheric or tropospheric ozone induce a climate forcing and, therefore, represent direct links between ozone and climate. Air pollution from a variety of human activities has led to increases in global tropospheric ozone (see Q2), causing a positive radiative forcing (warming) estimated to be +0.47 W/m^2 over the 1750–2019 time period, with a range of uncertainty spanning +0.24 to +0.70 W/m^2 (see Figure Q17-1). The large uncertainty in the climate forcing due to release of air pollutants reflects our limited knowledge of changes in the abundance of tropospheric ozone between 1750 and the mid-1950s as well

Radiative Forcing of Climate by Halocarbons

Climate forcing due to increases in controlled gases containing chlorine, bromine, and fluorine from human activities between 1750 and 2019

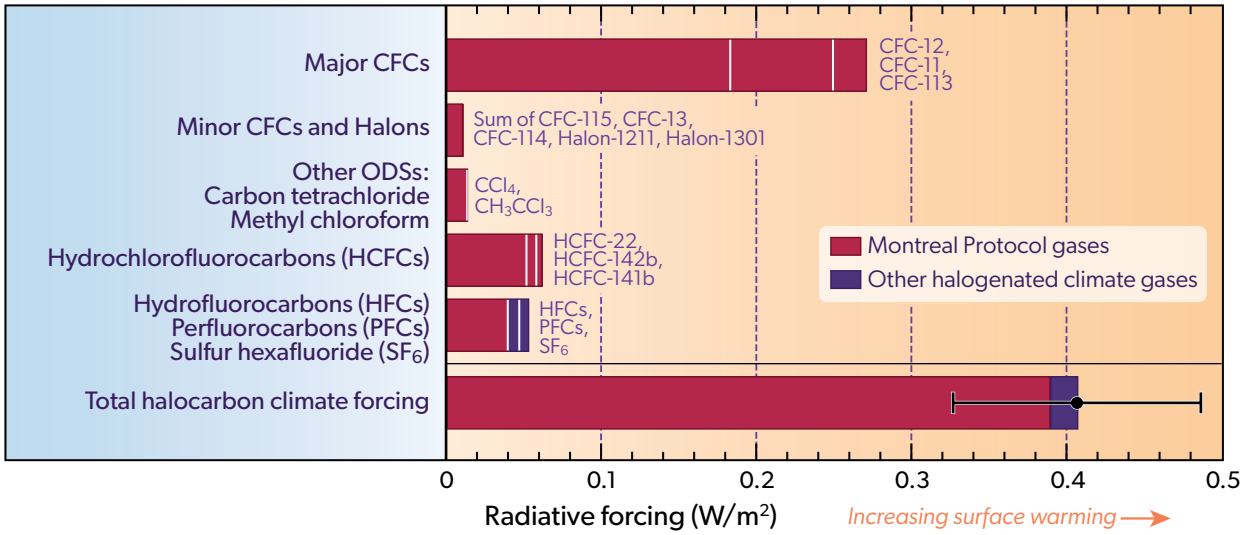

Figure Q17-2. Halocarbons and radiative forcing of climate. Halocarbon gases in the atmosphere represent an important contribution to the radiative forcing (RF) of climate since the start of the Industrial Era (see Figure Q17-1). Halocarbons are gases containing chlorine, bromine, or fluorine atoms, with at least one carbon atom, that contribute to RF by trapping infrared radiation released by Earth's surface. The rise in RF between 1750 and 2019 is shown for all halocarbons controlled either under the Montreal Protocol (red) or included in the Paris Agreement (blue) along with the RF due to the rise in SF_6. Note that while SF_6 is technically not a halocarbon because it lacks any carbon atoms, it is an important halogen-containing gas in the atmosphere. Separate contributions to RF of each gas or group of gases are based upon atmospheric abundance histories and the radiative efficiency specific to each compound. The gases listed in the right-hand labels begin with the largest contribution in each group and proceed in descending order, except for the entry for minor CFCs and halons, which are shown as one total value. The individual RF terms add together to form the bottom bar, representing the total RF due to controlled halocarbons, PFCs, and SF_6. The RFs of CFC-11 and CFC-12, the largest halocarbon contributors, are decreasing and will continue to decline as CFCs are gradually removed from the atmosphere (see Figure Q15-1). In contrast, the total RF of HCFCs, the intermediate-term ODS substitute gases, is projected to grow for about another one to two decades before decreasing. HFCs are the long-term ODS substitute gases. With the October 2016 Kigali Amendment, the Montreal Protocol now controls future production and consumption of HFCs with high Global Warming Potentials. As a result, nearly all of the RF due to halogen-containing GHGs is now controlled by the Montreal Protocol (bottom bar). The future RF of climate due to HFCs is expected to peak in about two decades under the provisions of the Kigali Amendment (see Q19).

as the difficulty in modeling the complex chemical processes that control the production of tropospheric ozone.

On the other hand, rising abundances of ODSs in the atmosphere since the middle of the 20th century have led to decreases in stratospheric ozone, causing a negative radiative forcing of –0.02 W/m^2 (cooling) over the 1750–2019 time period, with a range of uncertainty spanning –0.15 to +0.11 W/m^2 (see Figure Q17-1). The sign of the radiative forcing due to stratospheric ozone depletion is uncertain because this quantity is the difference between two terms of comparable magnitude, each of which has an associated uncertainty. The first term represents the trapping by ozone of outgoing infrared radiation released by the surface and lower atmosphere: this is a cooling term because less ozone results in less trapping of heat. The second term represents the absorption of solar UV radiation by ozone: this is a warming term because less ozone results in greater penetration of solar UV radiation into the lower atmosphere (troposphere). This radiative forcing due to stratospheric ozone depletion will diminish in the coming decades, as ODSs are gradually removed from the atmosphere.

It is clear that stratospheric ozone depletion is not a principal cause of present-day global warming. First, the climate forcing from ozone depletion is small. Second, the total radiative forcing of climate from other GHGs such as carbon dioxide, methane, halocarbons, and nitrous oxide is large and positive, leading to warming (see Figure Q17-1). The total forcing from these other GHGs is the principal cause of the observed warming of Earth's surface.

Ozone Depletion Potentials and Global Warming Potentials. A useful way of comparing the influence of individual emissions of halocarbons on ozone depletion and climate change is to compare Ozone Depletion Potentials (ODPs) and Global Warming Potentials (GWPs). The ODP and GWP are the effectiveness of an emission of a gas in causing ozone depletion and climate forcing,

Evaluation of Selected Ozone-Depleting Substances and Substitute Gases

Relative importance of equal mass emissions for ozone depletion and climate change

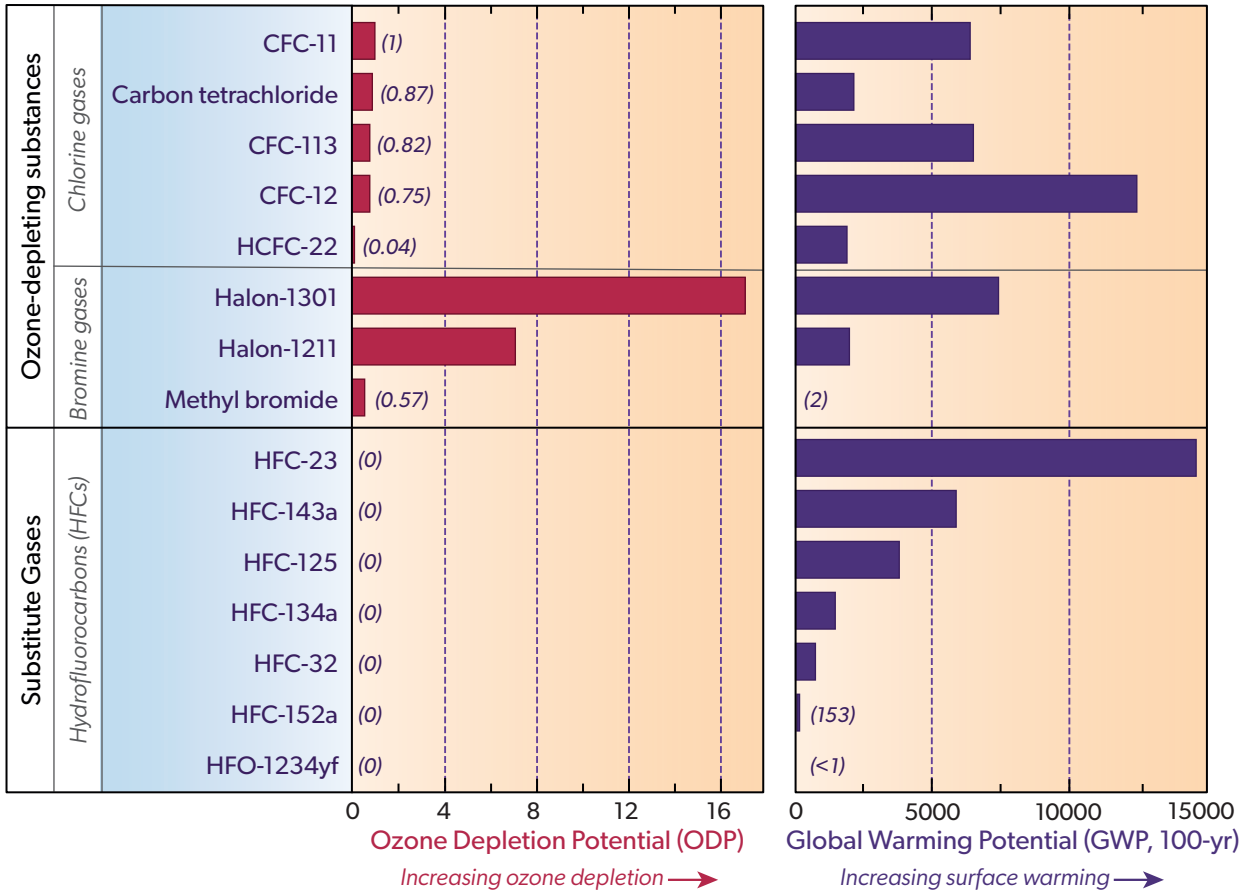

Figure Q17-3. ODPs and GWPs. The environmental impacts of ozone-depleting substances and their substitutes are commonly compared based upon their Ozone Depletion Potentials (ODPs) and Global Warming Potentials (GWPs) (see Table Q6-1). The ODPs and GWPs represent the magnitude of ozone depletion and climate forcing, respectively, of a given mass of gas emitted to the atmosphere, relative to that of CFC-11 (for ODP) or CO_2 (for GWP). Therefore, the ODP of CFC-11 and the GWP of CO_2 are assigned reference values of 1. The GWPs shown here are evaluated for a 100-year time interval after emission. The CFCs, halons, and HCFCs are ozone-depleting substances (ODSs) since they contain either chlorine or bromine (see Q6). HFCs, used as ODS substitutes, do not destroy ozone (ODPs equal zero) since they are mixtures of only hydrogen, fluorine, and carbon atoms. The ODPs of halons far exceed those of the CFCs, since all halons contain bromine. The GWPs of these gases span a wide range of values, from less than 1 (HFO-1234yf) to 14,700 (HFC-23).

respectively, relative to a reference gas (see Table Q6-1). The principal halocarbon gases are contrasted with each other in **Figure Q17-3**. The ODP of CFC-11 and the GWP of carbon dioxide are assigned reference values of 1. The CFCs and carbon tetrachloride all have ODPs near 1, indicating comparable effectiveness in causing ozone depletion per mass emitted. The principal halons have ODPs greater than 7, making them the most effective ozone-depleting substances per mass emitted. All HFCs have ODPs of zero since they contain no chlorine and bromine, and therefore do not directly cause ozone depletion (see Q6).

All halocarbons have non-zero GWPs and, therefore, contribute to the RF of climate. The GWP does not correspond strongly with the ODP of a gas because these quantities depend on different chemical and physical properties of the molecule. For example, while HFC-143a does not destroy ozone (ODP equals zero), each kilogram emitted is about 6000 times more effective than a kilogram of carbon dioxide in causing climate forcing. When HFCs are released to the atmosphere, their contribution to climate forcing depends on their GWPs, which vary over a wide range (less than 1 to 15,000).

Montreal Protocol regulations have led to reductions in CFC emissions and increases in HCFC emissions (see Q15). As a result of these actions, the total RF from ODSs stopped increasing and is now slowly decreasing because HCFCs have lower GWPs than

CFCs (see Q18). However, the overall RF of all halocarbons is slowly increasing because of growing contributions from non-ODS gases (HFCs, PFCs, and SF_6). The growth in the HFC contribution will be limited by the provisions of the 2016 Kigali Amendment (see Q19). It is important to note that despite having a GWP that is small in comparison to many other halocarbons and other greenhouse gases, carbon dioxide is the most important greenhouse gas produced by human activities because its emissions are large, its atmospheric lifetime is long, and its atmospheric abundance is far greater than those of all other greenhouse gases associated with human activities.

The Antarctic ozone hole and Southern Hemisphere climate. While stratospheric ozone depletion is not the principal cause of global climate change, the reoccurring Antarctic ozone hole has contributed to observed changes in climate parameters in the atmosphere and oceans of the Southern Hemisphere since the early 1980s. These research findings are explained in more detail in the box below.

The Antarctic Ozone Hole and Southern Hemisphere Surface Climate

Links between stratospheric ozone depletion and changes in surface climate were first found in research studies in the early 2000s, based on both observations and models. While increasing greenhouse gases (such as carbon dioxide, methane, and nitrous oxide) are the primary drivers of global climate change, the Antarctic ozone hole, which has occurred every spring since the early 1980s, was shown to contribute to observed changes in Southern Hemisphere (SH) surface climate during summer due to the effect of the ozone hole on atmospheric circulation.

The severe springtime depletion of ozone over the Antarctic leads to a strong cooling of the polar lower stratosphere persisting into early summer in the SH. This cooling increases the temperature contrast between the tropics and the polar region and strengthens stratospheric winds. As a result, in the SH there has been a poleward shift of tropospheric circulation features including the tropical Hadley cell (which determines the location of the subtropical dry zones) and the midlatitude jet stream (which is associated with weather systems). There is evidence from both models and observations that subtropical and midlatitude summer precipitation patterns in the SH have been affected by these changes. Model studies indicate that even though long-lived greenhouse gases that cause climate change exacerbate this shift in the summertime tropospheric circulation in the Southern Hemisphere, ozone depletion has been the dominant contributor to the observed changes since the early 1980s. Paleoclimate reconstructions suggest the current state of these climate features caused by the annually recurring ozone hole is unprecedented over the past 600 years.

Initial signs of the recovery of the ozone hole, particularly during September, are emerging (see Q10). During the 21st century, as the ozone hole further recovers due to the decline of stratospheric halogens, the ozone-depletion related climate impacts discussed above will lessen (see Q20). The influence of the ozone hole on SH circulation trends during summer has recently stabilized, due to the initial recovery of the area and depth of the ozone hole (see Q10). The Southern Hemisphere surface climate response to ozone depletion in other seasons is weaker than the summer response.

Q18 Are Montreal Protocol controls of ozone-depleting substances also helping protect Earth's climate?

Yes. Many ozone-depleting substances (ODSs) are also potent greenhouse gases that contribute to global warming when they accumulate in the atmosphere. Montreal Protocol controls have led to a substantial reduction in the emissions of ODSs over the last two decades. These reductions, while protecting the ozone layer, have the additional benefit of reducing the human contribution to climate change. Without Montreal Protocol controls, the global warming due to ODSs could now be nearly three times the present value. With the 2016 Kigali Amendment to the Montreal Protocol, climate protection was extended to include controls on HFCs, which do not deplete ozone but contribute to global warming (see Q19).

The success of the Montreal Protocol in controlling the production and consumption of ozone-depleting substances (ODSs) has protected the ozone layer (see Q14). The resulting reductions in emissions and atmospheric abundances of ODSs also decreased the human influence on climate because all ODSs are greenhouse gases (see Q17). By protecting both ozone and climate, the Montreal Protocol has provided a ***dual benefit*** to society and Earth's ecosystems. As shown in **Figure Q18-1** and described below, the dual benefit of the Montreal Protocol is highlighted by considering long-term ***baseline*** and ***world-avoided*** scenarios of ODS emissions, Ozone Depletion Potentials (ODPs), Global Warming Potentials (GWPs), equivalent effective stratospheric chlorine (EESC), and the radiative forcing (RF) of climate.

Baseline ODS scenario. The baseline scenario refers to actual past ODS emissions of the principal halogen source gases and projected emissions for the years 2021 to 2025. The baseline scenario is labeled "from observed ODS abundances" in Figure Q18-1 since, for 1960–2020, the emissions are based upon analysis of observed abundances of the principal ODS gases at Earth's surface (see Figure Q15-1). This scenario also includes emissions of the naturally occurring halogen source gases methyl chloride (CH_3Cl) and methyl bromide (CH_3Br). For this scenario the peak emission of ODSs occurs in the late 1980s (see Figure Q0-1).

For all of the emission scenarios shown in Figure Q18-1, the annual emissions of each gas are added together after being weighted (multiplied) by their corresponding Ozone Depletion Potential (ODP) (upper left) or Global Warming Potential (GWP) (upper right) (see Q17 and Table Q6-1). The ODP and GWP of a given gas quantify how effective the gas is at destroying ozone (ODP) or warming climate (GWP) for the emission of a certain mass of the gas, relative to the effect on ozone or warming of the emission of the same mass of CFC-11 (for ODP) or CO_2 (for GWP). In both cases, the reference gases (CFC-11 and CO_2) are assigned a value of 1, and the ODP and GWP for all other gases are scaled accordingly (see Table Q6-1 and Q17). For example, 1 kg of halon-1211 emissions is expressed as 7.1 kg of CFC-11-equivalent emissions because the ODP of halon-1211 is 7.1. Similarly, the GWP-weighted sum is expressed as CO_2-equivalent emissions because CO_2 is the reference gas, with an assigned GWP of 1. Likewise, 1 kg of carbon tetrachloride emissions is considered to be 2150 kg of CO_2-equivalent emissions because the GWP of carbon tetrachloride is 2150. GWP-100 values are shown here and throughout reflecting a choice of a time horizon of 100 years.

World-avoided ODS scenario. The baseline scenario of ODS emissions can be contrasted with a scenario of ODS emissions that the world has avoided by successfully implementing the Montreal Protocol (see Figure Q18-1). The world-avoided scenario is derived by assuming that, from 1987 onwards, emissions of ODSs increase at a rate of 3% per year. This growth rate is consistent with the strong market for ODSs in the late 1980s, which included a wide variety of current and potential applications and had the potential for substantial growth in developing countries.

CO_2 emission scenario. Long-term emissions of CO_2 are also shown in the upper right panel of Figure Q18-1. Atmospheric CO_2 is the principal greenhouse gas emitted by human activities. The CO_2 emission curve represents global emissions from the sum of each nation's reported emissions from the combustion of coal, oil, natural gas, as well as the fuels used by the world's ships and airplanes, cement manufacturing, and the release of CO_2 due to global deforestation.

ODP-weighted emissions. The ODP-weighted emission scenario based upon observed ODS abundances is one measure of how the overall threat to stratospheric ozone from ODSs has changed over time (see Figure Q18-1, upper left panel). Since most ODSs remain in the atmosphere for years (see "Atmospheric lifetime" column in Table Q6-1), when ODP-weighted emissions rise this means there will be an increase in ozone destruction for many future years. Conversely, when emissions decline, less ozone will be destroyed in future years than if emissions had remained high. Annual ODP-weighted emissions increased substantially between 1960 and 1987, the year the Montreal Protocol was signed (see Figure Q0-1). After 1987, annual ODP-weighted emissions began a long and steady decline to present-day values. The decline in emissions is expected to continue, causing the atmospheric abundances of all individual ODSs to eventually decrease (see Figure Q15-1). The

The Montreal Protocol Protection of Ozone and Climate from Global Emissions of Ozone-Depleting Substances (ODSs)

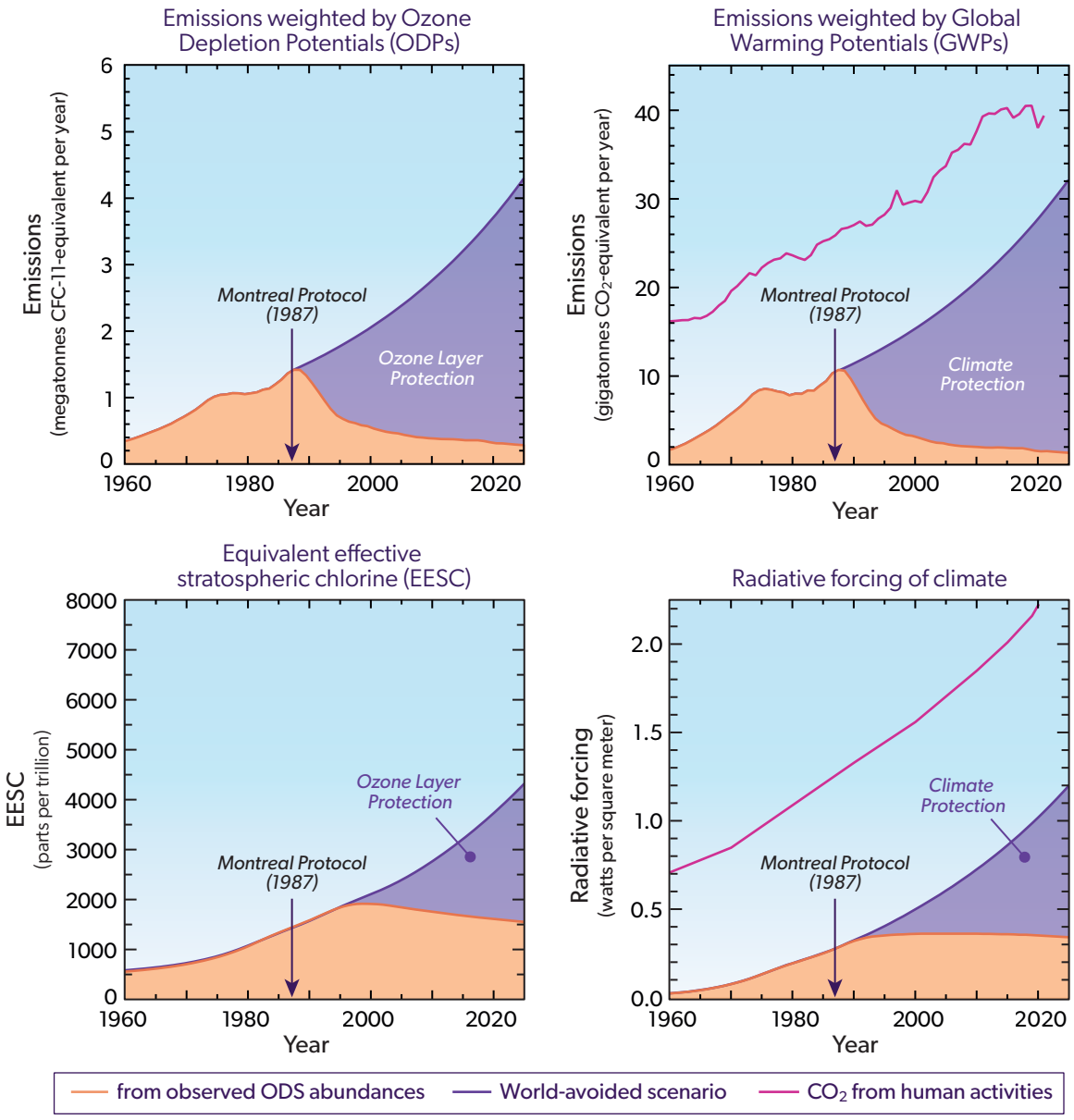

Figure Q18-1. Montreal Protocol protection of ozone and climate. The Montreal Protocol has protected the ozone layer and also reduced the potential for climate change, because ozone-depleting substances (ODSs) are greenhouse gases (GHGs). The baseline ODS scenario (orange line) includes actual emissions of all principal gases weighted either by their Ozone Depletion Potentials (ODPs) (upper left) or Global Warming Potentials (GWPs) (100-yr timeline) (upper right) coupled with projected emissions for years 2021 to 2025. With these weightings, emissions are expressed as CFC-11-equivalent or CO_2-equivalent mass per year. The lower panels show equivalent effective stratospheric chlorine (EESC) (see Figure Q15-1) and total radiative forcing (RF) of climate (see Figure Q17-2), as derived from the observed abundances of ODSs as well as projected abundances for 2021 to 2025. The world-avoided emission scenario (purple line) assumes a 3% per year growth in the emission of ODSs beyond 1987 values, consistent with the assumption for the No Protocol scenario shown in Figure Q14-1. The emission and RF of atmospheric CO_2 (magenta line) are shown for reference on the right panels. The magnitude of the dual benefit of the Montreal Protocol has steadily increased since 1987, as shown by the differences between the world-avoided scenario and the observed ODS abundance scenario (purple shaded region) in each panel.

(A megatonne = 1 million (10^6) metric tons = 1 billion (10^9) kilograms. A gigatonne = 1 billion (10^9) metric tons = 1 trillion (10^{12}) kilograms. A CFC-11-equivalent emission of an ODS is an emission amount that results in the same ozone depletion as the release of the same mass of CFC-11; a CO_2-equivalent emission of a non-CO_2 GHG is an emission amount that results in the same RF of climate over a 100-year time interval as the release of the same mass of CO_2. Emissions of CO_2 used in this figure are from the Global Carbon Project.

reductions in ODP-weighted emissions relative to the peak value in 1987 represent lower limits of the annual emissions avoided by the Montreal Protocol, which are a measure of its increasing success over time in protecting the ozone layer.

The upper limits of annual reductions in ODP-weighted emissions are derived from the world-avoided scenario. The difference between the world-avoided emission scenario and the baseline scenario (purple shaded region in Figure Q18-1, upper left panel) represents an estimate of the ozone layer protection provided by the Montreal Protocol.

GWP-weighted emissions. The GWP-weighted emission scenario based upon observed ODS abundances is a measure of how the overall threat to Earth's climate from ODSs has changed over time (see Figure Q18-1, upper right panel). As GWP-weighted emissions rise, the RF of climate in the future due to the accumulation of ODSs in the atmosphere also increases. The long-term changes in the GWP-weighted scenario are very similar to those in the ODP-weighted scenario. Both show an increase before 1987 and a decrease afterwards. This similarity follows from the dominant role that both CFC-11 and CFC-12 play in ozone depletion and climate forcing from ODSs. The difference between the world-avoided emission scenario and the baseline scenario (purple shaded region in Figure Q18-1, upper right panel) represents an estimate of the climate protection provided by the Montreal Protocol.

Annual GWP-weighted emissions of ODSs were a large percentage (about 20–40%) of global emissions of CO_2 between 1960 and 1987. Thereafter, this percentage has steadily decreased and was 2–3% of global CO_2 emissions in 2022. This past trend stands in sharp contrast to the world-avoided scenario, in which emissions of ODSs rise to more than 50% of CO_2 emissions in 2022. Another way to understand the climate benefit of the Montreal Protocol is to compare the height of the purple shaded region in 2022 to the rise in the emissions of CO_2 since 1987, as shown in Figure Q18-1 (upper right panel). These two quantities are nearly equal in magnitude, demonstrating that since 1987 the Montreal Protocol has avoided an increase in GWP-weighted emissions of ODSs that nearly equals the increase in global emissions of CO_2 over this same time period.

EESC scenarios. The EESC scenarios in Figure Q18-1 (lower left panel) provide a measure of the year-to-year potential of the atmospheric abundances of ODSs to destroy stratospheric ozone. Two scenarios are shown: the baseline that uses observed abundances of ODSs (with a projection to 2025) and the world-avoided scenario described above. The derivation of EESC from ODS atmospheric abundances is discussed in Q15 and the same EESC baseline scenario is shown in Figures Q13-1, Q14-1 (red curve), and Q15-1 for different time intervals. When ODS- weighted emissions declined after 1987, EESC did not decrease in a proportional manner because of the long atmospheric lifetimes of the principal ODSs (see Table Q6-1). As shown in Figure Q18-1, EESC reached its peak value nearly a decade after the peak in ODP-weighted emissions, and by 2022 the decrease in EESC from its peak value was only about 18%, compared to the 80% decrease in ODP-weighted emissions achieved by 2022. Conversely, had the emissions of ODSs followed the world-avoided scenario, EESC would be more than twice the value in today's stratosphere. In this case, computer simulations show global total ozone values in 2020 are about 17% lower than the 1964–1980 average. Even larger depletions occur in subsequent years. The Montreal Protocol and its amendments and adjustments have provided vitally important protection to the global ozone layer and climate.

Radiative forcing (RF) scenarios. The RF of climate scenarios in Figure Q18-1 (lower right panel) provide a measure of the year- to-year contribution to climate change from the atmospheric abundances of ODSs. The RF of an ODS is equal to the net increase in its atmospheric abundance since 1750 multiplied by its radiative efficiency, which quantifies how effective a given ODS molecule is at retaining infrared radiation. The RF of ODSs up to the present is calculated using observed atmospheric abundances. The RF due to ODSs increases smoothly from 1960 onward, peaks in 2010, and decreases very gradually in subsequent years. The decline of RF of climate in response to ODS emission reductions is slow because of the high abundances of the two principal contributing gases, CFC-11 and CFC-12, and their long atmospheric lifetimes of about 50 and 100 years, respectively.

Increasing the benefits of the Montreal Protocol. The benefit of the Montreal Protocol for protection of climate was expanded in 2016 through the Kigali Amendment, which placed controls on the production and consumption of some hydrofluorocarbons (HFCs) (see Q19). HFC compounds do not contain chlorine or bromine, and therefore do not deplete ozone. Many HFC gases have a high radiative efficiency and a long atmosphere lifetime, which leads to significant global warming (see Figure Q19-2). The ozone layer and climate benefits of the Montreal Protocol could be further increased by expanded capture and destruction of halons, chlorofluorocarbons (CFCs), and hydrochlorofluorocarbons (HCFCs) in banks, by avoiding emissions in continued use of ODSs as feedstock for the production of other chemicals, and by eliminating future emissions of halogen source gases not controlled by the Montreal Protocol, such as dichloromethane (CH_2Cl_2). Banks are largely associated with ODSs contained in refrigeration, air conditioning, fire protection equipment, insulating foams, and stockpiles for servicing long-term applications. Atmospheric release of ODSs from existing banks is projected to contribute more to ozone depletion in the coming decades than the limited production and consumption of ODSs (HCFCs and CH_3Br) allowed by the Montreal Protocol after 2023. If all available options were implemented to avoid future atmospheric release of ODSs starting in 2023, the return of EESC to 1980 values would be advanced by about a decade for both the midlatitude (see Fig Q14-1) and polar stratosphere.

Q19 How has the protection of climate by the Montreal Protocol expanded beyond the regulation of ozone-depleting substances?

At the 28th Meeting of the Parties to the Montreal Protocol held in Kigali, Rwanda, in October 2016, the Montreal Protocol was amended to control the production and consumption of hydrofluorocarbons (HFCs). The Montreal Protocol phaseout of chlorofluorocarbons (CFCs) led to the temporary use of hydrochlorofluorocarbons (HCFCs). The subsequent phaseout of HCFCs led to expanded long-term use of HFCs, because HFCs pose no direct threat to the ozone layer. However, HFCs are greenhouse gases and therefore contribute to climate change. Limiting the production and consumption of those HFCs with high global warming potentials is projected to avoid 0.3 to 0.5°C of global warming over this century. The Kigali Amendment marks the first time the Montreal Protocol has adopted regulations solely for the protection of climate.

The control of ozone-depleting substances (ODSs) by the Montreal Protocol provides the dual benefit of protecting Earth's ozone layer and global climate (see Q18). The widespread global use of hydrofluorocarbons (HFCs) and their projected future growth in the coming decades has been recognized by the Montreal Protocol as a potentially significant contribution to climate change from human activities. In response, the Kigali Amendment was adopted to control production and consumption of HFCs with high Global Warming Potentials (GWPs) (see Q17). Full compliance with the provisions of the Kigali Amendment will significantly enhance the climate-protection benefit of the Montreal Protocol.

Hydrofluorocarbons (HFCs). HFCs are replacement compounds for ODSs that were chosen because they contain no chlorine or bromine that cause ozone depletion. HFCs are widely used in the residential air-conditioning and refrigeration sectors and as foam-blowing agents, spray-can propellants, and feedstocks for the production of other chemicals. These uses are growing as the global phaseout of hydrochlorofluorocarbons (HCFCs), the early replacement compounds, nears completion. The GWPs of HFCs vary over a wide range due to differences in their physical and radiative properties (see Table Q6-1 and Figure Q17-3). For example, the GWP of HFC-134a (primarily used in air conditioning and refrigeration) is 1470, which means that after release to the atmosphere, each kilogram of HFC-134a is 1470 times more effective than a kilogram of CO_2 in increasing climate forcing over a century-long time period. In contrast, the GWP of HFO-1234yf, a substitute for HFC-134a, is less than 1.

HFC-23. HFC-23 is considered separately in the Kigali Amendment because this gas is primarily produced as an unwanted by-product in the manufacture of HCFC-22 and HFCs. The global warming potential of HFC-23 is quite large (14,700), in part due to its long atmospheric lifetime of 228 years. Although many methods exist to chemically destroy HFC-23 at production facilities, this compound continues to be released to the atmosphere. For example, the atmospheric abundance of HFC-23 increased by 44% between 2009 and 2019. In 2019, the radiative forcing of HFC-23 was 0.006 W/m^2, which is approximately 15% of the total forcing from all HFCs. The Kigali Amendment phases down, in conjunction with the other HFCs, unwanted by-production of HFC-23, but provides no specific control measures for emissions of HFC-23. Instead, the amendment directs nations to destroy HFC-23 to the extent practicable in order to avoid future emissions and the associated increased climate forcing.

Climate implications of HFC use. The total global emission of HFCs expressed in terms of CO_2-equivalent emissions has grown steadily since 2000, equaling about 1 gigatonne CO_2-equivalent per year in 2020 (see **Figure Q19-1**). The primary emissions of HFCs are of HFC-134a as well as HFC-143a, HFC-125 and HFC-32, which are widely used in blended refrigerants such as R404A (52% HFC-143a, 44% HFC-125, and 4% HFC-134a) and R410A (50% HFC-32, 50% HFC-125). Recent growth in the consumption (and emissions) of HFCs is due in part to replacing HCFCs that are being phased out under the Montreal Protocol with HFCs. In 2019, the atmospheric abundances of HFCs contributed about 10% of climate forcing from all halocarbon compounds (see Figure Q17-2) and less than 1% of the total climate forcing from all other long-lived greenhouse gases (see Figure Q17-1). Projections based on current production and consumption patterns and future economic growth indicate that, without the Kigali Amendment, HFC emissions could have reached around 5 gigatonnes CO_2-equivalent per year by 2050 and nearly double that value by 2100 (see Figure Q19-1). This projected emission value for 2050 is about one half of the peak in CO_2-equivalent emissions of ODSs in 1987 (see Figure Q18-1). Thus, in the absence of the Kigali Amendment, the projected growth in HFC emissions in the coming decades offsets a significant amount of the climate protection gained from reductions in ODS emissions under the Montreal Protocol.

Kigali Amendment. The future of HFC emissions was changed by the Montreal Protocol with the adoption of the Kigali Amendment in 2016. The amendment requires a phasedown of the global pro-

Projected Emissions of Hydrofluorocarbons (HFCs)

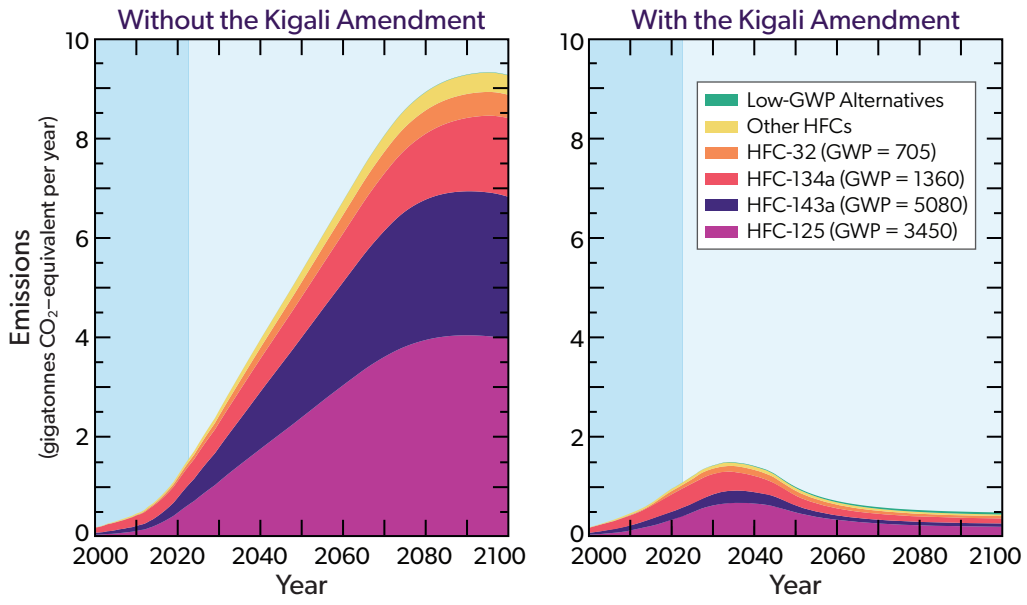

Figure Q19-1. HFC emissions and the Kigali Amendment. The Kigali Amendment to the Montreal Protocol limits the production and consumption of a group of hydrofluorocarbons (HFCs) with high global warming potentials (GWPs). HFCs are considered replacement compounds for ozone-depleting substances (ODSs) because HFCs lack chlorine and bromine, and therefore pose no direct threat to the ozone layer. Avoiding substantial emissions of high-GWP HFCs through the implementation of the Kigali Amendment will increase future climate protection. HFCs have a wide range of GWPs given their different physical and chemical properties (see Table Q6-1 and Figure Q17-3). The panels show emissions of widely used high-GWP HFCs. The emissions are weighted by the 100-yr GWP of each compound; with this weighting, emissions are expressed as CO_2-equivalent mass per year. In the left panel, emissions are based upon an analysis of atmospheric observations up to 2013 and projections to 2100 that represent an upper range to future global emissions in the absence of the Kigali Amendment and national regulations. The right panel shows GWP-weighted emissions based on atmospheric observations up to 2020 as well as projections to 2100, again assuming international compliance with the provisions of the Kigali Amendment. The projections in the right panel include a category termed low-GWP alternatives that is comprised of refrigerant compounds that have GWPs much lower than the refrigerants they replace. Low-GWP alternatives include a subset of HFCs known as hydrofluoroolefins (HFOs), which are also composed only of hydrogen, fluorine and carbon atoms. The chemical structure of HFOs results in these compounds being more reactive in the lower atmosphere (troposphere) than other HFCs and, consequently, HFOs have shorter lifetimes after atmospheric release (see Table Q6-1). As a result, emissions of HFOs cause substantially lower radiative forcing than emissions of the same mass of high-GWP HFCs.

(A gigatonne = 1 billion (10^9) metric tons = 1 trillion (10^{12}) kilograms. A CO_2-equivalent emission of a non-CO_2 GHG is an emission amount that results in the same RF of climate over a 100-year time interval as a release of the same mass of CO_2.)

duction and consumption of high-GWP HFCs by more than 80% (in CO_2-equivalent) from the baseline level over the next 30 years. The phasedown schedule accommodates the concerns and interests of developed and developing countries, including those with high ambient temperatures that are likely going to have future increased demand for the use of air-conditioners. The Kigali Amendment entered into force on 1 January 2019. Figure Q19-1 shows how the amendment provisions dramatically reduce projected emissions of HFCs in the coming decades. The emissions of HFCs that are avoided by 2100 total about 420 gigatonnes CO_2-equivalent, which is more than 10 years of present-day annual emissions of CO_2 due to human activities.

Expanding climate protection. The Kigali Amendment substantially expands the protection of climate afforded by the Montreal Protocol (see Q18). With full implementation of the amendment, annual global emissions of HFCs reach their peak value before 2040 (see Figure Q19-1). Without the amendment, yearly emissions are projected to increase until market saturation is reached in the second half of the century, at a value of about 10 gigatonnes CO_2-equivalent per year, nearly five times more than the emission peak under the amendment. Furthermore, as shown in **Figure Q19-2**, the long-term radiative forcing of climate, which is proportional to atmospheric abundances, is substantially reduced. Without the amendment, projected radiative forcing from HFCs increases throughout this century, reaching a value of about 0.6 W/m^2 in 2100. In this scenario, radiative forcing due to HFCs by the end of the century exceeds that of nitrous oxide and rivals that of methane. With the amendment, the radiative forcing of climate by HFCs reaches a peak value before 2050 and gradually decreases to about 0.07 W/m^2 in 2100. The ranges of radiative forcing values for meth-

Climate Benefit of the Kigali Amendment

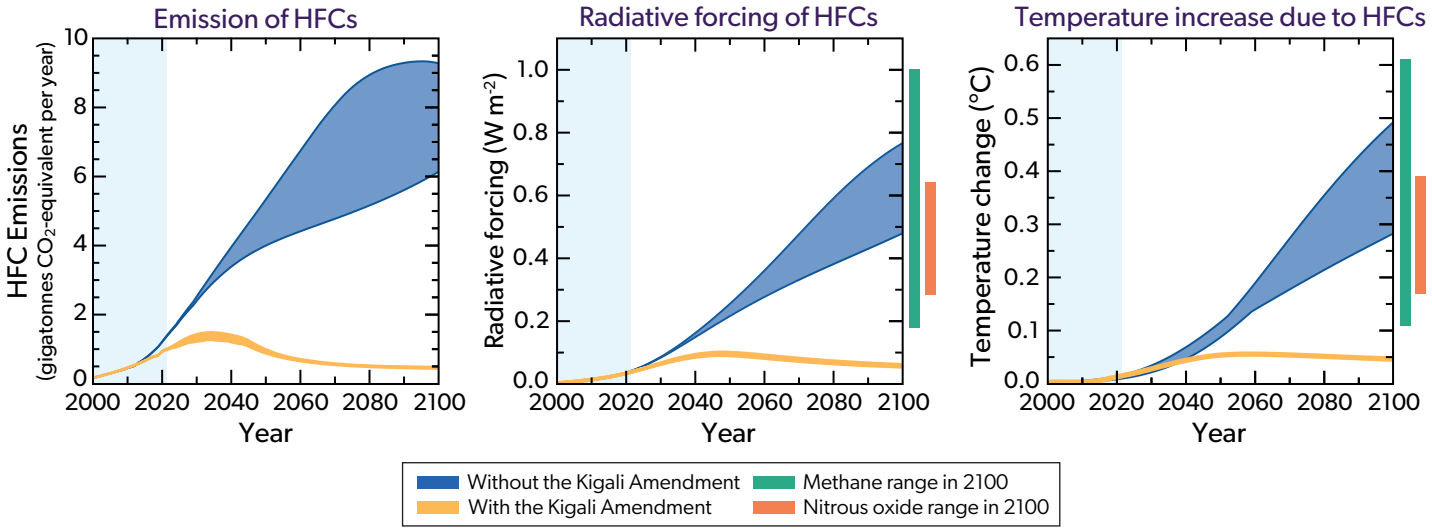

Figure Q19-2. Kigali Amendment Climate Protection. The successful implementation of the Kigali Amendment will enhance the protection to Earth's climate afforded by the Montreal Protocol. The panels display the CO_2-equivalent emissions (left), radiative forcing (middle) and surface temperatures (right) for HFC emission scenarios without (blue shaded regions) and with (gold lines) the implementation of the Kigali Amendment and national regulations. Historical emissions of HFCs are derived from atmospheric observations. Emissions for latter years are based upon projections of production and consumption patterns as well as future economic growth. All emissions are weighted by the 100-yr GWP of each compound (CO_2-equivalent emissions). Emissions of HFC-23 are excluded. The emission projections without the Kigali Amendment and national regulations are based on lower and upper ranges of projected HFC consumption. The increases in global mean surface temperature from HFC emissions are shown beginning in year 2000. For comparison, the radiative forcing and surface temperature increases are shown for methane (CH_4) and nitrous oxide (N_2O) in the middle and right panel margins, respectively, for year 2100 based on accumulated emissions since 1750. Compliance with the Kigali Amendment has the potential to avoid a 0.3 to 0.5°C rise in global surface temperature over this century due to restrictions on the future emission of high-GWP HFCs.

(A gigatonne = 1 billion (10^9) metric tons = 1 trillion (10^{12}) kilograms. The end of century values for CH_4 and N_2O are based upon the Shared Socioeconomic Pathway (SSP) SSP1-2.6 (lower limit) and SSP3-7.0 (upper limit) scenarios.)

ane and nitrous oxide in 2100 as shown in Figure Q19-2 far exceed the 0.07 W/m^2 forcing due to HFCs under the Kigali Amendment.

The benefit of avoiding HFC radiative forcing over many decades as a result of the Kigali Amendment provisions can be expressed as an avoided increase in globally averaged surface temperature. The increase in temperature by the year 2100 due to future atmospheric growth of HFCs without the Kigali Amendment and national regulations is projected to be between 0.3 and 0.5°C (see Figure Q19-2). In contrast, the temperature increase is projected to be about 0.06°C with full implementation of the amendment, which is significantly less, for example, than the warming expected from projected abundances of methane and nitrous oxide in 2100. Currently, global warming due to all emissions from human activities is about 1.2°C since 1750, the start of the Industrial Era. The goal of the United Nations Framework Convention on Climate Change Paris Agreement is to limit global warming to well below 2.0°C since the start of the Industrial Era and to pursue efforts to limit global warming to 1.5°C. The temperature increase of 0.3 to 0.5°C avoided by the Kigali Amendment contributes substantially to the achievability of this goal.

Low-GWP substances. The Kigali Amendment encourages the use of low-GWP substances or other alternatives to replace high-GWP HFCs in the coming decades (see Table Q6-1 and Figure Q17-3). Other alternatives include propane, ammonia, and other climate-friendly technologies. The low-GWP substances include a subset of HFCs known as hydrofluoroolefins (HFOs), which are also composed only of hydrogen, fluorine and carbon atoms. The chemical structure of HFOs includes a double carbon bond, causing these compounds to be more reactive in the lower atmosphere (troposphere) than other HFCs. Consequently, HFOs have very short atmospheric lifetimes. One such compound, HFO-1234yf, has a lifetime of only 12 days, in contrast to HFC-23, HFC-143a, and HFC-134a with lifetimes of 228, 52, and 14 years, respectively (see Table Q6-1). The short atmospheric lifetimes of HFOs lead to very low GWPs. As a result, the emission of an HFO results in substantially lower climate forcing than the forcing caused by emission of the same mass of high-GWP HFCs (see Figure Q19-1).

The projections of emissions under the Kigali Amendment include a group of compounds labeled Low-GWP Alternatives in Figure Q19-1. These compounds are expected to cover the application demand from sectors in which the use of high-GWP HFCs is phased

down. Even with the emissions of a large mass of these low-GWP alternatives, the future projected contribution to climate change is much less than contributions from projected emissions of high-GWP HFCs in the absence of the Kigali Amendment.

Other environmental consequences of HFC use. The atmospheric abundance of trifluoroacetic acid (TFA, chemical formula $C_2HF_3O_2$) is expected to increase in the coming decades due to future emissions of HFCs (including HFOs), HCFCs, and related compounds. When these compounds breakdown in the atmosphere, they produce TFA, a persistent, long-lived chemical with potentially harmful effects on animals, plants, and humans. The current concentration of TFA in rainwater and ocean water is generally very far below toxicity limits. Potential future environmental impacts of TFA are a subject of active research.

The Future. The phasedown of HFCs under the Kigali Amendment sets a path in which HFCs play a very limited role in future climate forcing. Achieving the maximum climate protection from the implementation of the amendment requires that compounds replacing high-GWP HFCs have much smaller or negligible GWPs. Technological developments related to low-GWP replacement substances or other alternatives along with improved refrigeration and air conditioning equipment will help achieve this maximum protection. The release of greenhouse gases in generating electricity for powering refrigeration and air conditioning equipment contributes to the indirect climate forcing from this sector. Improvements in the energy efficiency of equipment in this sector during the transition to low-GWP alternative refrigerants could potentially double the direct climate benefits of the Kigali Amendment. The combination of low-GWP replacement compounds, energy efficiency improvements, and the growth in renewable energy sources has great potential to minimize the direct and indirect contributions to climate forcing from global refrigeration and air conditioning applications.

Q20 How is stratospheric ozone expected to change in the coming decades?

Recovery of the global ozone layer from the effects of ozone-depleting substances (ODSs) is expected around the middle of the 21st century, assuming global compliance with the Montreal Protocol. Recovery will occur as ODSs and reactive halogen gas abundances in the stratosphere decrease in the coming decades. In addition to responding to ODSs, ozone abundances will increasingly be influenced by climate change. The impacts of future climate change on the ozone layer will vary between the tropics, midlatitudes, and polar regions, and strongly depend on future emissions of carbon dioxide (CO_2), methane (CH_4), and nitrous oxide (N_2O). During the long recovery period, large volcanic eruptions could temporarily reduce global ozone amounts for several years.

The expected recovery of the global and polar ozone layer is a direct consequence of the success of the Montreal Protocol in reducing the global production and consumption of ODSs. Currently, the atmospheric abundances of most major ODSs and the associated annual values of equivalent effective stratospheric chlorine (EESC) are in decline (see Q15). In contrast to the diminishing role of ODSs, changes in climate are expected to have an increasing influence on future levels of total ozone. Climate change is driven by the projected growth in the abundance of greenhouse gases (GHGs), primarily carbon dioxide (CO_2), methane (CH_4), and nitrous oxide (N_2O). Increasing amounts of GHGs will lead to changes in temperature, chemistry, and the circulation of the stratosphere, all of which affect ozone. Chemistry-climate models can be used to project how ozone is expected to respond to changes in ODSs and climate in particular geographic regions during the recovery period. Sporadic events such as major volcanic eruptions and wildfires, or deliberate actions such as the injection of aerosols into the stratosphere to mitigate global warming may also influence future ozone levels.

Using chemistry-climate models. Chemistry-climate models (CCMs) are complex computer programs that simulate temperature, winds, radiation, and the chemical composition of the atmosphere, including stratospheric ozone. The simulations of ozone are conducted as a function of time, altitude, and geographic location. Projections of total ozone presented here are based on the results from a group of chemistry-climate models that account for the influences of changes in ODSs and GHGs. These models show how changes in ozone are expected to vary across geographic regions by evaluating the complex interactions of the processes that control ozone and climate involving radiation, chemistry, and transport of chemicals by stratospheric winds. Model inputs include historical and projected concentrations of ODSs, GHGs (including CO_2, CH_4, and N_2O), air pollutant gases, as well as incoming solar radiation. The results from chemistry-climate model simulations are used to identify particular processes that are important for future abundances of ozone. For example, model projections driven by increases in the atmospheric abundance of GHGs over the coming decades show a strengthening in the global-scale atmospheric circulation that brings air from the troposphere into the stratosphere in the tropics, moves stratospheric air poleward into both hemispheres, and then returns air to the troposphere at middle to high latitudes. These circulation changes will significantly alter the global distribution of ozone and the atmospheric lifetimes of ODSs and other long-lived gases (see Q6). Also, while Earth's surface is expected to continue to warm in response to positive radiative forcing of climate from GHGs (see Q17), the stratosphere is expected to continue to cool. A colder upper stratosphere leads to increases in ozone because lower temperatures slow down the gas-phase reactions responsible for ozone loss. Conversely, colder conditions at lower altitudes in the polar stratosphere have the potential to exacerbate ozone loss, especially if the presence of polar stratospheric clouds (PSCs) increases.

Methane and nitrous oxide are both involved in the chemistry that determines levels of stratospheric ozone. The main effect of higher amounts of CH_4 is to increase ozone, while that of rising N_2O is to decrease ozone. The stratospheric decomposition of CH_4 leads to more reactive hydrogen gases that produce ozone in the lowest parts of the stratosphere and increases the conversion of reactive chlorine into its reservoir gas HCl (see Q7). The decomposition of CH_4 also leads to larger abundances of H_2O, which cool the upper stratosphere, slowing down ozone loss reactions. Conversely, the decomposition of N_2O produces reactive nitrogen gases that destroy ozone (see Q8). The effect of higher amounts of N_2O on the depletion of the ozone layer becomes increasingly important as halogen levels decline.

Simulating recent ozone changes. Comparisons of model results with observations help confirm the causes of ozone depletion and increase confidence in model projections of future ozone amounts. Two important measures are the globally averaged total column ozone outside of polar regions (see Q3) and total ozone in the Antarctic during October (the month of peak ozone depletion). These observations are compared to simulations from a group of chemistry-climate models in **Figure Q20-1**. Both time series of ozone show substantial depletion since 1980. The average model values of ozone follow the observed general decline in both regions, suggesting that the main processes involved in ozone depletion are well represented by these models.

Changes in Global and Antarctic Ozone

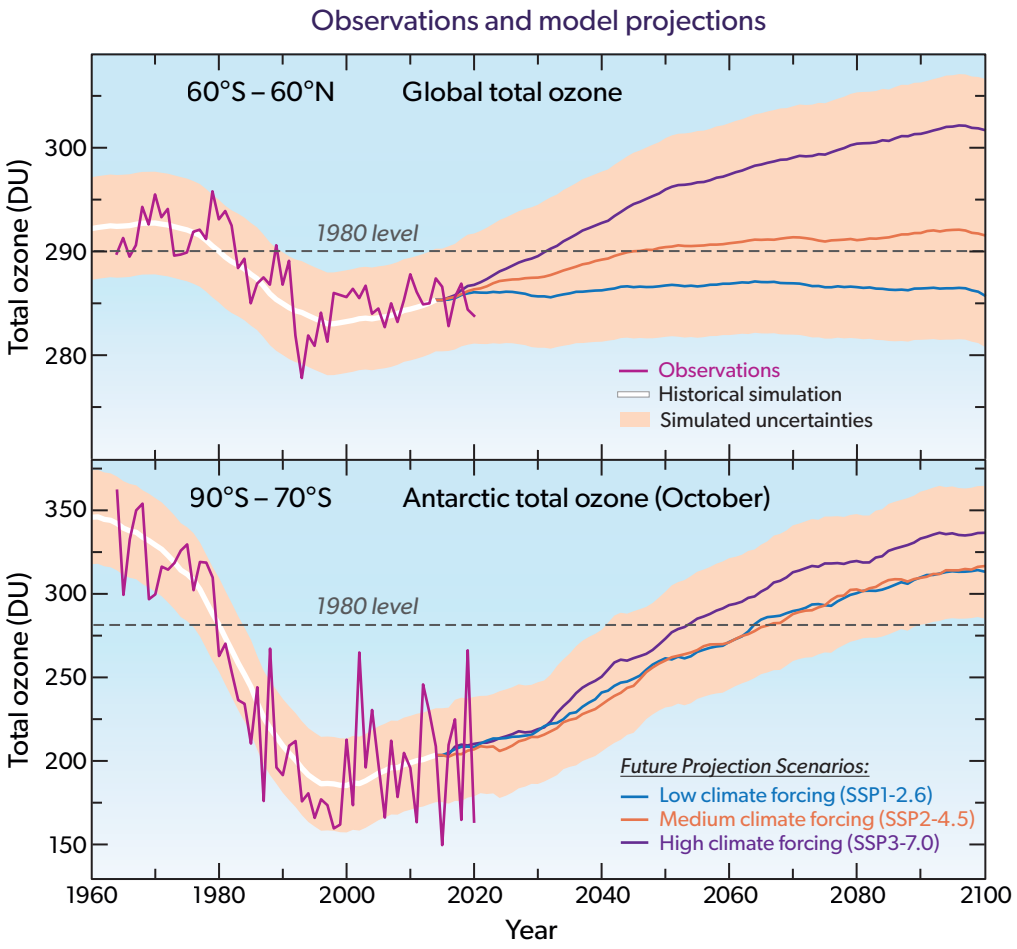

Figure Q20-1. Simulations of ozone depletion. Chemistry-climate model (CCM) simulations that account for changes in ozone-depleting substances (ODSs) and greenhouse gases (GHGs) are widely used to assess past ozone changes and project future values of ozone. Agreement between model results and observations increases confidence in the model projections and our understanding of the processes leading to ozone depletion. Observed values of total ozone (in Dobson units, DU) annually averaged over 60°S–60°N latitude (top panel) and total ozone values over 70°S–90°S during October (bottom panel) decreased during the latter decades of the prior century (magenta lines). Future ODS projections assume compliance with the Montreal Protocol, and future abundances of GHGs follow either the SSP1-2.6 (low climate forcing), SSP2-4.5 (medium climate forcing), or SSP3-7.0 (high climate forcing) scenario for 2015–2100. The simulation uncertainties for modeled ozone represent the standard deviation about the multi-model mean (MMM), either added to the SSP3-7.0 MMM (upper limit) or subtracted from the SSP1-2.6 MMM (lower limit). As ODS abundances decrease in this century, CCMs project global total ozone to increase steadily and exceed the 1980 value by mid-century for the medium climate forcing scenario. Antarctic ozone during October is projected to exceed the 1980 values around mid-century for all three scenarios.

There are significant year-to-year variations in global and Antarctic ozone that are not captured by these simulations. The differences between the observed and modeled values of ozone are due to factors such as interannual meteorological variability that are not well represented in these simulations. Over the time period 1996–2020, observed global ozone has exhibited considerable variability and risen slightly, by less than 1% (see Q12). Antarctic ozone during October has exhibited even more year-to-year variability, but there are emerging indications that the ozone hole has diminished in size and depth (maximum amount of ozone depletion) since 2000, particularly during September when the effects of meteorological variability are smaller (see Q10).

Long-term total ozone projections. Total ozone changes derived from chemistry-climate models are shown for 1960 to 2100 in Figure Q20-1. These simulations use the projected abundances of ODSs given in the 2018 Scientific Assessment of Ozone Depletion report. A computation of EESC (see Q15) based on this 2018 projection of ODSs shows a return to the 1980 level in years 2061 and 2077 for the midlatitude and polar stratospheres, respectively.

The model simulations shown in Figure Q20-1 use projections of CO_2, CH_4, and N_2O termed the Shared Socioeconomic Pathways (SSPs). Each SSP provides an estimate of future abundances of GHGs based on projected emissions, which are constructed using various assumptions of population growth and economic development, as well as technological innovation and political decisions related to the environment. Figure Q20-1 shows the evolution of annually averaged ozone outside the polar regions (60°S–60°N) (top) and ozone during October at 70°S–90°S (bottom), for a high climate forcing scenario (SSP3-7.0; purple line), a medium scenario (SSP2-4.5; dark orange line), and a low scenario (SSP1-2.6; blue line). These three lines represent the multi-model mean (MMM) projection from numerous CCMs.

These simulations show that the future recovery of the ozone layer outside of the polar regions will be governed mostly by GHGs, assuming continued adherence to the Montreal Protocol. The wide range of possible future levels of CO_2, CH_4, and N_2O is an important limitation to providing accurate future projections of ozone globally and for the ozone hole (Figure Q20-1), as well as in other geographic regions. For 60°S–60°N, total ozone recovers to the 1980 level more rapidly under the high climate forcing scenario because large future increases in both CO_2 and CH_4 tend to increase ozone. Under the low climate forcing scenario, the MMM of the CCMs projects that ozone over 60°S–60°N may not reach the 1980 level by the end of this century. In this low climate forcing simulation, future declines in total ozone driven by rising N_2O outweigh the small future ozone increases caused by CO_2 and CH_4. For the MMM of the medium climate forcing scenario (dark orange line in Figure Q20-1), total ozone over 60°S–60°N is projected to return to the 1980 level around year 2040.

The one-standard deviation range of computed values of ozone from these CCMs for all three scenarios is shown by the orange shaded region in Figure Q20-1 (see caption), which depicts the uncertainty in the model projections of ozone for both regions. There is a considerable range of model projections for total ozone at the end of the century for 60°S–60°N, because of sensitivity to the actual future abundance of GHGs for the three scenarios considered here, as well as variations among CCMs regarding how the stratospheric circulation will actually respond to a specific GHG scenario. The CCM simulations in Figure Q20-1 show that for the Antarctic ozone hole (October, 70°S–90°S) the future evolution of total ozone is largely governed by ODSs, with modest sensitivity to GHGs. Here, total ozone is projected to return to the 1980 level in 2066 for both the low and medium climate forcing scenarios (blue and dark orange lines, Figure Q20-1). Under the high climate forcing scenario, a more rapid recovery of October total ozone for 70°S–90°S is projected, with a return to the 1980 level at mid-century. Because of the impact of GHGs, these recovery years for the return of Antarctic total ozone to the 1980 level precede 2078, which is the year EESC is projected to return to its 1980 level for the polar stratosphere.

The multi-model mean of CCM simulations conducted for Northern Hemisphere (NH) midlatitudes (35°N–60°N) and Southern Hemisphere (SH) midlatitudes (35°S–60°S) (results not shown) project a return of total ozone to the 1980 level around years 2035 and 2045, respectively, for the medium climate forcing scenario. The faster return of total ozone to the 1980 level forecast for NH midlatitudes under this scenario is caused by a greater sensitivity of ozone to future abundances of GHGs in the NH compared to the SH, as explained below. The return to the 1980 level of total ozone for both NH and SH midlatitudes occurs considerably sooner than year 2061, when EESC is projected to return to the 1980 level. Finally, the MMM of CCM simulations for the tropics (20°S–20°N) (results not shown) under the medium climate forcing scenario indicates that total ozone will remain below the 1980 level until the end of this century.

Figure Q20-2 illustrates, for six geographic regions, the combined effect on ozone of future changes in ODSs, the GHGs CO_2, CH_4, and N_2O (white line marked "Sum of all gases") as well as the individual effect on ozone of each GHG and all ODSs. These effects on ozone are determined by varying the abundance of each quantity individually, while holding the abundances of the others constant at their level in 1960. All of the results shown in Figure Q20-2 are for the medium climate forcing SSP2-4.5 scenario and rely on simulations from a single CCM. As such, the timing of the recovery of ozone to the 1980 level differs slightly from the values stated above, which are based on the MMM of simulations from numerous CCMs. In Figure Q20-2 the change of ozone is shown relative to the 1960 level to more clearly display the results prior to 1980.

The breakdown of individual drivers of future ozone for these six selected regions shown in Figure Q20-2 is an illustrative example of the complexity of projecting the future recovery of stratospheric ozone, as the sensitivity to various factors differs markedly between regions.

Future changes in total ozone for the various regions are described with respect to a return to the level in year 1960 (see figure caption):

- **Antarctic.** Total ozone changes are largest in the Antarctic region in springtime (October). Chemistry-climate models show that ODSs are the predominant factor in Antarctic ozone depletion in the past and in the coming decades. The future increase of CO_2 and CH_4 in this scenario acts to increase ozone, while the future increase in N_2O decreases ozone. All of these impacts on ozone are smaller than the present impact of ODSs, and the effects of CO_2, CH_4, and N_2O nearly cancel one another later in the century. As a result, changes in total ozone when all forcings are considered (white line) mostly follow the change driven by ODSs (dark pink shaded region). Although meteorological variability in the Antarctic in late winter/early spring when ozone depletion occurs causes a substantial range in the observations and model projections (see Figure Q20-1), Antarctic total ozone is projected to remain below the 1960 level throughout the rest of this century.
- **Arctic.** Total ozone changes in the Arctic during spring (March) are considerably smaller than in the Antarctic (see Q11). After midcentury, Arctic total ozone increases to values above those expected from future reductions in ODSs alone because of the strengthening of atmospheric circulation and enhanced stratospheric cooling associated with increases in GHGs such as CO_2. For this medium climate forcing scenario, Arctic spring total ozone is projected to exceed the 1960 level after around 2065.

Total Ozone Changes in Response to Ozone-Depleting Substances and Greenhouse Gases

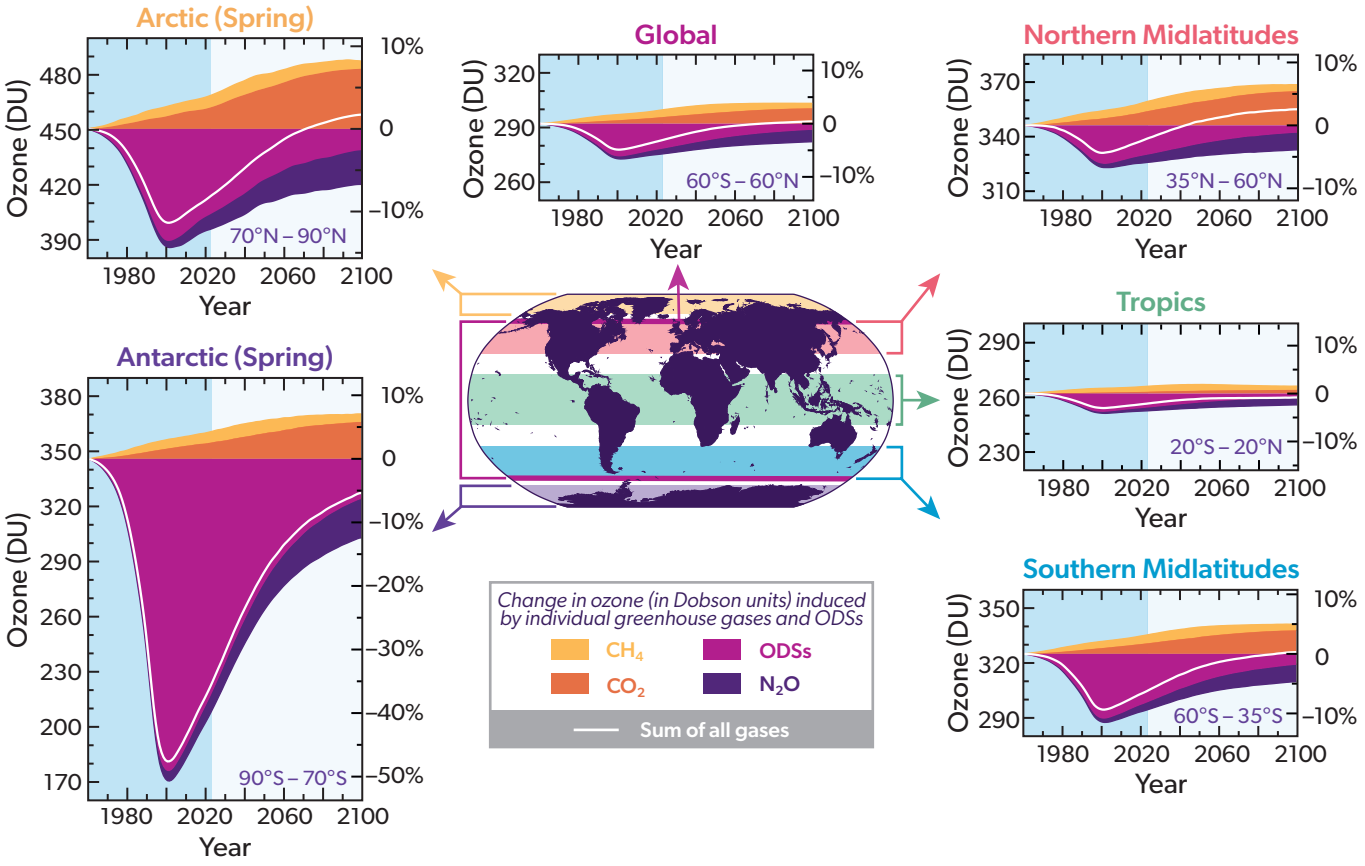

Figure Q20-2. Total ozone changes in response to greenhouse gases and ODSs. Results from model simulations of a single CCM show the sensitivity of total ozone to individual changes in the abundances of the greenhouse gases CO_2, CH_4, and N_2O as well as to ODSs starting in 1960. These total ozone changes (in Dobson units, DU) are shown for spring in the polar regions (March for the Arctic and October for the Antarctic) and for the annual average for the Tropics, for both the northern and southern midlatitudes, and for the global average outside of the polar regions ("Global"). The solid shaded regions illustrate how each particular gas (or family of gases for ODSs) affects total ozone, with negative contributions shown below the 1960 level of ozone and positive contributions shown above. These simulations use CO_2, CH_4, and N_2O from the medium climate forcing (SSP2-4.5) scenario of Figure Q20-1. The abundances of the greenhouse gases and ODSs are varied individually while the others are kept constant at their level in 1960 to compute the individual constituent's contribution to prior and projected total ozone. Increasing CO_2 results in lower temperatures throughout the stratosphere. Lower temperatures slow down the rate of most ozone destruction chemical reactions, particularly those that regulate the abundance of ozone outside of polar regions, leading to an increase in ozone. Increasing CO_2 also enhances the transport of ozone from the tropics to middle and high latitudes by stratospheric winds. Increasing CH_4 leads to changes in stratospheric chemistry that augment the increase in ozone driven by stratospheric cooling. Conversely, the expected future increase in N_2O results in significant decreases in ozone due to chemical effects. As the atmospheric abundance of ODSs declines towards the end of this century, ozone reductions due to increasing N_2O may become more prominent. The white "Sum of all gases" line on each panel represents the combined effect on ozone of CO_2, CH_4, N_2O, and ODSs.

(These projections use abundances for CO_2, CH_4, N_2O from the SSP2-4.5 scenario and ODSs from the baseline (A1) projection of the 2018 Scientific Assessment of Ozone Depletion report.)

- **Northern and Southern Midlatitudes.** Changes in the annual averages of total ozone in midlatitudes are much smaller than the springtime losses in polar regions. In the northern midlatitudes, the all-forcings simulation (white line) indicates a return of total ozone to the 1960 value around 2045, even though EESC remains above its 1960 value until the end of the century. In the southern midlatitudes, total ozone returns to the 1960 level around 2085, about four decades later than projected for the Northern Hemisphere. The maximum ozone depletion near year 2000 is much larger for the Southern Hemisphere, and total ozone more closely follows the depletion driven by ODSs. This behavior reflects the influence of the Antarctic

ozone hole on the southern midlatitudes, driven by the transport of ozone-depleted air following the breakup of the polar vortex in late spring (see Q10). The larger value of midlatitude total ozone from mid-century to the end of this century when all forcings are considered (white lines) compared to ozone depletion due only to ODSs (dark pink shaded region) reflects the influence of changes in stratospheric circulation and upper stratospheric temperatures by CO_2 and CH_4 for this medium climate forcing scenario, especially in the NH.

- **Tropics.** Total ozone changes in the tropics are smaller than in any other region. Ozone is less sensitive to ODSs in the tropical stratosphere because of the dominant roles of production and transport in controlling ozone and the low amounts of reactive halogens available in this region (see Q12). Total ozone gradually increases until around 2060, and then remains fairly constant and slightly below the 1960 level until the end of the century. The near-constant value of tropical ozone during the latter part of the century is primarily due to climate-change-induced strengthening of the stratospheric circulation, which leads to enhanced transport of ozone out of the tropics and into midlatitudes. This circulation change also influences the Arctic and midlatitude regions, as noted above.
- **The globe.** The annual average of global (60°S to 60°N) total ozone is projected to return to the 1960 level around 2075, even though EESC remains above its 1960 value until the end of the century. Chemistry-climate model analysis suggests that the early return of total ozone relative to EESC, as well as the end-of-century rise, are primarily a result of upper stratospheric cooling and strengthening of the stratospheric circulation caused by increasing GHGs. Towards the latter part of this century, increased abundances of N_2O may lead to more ozone depletion (dark blue shaded region) than ODSs (dark pink shaded region).

Future ultraviolet radiation. Projections of long-term changes in total ozone can be used to estimate long-term changes in solar ultraviolet (UV) radiation reaching Earth's surface (see Q16). The UV-B component of ultraviolet radiation (see Q2) decreases as total ozone increases. Based on the ozone increases in the chemistry-climate model projections, clear-sky (cloud-free) UV-B radiation is expected to be below the 1960 value by the end of the century across much of the globe in regions that are not currently affected by high levels of tropospheric air pollution. Clear-sky UV-B radiation values are expected to remain high in Antarctica, where total ozone is expected to remain below its 1960 value even at the end of this century.

Volcanoes, wildfires, and climate intervention. There are several factors not included in chemistry-climate model projections shown above that have the potential to affect future amounts of total ozone. For example, explosive volcanic eruptions have temporarily reduced global total ozone in the past (see Q13) by enhancing the stratospheric sulfate aerosol layer. Large volcanic eruptions that occur while EESC values remain high are expected to reduce total ozone for a few years. Such volcanic eruptions are an additional source of uncertainty that is not included in the ozone projections in Figures Q20-1 and Q20-2. Extreme wildfires can generate deep thunderstorms, termed pyrocumulonimbus (pyroCb) clouds, that inject particles from biomass burning into the stratosphere. The biomass burning particles consist of organic carbon, inorganic components and a significant fraction of black carbon that enhance the absorption of solar radiation. These pyroCb particles likely impact the ozone layer and climate in a manner that differs substantially from the impact of sulfate aerosols.

Numerous climate intervention (also called geoengineering) methods have been proposed to reduce climate forcing from human activities. A widely discussed method is the intentional enhancement of sulfate aerosols in the stratosphere from direct injections of sulfur-containing substances, known as Stratospheric Aerosol Injection (SAI). With sufficient enhancement, the added aerosols would cool the Earth's surface through increased reflection of sunlight back to space, similar to the effect observed after volcanic eruptions that inject sulfate into the stratosphere (see Figure Q13-1). While SAI could reduce some of the impacts of global warming, it cannot restore past climatic conditions and may cause unintended side effects, including changes in the concentration of stratospheric ozone, a delay in the recovery of the ozone hole, and changes to the atmospheric circulation. Aerosol heating of the lowermost stratosphere by SAI using sulfates could result in further residual impacts, including changes in regional surface temperature and precipitation patterns. How much aerosol injection would be needed and the duration of that injection would depend on the desired climate outcomes and the trajectory of greenhouse gas emissions and decarbonization efforts. The sign of stratospheric ozone changes will depend on the details of the SAI implementation as well as the concentrations of EESC and N_2O at the time of injection. Changes in stratospheric water vapor due to variations in temperature and circulation resulting from SAI may also play a role in governing how stratospheric ozone would be affected by SAI.

Studies are currently being conducted to determine materials for SAI other than sulfate that have chemical and radiative properties that would reduce the effect of SAI on ozone and stratospheric heating. These studies are just beginning; significant laboratory and modeling work on materials other than sulfate is needed before their effects on ozone and stratospheric transport can be reliably estimated.

TERMINOLOGY

CCM	chemistry-climate model
CFC	chlorofluorocarbon, a group of industrial compounds that contains at least one chlorine, fluorine, and carbon atom
CFC-11-equivalent	a unit for the measure of the mass of emission of an ODS, equal to the product of the actual mass emission of the ODS times its ODP
CO_2-equivalent	a unit for the measure of the mass of emission of a GHG, equal to the product of the actual mass emission of the GHG times its GWP
DU	Dobson unit, a measure of total column ozone; 1 DU = 2.687×10^{16} molecules/cm^2
EEAP	Environmental Effects Assessment Panel of the Montreal Protocol
EESC	equivalent effective stratospheric chlorine, a measure of the total amount of reactive and reservoir chlorine and bromine gases in the stratosphere that is available to deplete stratospheric ozone
GHG	greenhouse gas
gigatonne	1 billion (10^9) metric tons = 1 trillion (10^{12}) kilograms
GWP	global warming potential, a measure of the effectiveness of the emission of a gas to cause an increase in the radiative forcing of climate, relative to the radiative forcing caused by the emission of the same mass of CO_2; all GWPs used here are for a 100-year time interval
halogen	elements fluorine, chlorine, bromine, iodine, and astatine that form group 7A of the periodic table
halon	a group of industrial compounds that contain at least one bromine and carbon atom; may or may not contain a chlorine atom
HCFC	hydrochlorofluorocarbon, a group of industrial compounds that contain at least one hydrogen, chlorine, fluorine, and carbon atom
HFC	hydrofluorocarbon, a group of industrial compounds that contain at least one hydrogen, fluorine, and carbon atom and no chlorine or bromine atoms
HFO	hydrofluoroolefin, a group of industrial compounds that contain at least one hydrogen, fluorine, and carbon atom and no chlorine or bromine atoms, and also include a double carbon bond that causes these gases to be more reactive in the troposphere than other HFCs
IPCC	Intergovernmental Panel on Climate Change
kilotonne	1000 metric tons = 1 million (10^6) kilograms
megatonne	1 million (10^6) metric tons = 1 billion (10^9) kilograms
MMM	multi-model mean
mPa	pascal (Pa) is a unit of pressure; 1 mPa (millipascal) equals 0.001 Pa.
nm	nanometer, one billionth of a meter (10^{-9} m)
ODP	ozone depletion potential, a measure of the effectiveness of the emission of a gas to deplete the ozone layer, relative to the ozone depletion caused by the emission of the same mass of CFC-11
ODS	ozone-depleting substance
ozone layer	the region in the stratosphere with the highest concentration of ozone, between about 15 and 35 km altitude
ppb	parts per billion; 1 part per billion equals the presence of one molecule of a gas per billion (10^9) total air molecules
ppm	parts per million; 1 part per million equals the presence of one molecule of a gas per million (10^6) total air molecules
ppt	parts per trillion; 1 part per trillion equals the presence of one molecule of a gas per trillion (10^{12}) total air molecules
PFC	perfluorocarbon, a group of industrial compounds that contain only carbon and fluorine atoms
PSC	polar stratospheric cloud
RF	radiative forcing of climate

SAI	stratospheric aerosol injection
SAOD	stratospheric aerosol optical depth
source gas	a halogen-containing chemical with a sufficiently long atmospheric lifetime that its emissions contribute to the stratospheric abundance of chlorine or bromine molecules, which participate in chemical reactions that deplete ozone
SAP	Scientific Assessment Panel of the Montreal Protocol
SSP	Shared Socioeconomic Pathway
stratosphere	layer of the atmosphere above the troposphere that extends up to around 50 km altitude, and that includes the ozone layer
TEAP	Technology and Economic Assessment Panel of the Montreal Protocol
TFA	trifluoroacetic acid, a decomposition product of HFCs, HCFCs, and HFOs
troposphere	lower layer of the atmosphere that extends from the surface up to about 10–15 km (6–9 miles) altitude
UNEP	United Nations Environment Programme
UNFCCC	United Nations Framework Convention on Climate Change
UV	ultraviolet radiation
UV-A	ultraviolet radiation between wavelengths of 315 and 400 nm
UV-B	ultraviolet radiation between wavelengths of 280 and 315 nm
UV-C	ultraviolet radiation between wavelengths of 100 and 280 nm
UVI	ultraviolet radiation index
VSL	very short-lived
WMO	World Meteorological Organization

CHEMICAL FORMULAE AND NOMENCLATURE

Chlorine Compounds

Cl	atomic chlorine
ClO	chlorine monoxide
$(ClO)_2$	chlorine monoxide dimer, chemical structure ClOOCl
$ClONO_2$	chlorine nitrate
HCl	hydrogen chloride (hydrochloric acid)
CCl_4	carbon tetrachloride
CH_2Cl_2	dichloromethane
CH_3CCl_3	methyl chloroform
CH_3Cl	methyl chloride
CCl_3F	CFC-11
CCl_2F_2	CFC-12
CCl_2FCClF_2	CFC-113
CHF_2Cl	HCFC-22
CH_3CCl_2F	HCFC-141b
CH_3CClF_2	HCFC-142b

Bromine Compounds

Br	atomic bromine
BrO	bromine monoxide
BrCl	bromine monochloride
CH_2Br_2	dibromomethane
$CHBr_3$	bromoform
CH_3Br	methyl bromide
$CBrClF_2$	halon-1211
$CBrF_3$	halon-1301
$CBrF_2CBrF_2$	halon-2402

Other Halogens

CHF_3	HFC-23
CH_2F_2	HFC-32
CHF_2CF_3	HFC-125
CH_2FCF_3	HFC-134a
CH_3CF_3	HFC-143a
CH_3CHF_2	HFC-152a
CF_3CFCH_2	HFO-1234yf
CF_4	carbon tetrafluoride
C_2F_6	perfluoroethane
CF_3I	trifluoroiodomethane
$C_2HF_3O_2$	trifluoroacetic acid
IO	iodine monoxide
SF_6	sulfur hexafluoride

Other Gases

CH_4	methane
CO	carbon monoxide
CO_2	carbon dioxide
H	atomic hydrogen
H_2O	water vapor
HNO_3	nitric acid
H_2SO_4	sulfuric acid
N_2	molecular nitrogen
N_2O	nitrous oxide
NO_x	nitrogen oxides
O	atomic oxygen
O_2	molecular oxygen
O_3	ozone

AUTHORS AND CONTRIBUTORS

Co-Chairs of the Scientific Assessment Panel (SAP) of the Montreal Protocol and Assessment Co-Chairs

David W. Fahey	NOAA Chemical Sciences Laboratory	USA
Paul A. Newman	NASA Goddard Space Flight Center	USA
John A. Pyle	University of Cambridge and the National Centre for Atmospheric Science (NCAS)	UK
Bonfils Safari	University of Rwanda, College of Science and Technology	Rwanda

Lead Author

Ross J. Salawitch	University of Maryland, College Park	USA

Authors

Laura A. McBride	Albright College	USA
Chelsea R. Thompson	NOAA Chemical Sciences Laboratory	USA
Eric L. Fleming	Science Systems and Applications, Inc. (SSAI) at NASA Goddard Space Flight Center	USA
Richard L. McKenzie	National Institute of Water and Atmospheric Research (NIWA)	New Zealand
Karen H. Rosenlof	NOAA Chemical Sciences Laboratory	USA
Sarah J. Doherty	University of Colorado, Cooperative Institute for Research in Environmental Sciences (CIRES) at NOAA Chemical Sciences Laboratory	USA
David W. Fahey	NOAA Chemical Sciences Laboratory	USA

Contributing Authors

Simon Alexander	Australian Antarctic Division	Australia
Germar Bernhard	Biospherical Instruments, Inc.	USA
Lucy Carpenter	University of York	UK
Gabriel Chiodo	ETH Zürich, Institute for Atmospheric and Climate Science	Switzerland
Robert Damadeo	NASA Langley Research Center	USA
John S. Daniel	NOAA Chemical Sciences Laboratory	USA
Sean Davis	NOAA Chemical Sciences Laboratory	USA
Vitali Fioletov	Environment and Climate Change Canada	Canada
Hella Garny	Deutsches Zentrum für Luft und Raumfahrt (DLR), Institut für Physik der Atmosphäre (IPA)	Germany
Brad Hall	NOAA Global Monitoring Laboratory	USA
Birgit Hassler	Deutsches Zentrum für Luft und Raumfahrt (DLR), Institut für Physik der Atmosphäre (IPA)	Germany
James Haywood	University of Exeter and Met Office Hadley Centre	UK
Lei Hu	University of Colorado, Cooperative Institute for Research in Environmental Sciences (CIRES) at NOAA Global Monitoring Laboratory	USA
Yue Jia	University of Colorado, Cooperative Institute for Research in Environmental Sciences (CIRES) at NOAA Chemical Sciences Laboratory	USA
Bryan Johnson	NOAA Global Monitoring Laboratory	USA
James Keeble	University of Cambridge, Department of Chemistry	UK
Johannes C. Laube	Forschungszentrum Jülich, Institute for Energy and Climate Research: Stratosphere (IEK-7)	Germany
Eric Nash	Science Systems and Applications, Inc. (SSAI) at NASA Goddard Space Flight Center	USA
Stefan Reimann	Swiss Federal Laboratories for Materials Science and Technology (Empa)	Switzerland
Matt Rigby	University of Bristol, School of Chemistry	UK
Michelle L. Santee	NASA Jet Propulsion Laboratory, California Institute of Technology	USA
Susan Tegtmeier	University of Saskatchewan, Institute of Space and Atmospheric Studies	Canada
Simon Tilmes	National Center for Atmospheric Research (NCAR), Atmospheric Chemistry Observations & Modeling	USA
Walter Tribett	University of Maryland, College Park	USA
Guus J. M. Velders	National Institute for Public Health and the Environment (RIVM) & Utrecht University	Netherlands
Peter von der Gathen	Alfred Wegener Institute, Helmholtz Centre for Polar and Marine Research	Germany
Krzysztof Wargan	Science Systems and Applications Inc. (SSAI) at NASA Goddard Space Flight Center	USA
Mark Weber	Universität Bremen, Institute of Environmental Physics	Germany
Paul Young	Lancaster University	UK

The *Twenty Questions and Answers About the Ozone Layer: 2022 Update* is a component of the Scientific Assessment of Ozone Depletion: 2022 report. The report is prepared quadrennially by the Scientific Assessment Panel (SAP) of the Montreal Protocol on Substances that Deplete the Ozone Layer. The motivation behind this publication is to tell the story of ozone depletion, ozone-depleting substances, and the success of the Montreal Protocol. This 2022 Update coincides with the 35th anniversary of the signing of the Montreal Protocol in 1987.

Lead Author
Ross J. Salawitch

Coauthors
Laura A. McBride
Chelsea R. Thompson
Eric L. Fleming
Richard L. McKenzie
Karen H. Rosenlof
Sarah J. Doherty
David W. Fahey

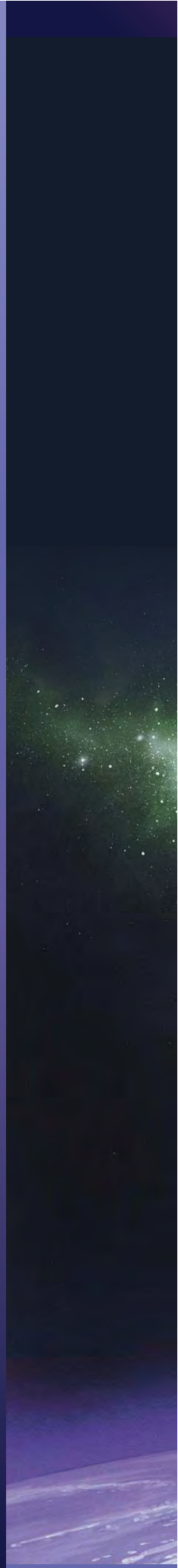

World Meteorological Organization
United Nations Environment Programme
National Oceanic and Atmospheric Administration
National Aeronautics and Space Administration
European Commission